Vol 5 Spring 2014

SCIENTIA

Undergraduate Journal of Scientific Research
University of Notre Dame

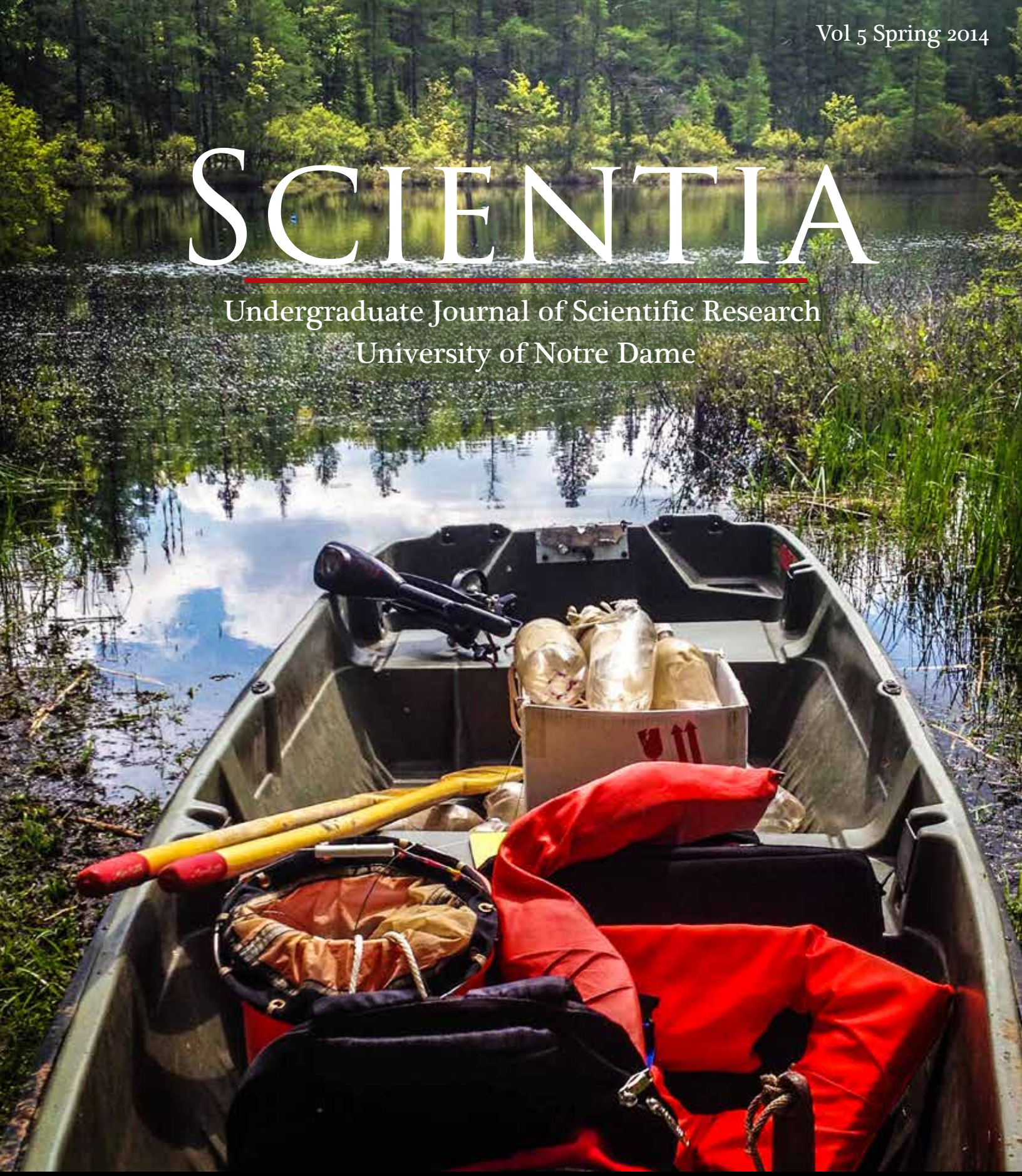

UNIVERSITY OF NOTRE DAME
College of Science

CHARLES EDISON FUND

A Letter From Dean Crawford

The University of Notre Dame is founded on the virtues of men and women who have built our community for more than 170 years. I witness the virtues of Our Lady's University whenever I am in the presence of our science students, especially our undergraduate researchers, each and every day.

Our undergraduate researchers are ambitious. They have the inner drive to achieve great things for the sake of the common good. Many of our researchers work countless hours in the lab to help find treatments and cures for some of the most challenging health concerns of our day.

Our undergraduate researchers are curious. Curiosity as a virtue involves the habit of seeking new knowledge by observation and investigation. Our undergraduate researchers explore, challenge the status quo, and seek new solutions that improve the depth of human understanding and push the frontiers of science forward.

Our undergraduate researchers are diligent. Diligence is the virtue of hard work, keeping at the task in order to make sure it is accomplished. It involves not only the degree of labor exerted at any particular moment, but also the sustained performance of that effort across long periods of time as needed.

As you read through this fifth volume of *Scientia*, you will see that our researchers are also dedicated, passionate, determined, persistent, and full of wonder. I am so proud of this publication, which highlights the incredible work they have completed over the last year. I hope you enjoy reading this volume of *Scientia* as much as I did.

Yours in Notre Dame,

Gregory P. Crawford, Ph.D.
William K. Warren Foundation Dean of the College of Science
Professor of Physics

Editorial Board 2013-2014

Acknowledgments: *Scientia*, comprised of exclusively undergraduate work, is sincerely thankful to the students who have submitted their research. Additionally, the Editorial Board expresses its gratitude for the dedication and guidance of our faculty advisor, Dominic Chaloner, Ph.D., the Dean of the College of Science, Gregory Crawford, Ph.D., for his inspiration, enthusiasm, and support for our mission, Marissa Gebhard and Stephanie Healey for helping us through the publication process, and the College of Science and The Charles Edison Fund for their financial support.

From the Editors

We are pleased to present the fifth volume of *Scientia*, the undergraduate journal of scientific research. This year's edition carries on our proud tradition of presenting top research produced by undergraduates, written by undergraduates, and reviewed by our undergraduate peers.

The very name of this journal, *Scientia*, is derived from the work of Sir Francis Bacon, who claims that *scientia*, knowledge of the natural world, is itself the proper partner of *potentia*, or power. *Scientia* embodies the mission of the College of Science to prepare tomorrow's scientific leaders to think big while also inspiring them to make a difference, and to share their knowledge and discoveries in ways that encourage collaboration, advance learning, and contribute to the common good. In the pages of this journal, you will discover articles on topics ranging from the application of nanotechnology in human health to the use of mass spectroscopy in identifying the binding sites of specific proteins. Even so, these articles only touch on the vast variety of research done by undergraduates across campus.

One of the goals of *Scientia* is to drive undergraduate participation in the publication and peer review process, but more broadly to foster scientific communication across disciplines and among students and faculty. Beyond the publication of this print journal, we also celebrate the success of our monthly "Talk Science" seminars. Now in its fourth year, "Talk Science" serves as an opportunity for undergraduates and faculty to give talks on their research in a fun and informal setting. We thank all of our student and faculty presenters this year, who are listed on the final page of the journal.

As we prepare to graduate from Notre Dame, we look back on our involvement with *Scientia* with great fondness. Though we must say goodbye, we are so thrilled to announce Orrin Belden and Katrina Magno as *Scientia*'s next editors-in-chief. Orrin and Katrina both joined *Scientia* as freshmen, and have since contributed articles to the journal, and have been involved in the peer review, layout, and publication process. This year, as managing editors, they have done phenomenal work coordinating many aspects of *Scientia*, including not only the journal itself, but also our "Talk Science" seminars. We are confident that they will do a superb job as editors-in-chief.

In closing, we thank all of the people whose support has contributed to the continued success of *Scientia*. In particular, we would like to recognize Greg Crawford, dean of the college of science; the staff of the dean's office; and Prof. Dom Chaloner, our faculty advisor. We gratefully acknowledge all of the students who submitted their papers for review, as well as their faculty mentors. Finally we thank all of our staff members, particularly our layout team and our section editors for all of their fantastic work throughout the year. Without them *Scientia* would not be possible.

In Notre Dame,

Rachel Cotton

Rachel Cotton
Scientia Co-Editor-in-Chief

Rebecca Marton

Rebecca Marton
Scientia Co-Editor-in-Chief

Contents

News

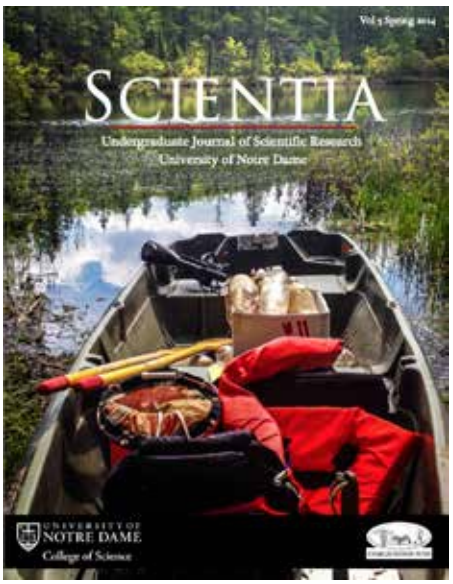

▲ On the Front & Back Covers

The University of Notre Dame Environmental Research Center - East (UNDERC) is the home of Notre Dame's ecology and environmental biology research. The center totals over 7,000 acres in size with 30 lakes and bogs.

Biology

Chemistry

Physics

Health

New Faculty Join the College of Science

LUQUN SHEN & JOHN KWON

Dan Bardayan, associate professor of physics, earned his B.S. at Tennessee Technological University and his Ph.D. at Yale University. At Yale, he performed the first measurement with a short-lived reaccelerated beam in the U.S. and was awarded the American Physical Society's Dissertation in Nuclear Physics Award in 2001. He comes to Notre Dame after spending the past decade studying nuclear reactions occurring in stellar explosions as a senior scientist at Oak Ridge National Laboratory. His research focuses on understanding the properties of exotic nuclei that normally exist only in the cores of massive stellar explosions. These exotic nuclei can also be produced and studied on Earth at the Notre Dame Nuclear Science Laboratory before they quickly decay.

Maxime Brodeur, assistant professor of physics, earned his B.Sc. in physics from l'Université de Montréal and his Ph.D. from the University of British Columbia. He performed his doctoral research at TRIUMF, Canada's national lab for particles and nuclear physics where he measured the masses of very exotic nuclei to high precision. He went on to do his postdoctoral work at Michigan State University. His current research focuses on nuclear astrophysics and seeks to explain the synthesis of the nuclei we observe in the universe. More specifically, he studies the rapid neutron capture process (r-process), which happens in very explosive events and is responsible for the production of approximately half of the nuclides heavier than iron. To study this process, he plans on synthesizing some of these very neutron-rich nuclei before trapping them to measure their mass or decay properties.

Alexandra Jilkine, assistant professor of applied and computational mathematics and statistics, earned her B.S. at the University of Manitoba, and her M.S. and Ph.D. at the University of British Columbia. She studies mathematical biology with applications in cell biology. In particular, her research focuses on how cells reorganize their cellular components in a process called polarization and how a cell's external environment biases this process. Because loss of cell polarity is observed in many cancers during transformation and progression, understanding the molecular mechanisms involved in the establishment and maintenance of cell polarity could lead to a better understanding of how tissues can regenerate and develop cancer. This research has the potential to suggest new therapeutic approaches that would specifically target cancer cells.

Andrei Jorza, assistant professor of mathematics, earned his B.A. at Harvard University and his Ph.D. from Princeton University. After, he did his postdoctoral work at the California Institute of Technology. His research focuses on solving Diophantine equations by studying the deep connections between the geometric symmetries of equations and the symmetries of arithmetically meaningful analytic functions. He is currently exploring variants of the million-dollar Birch and Swinnerton-Dyer conjecture, one of today's leading open problems in number theory.

Alan Lindsay, assistant professor of mathematics, received his B.S. at the University of Edinburgh and completed his Ph.D. in Applied Mathematics at the University of British Columbia in 2010. Prior to his position at Notre Dame, he was a postdoctoral fellow at the University of Arizona and a lecturer at the Heriot-Watt University. His research spans interface dynamics, micro-electro mechanical systems, and partial differential equations. Currently, he is investigating physical and ecological models through the application of partial differential equations.

Adam Martin, assistant professor of physics at the University of Notre Dame, obtained his B.S. at the University of Wisconsin-Madison and pursued his Ph.D. in Physics at Boston University. His thesis focused on an alternative approach to light composite higgs, known as the Little Higgs mechanism, to find a potential dark matter candidate. He was a postdoctoral fellow at Yale University and Fermilab, where he continued his work on Little Higgs and the Higgs Boson, also known as the "God particle." Martin continues this work here at the University of Notre Dame.

Athanasia Panopoulos is the Gallagher Family Assistant Professor of Stem Cell Biology. She received her B.S. at the University of Michigan and obtained an M.S. and Ph.D. at the MD Anderson Cancer Center. She then performed her postdoctoral studies at The Salk Institute in La Jolla. As an assistant professor at the University of Notre Dame, her work focuses on somatic cell reprogramming, a process by which somatic cells revert back to a pluripotent stem cell state. This system has provided researchers new methods to study development and disease. Her lab uses somatic cell reprogramming to understand blood stem cell development, and to identify strategic cancer targets.

John Parkhill, an assistant professor of physical and analytical chemistry, received his B.S. in Chemistry and Mathematics at the University of Chicago. He pursued his Ph.D. at University of California, Berkley in Theoretical Chemistry and continued his academic career as a postdoctoral fellow at Harvard University. At the University of Notre Dame, his research focuses on elucidating a more predictive and practical method for electronic dynamic modeling using physical models, computational models, and energy material simulations.

Anand Pillay, the William J. Hank Family Professor of Mathematics, obtained his B.A. in Mathematics and Philosophy at Oxford University. At London University, he received his M.S. and Ph.D. in Mathematics in 1974 and 1978, respectively. Prior to his time at Notre Dame, Pillay served at the University of Illinois as the Swanlund Chair, 1996-2006, and then Swanlund Chair Emeritus from 2006. His research interests lie in the study of pure model theory and correlating model theory and other diverse subjects in mathematics, including algebra, geometry, and number theory.

Science Policy Ethics Seminar Takes Students to Washington, D.C.

DANIEL PAPE

While many students spent their spring breaks lying on a beach or hitting the ski slopes, students in the College of Science and Center for Social Concerns seminar *Science Policy Ethics: Guiding Science Through the Regulation of Research and Funding* traveled to Washington, D.C., to meet with those at the intersection of science and government. Now in its second year, the student-created seminar explores the life cycle of science in Washington through the framework of values, ethics, and Catholic Social Teaching. Specifically, the seminar examines why Congress invests federal funds into scientific research, how research is regulated and priorities are set, and how science is communicated among scientists, lobbyists, government, federal agencies, and industry.

Student leaders Katrina Magno ‘15 and Rachel Cotton ‘14 wrote the syllabus, invited speakers, and scheduled meetings for the week in Washington, D.C., working with Greg Crawford, dean of the College of Science, Kyle Lantz in the Center for Social Concerns, and Notre Dame’s Office of Federal and Washington Relations. Lantz described the applicability of the seminar for science students intending to pursue careers in research. “In the future, students will be exposed to significant shareholders in the world of science,” Lantz said. “This was a great opportunity for them to directly act in their field of study.” In addition to Magno and Cotton, the class was made up of 13 undergraduate and graduate students from across the College of Science.

Before spring break, the class met weekly to hear from speakers with experience in science policy, communication, ethics, or Catholic Social Teaching. Speakers during the first two classes included Dean Crawford; Kathie Olsen, Ph.D., founder and managing director of ScienceWorks, who spoke about her time leading the National Science Foundation’s multibillion dollar budget; Don Howard, director of the Reilly Center for Science, Technology, and Values who offered philosophical insight on social concerns for scientists; and Margie Pfeil, assistant professor of theology, who led a discussion on how Catholic Social Teaching applies to science.

The class also examined examples in specific disciplines. Peter Burns, Massman Professor of Civil Engineering and director of the Energy Frontier Research Center (ND-EFRC), spoke about running the EFRC, which was established with a grant from the U.S. Department of Energy to study clean nuclear power. Sharon Stack, Ann F. Dunne and Elizabeth Riley director of the Harper Cancer Research Institute and

The class poses for a photo with Nobel Prize Winner John Mather, Ph.D. at NASA's Goddard Space Flight Center in Washington, D.C.

professor of chemistry and biochemistry, spoke on the NIH grant application process with respect to cancer research; and Norb Wiech, Ph.D., CEO of Lysomics, described the barriers restricting the transition of drugs from the lab to patients. The final class prior to the trip examined environmental policy and communication, and featured Joyce Coffee, managing director of the Notre Dame Global Adaptation Index; and Jennifer Tank, Ludmilla F., Stephen J., and Robert T. Galla Professor of Biological Sciences.

The week in Washington, D.C., was the capstone of the course. The group met with a number of individuals and federal agencies, including Teresa Fryberger, Ph.D., of the National Academy of Sciences' Board on Chemical Sciences and Technology, and Patrick Kelley, M.D., of the Institute of Medicine Board on Global Health.

A highlight of the week was the visit to the NASA Goddard Space Flight Center, where the group met with Michelle Thaller, Ph.D., and Nobel Prize winner John Mather, Ph.D. Students toured the astrobiology laboratories and the largest Class 10 clean room in the world, where the James Webb Space Telescope is currently being assembled. Rear Admiral Matthew Klunder and Larry Shuette, Ph.D., who lead the Office of Naval Research, described some of the basic and applied research projects of interest to the Navy. At the Defense Advanced Research Projects Agency (DARPA), the group met with deputy director Steven Walker '87, Ph.D. '97, and Mike Arnone '94, of DARPA Public Affairs.

Dominic Chaloner, associate research professor in the College of Science, also joined the group for several meetings in Washington. "The Science Policy Ethics Seminar visit to Washington D.C., provided Notre Dame students with unparalleled insights about the many issues confronting a variety of government and government related-agencies; specifically how those agencies develop and implement solutions to many of the world's challenges," said Chaloner.

At the Food and Drug Administration (FDA), the group heard from Rear Admiral Sandra Kweder, M.D., deputy director of the Office of New Drugs, and Larry Bauer and Chris Leptak, M.D., Ph.D., from the FDA Rare Diseases program. At the Sabin Vaccine Institute, the group discussed global health and neglected tropical diseases with Emily Conron '13, Neeraj Mistry, and National Institutes of Health (NIH) Bioethicist Sam Garner. The group also spent time at the NIH and the Uniformed Services University of the Health Sciences, led by Captain Phil Coyne '76, M.D., who gave students an overview of the funding landscape for global infectious diseases.

On Capitol Hill, the group met with Congresswoman Jackie Walorski (IN-02), and the Chief of Staff from Congressman Larry Bucshon's Office (IN-08), a member of the House Committee on Science, Space, and Technology. Notre Dame's Office of Federal and Washington Relations, including Vice President John Sturm '69, Leslee Gilbert of Van Scoyoc Associates, and Laura Dean of ScienceWorks, spoke with the students on the role of their office in furthering the interests of Notre Dame in Washington.

"To have been given the opportunity to take advantage of Notre Dame's extensive alumni network and connections in the Washington D.C. area in order to explore both the intricacies of public policy and cutting-edge scientific innovation simultaneously—in addition to a critical analysis through the lens of Catholic Social Teaching—was an unforgettable experience," said sophomore Science-Business major Michael Fliotsos.

The College of Science and the Center for Social Concerns have plans to offer the course annually in the spring semester. The seminar will continue to be student-led and will facilitate the ongoing dialogue on science policy and funding among leaders in Washington and Notre Dame, using the University's most valuable resource—its students.

Ruth M. Hillebrand Center for Compassionate Care in Medicine

LAURA ANDERSON

The education required to produce exceptional healthcare professionals transcends what can be taught in the classroom. Direct interaction with patients is a demand that must be answered with care focused on the need to ease the pain of others, physically and emotionally. As Notre Dame's mission statement emphasizes, the university seeks to educate the heart and the mind. Following this purpose, the Notre Dame College of Science has recently gained an invaluable resource with the introduction of the Ruth M. Hillebrand Center for Compassionate Care in Medicine. The Center for Compassionate Care in Medicine was established in 2004 by Joseph Hillebrand to realize the dream of his sister, Dr. Ruth Hillebrand. A Manhattan-based clinical psychologist who specialized in treating people with eating disorders, Dr. Hillebrand recognized the need to foster a sense of compassion within the health professions. She devoted her life to promoting care, sensitivity, and emotional dedication in medicine after her own terminal diagnosis of mesothelioma was delivered in a blunt and desultory manner by a physician she had met only once before. This experience left Dr. Hillebrand with a strong desire to change the way doctors, nurses, and other health professionals attend to patients.

Since 2011, the center has been under the direction of Professor Dominic Vachon with the objective of "trying to connect the pieces and bring the science of compassion into medical practice." In order to fill this disparity within the education of aspiring healthcare professionals, the Center offers multiple care-focused courses that undergraduate and medical schools may not. Indeed, many medical schools supply "brief, surface level" exposure to effective communication skills and even less emphasis on compassionate care dynamics in patient-physician interactions. Notre Dame graduates who participated in Hillebrand Center classes have remarked that the courses "gave them a solid foundation" in compassionate care, which allowed them to feel "at ease and comfortable" in their new roles and as result, provided time "to focus on honing their skills" in medical school and beyond. Vachon teaches courses designed to expose students to medical counseling skills, hospice and palliative care, as well as the importance of spirituality in healthcare. Programs such as the Pathos Project aim to teach students about patient-centered healthcare and the science of compassion by bringing in guest lecturers from various medical fields and by offering the courses to students from all disciplines, including science, nursing, and business.

The Center for Compassionate Care in Medicine has played an integral role in the planning of many campus events, including lecture series pertaining to relevant medical care as well as events that focus on the sense of spirituality involved in compassionate care. In November 2013, seven Tibetan Buddhist monks from Dehra Dun, India visited Notre Dame to conduct a weeklong presentation on compassion. As part of the week's festivities, the monks constructed a Peace Sand Mandala and gave a talk entitled, "The Power and Practice of Compassion: Taking in Harshness and Giving Out Kindness." The events were overwhelmingly well attended and taught many students, teachers, and faculty about the strength of compassion.

The Center for Compassionate Care in Medicine bridges the gap between the science and the spirituality of healthcare by appealing to the innate senses of empathy and tenderness. It is the goal of the Hillebrand Center to facilitate the constant underlying sense of compassion that proves to be so vital during the trials of the health professions.

Vachon talks to students participating in the program offered through the center.

Notre Dame Reaching for the Stars: Sarah L. Krizmanich Telescope

CHARLEY JANG

On September 9, 2013, the long awaited 0.8-m Sarah L. Krizmanich telescope was installed on the roof of the Jordan Hall of Science. This was a momentous occasion for both the Krizmanich family and the students of Notre Dame. By dedicating the telescope to Sarah, the family was able to immortalize the curiosity and immense passion for learning she possessed. "A telescope is like a time machine. Telescopes allow you to see into the past from the Moon, which is seconds, to a galaxy, which is millions of years. I wanted the family to remember Sarah as it is similar in that telescopes produce memories," said Professor Peter Garnavich of the Department of Physics. The presence of the telescope will serve as a reminder and tool to pursue our childlike curiosity and imagination. With this in mind, the University plans to open the telescope to the public through community outreach events and cooperative observing with local astronomy groups.

Physics Professor Peter Garnavich inside the dome housing the new Sarah L. Krizmanich Telescope

The aperture of the mirror makes it the largest telescope in Indiana, thus providing undergraduates, graduate students, and faculty with the unprecedented opportunity to conduct research quality observations on campus. "The telescope is unique in that it is so large for a University site. Telescopes like these are usually in deserts and mountains," said Professor Peter Garnavich, a professor of astrophysics and cosmology. In fact, several students have already published papers through their observations with significantly smaller telescopes. The Krizmanich telescope will allow students and faculty more freedom to try new methods and techniques in using the telescope and collecting data. It will also be utilized to test new instrumentation being developed by the University's Department of Physics. The overall design of telescopes has remained the same for hundreds of years, but what changes is their instrumentation. Over time, the Department hopes to make the telescope even better. "This guy will reach a magnitude I haven't reached in five years. It is a lot of science waiting," said Professor Garnavich. This new resource, combined with Notre Dame's access to the Large Binocular Telescope (LBT), located in the Pinaleno Mountains of southeastern Arizona, will advance the University's astrophysical research to a dramatically new level.

Currently, minor adjustments are being made to the telescope in order to maximize its capabilities. In the upcoming weeks, a charge-coupled device (CCD), which is a specialized image collector, will be added. Observers will also be able to collect data using certain filter sets, thus isolating specific details of star-forming regions and distant galaxies. This, along with the installment of the appropriate dome aperture wiring, will allow students and faculty to control and observe through the telescope remotely.

"Our number one goal is to get it working for science and ready for research. The first level is undergraduate research, the second level is graduate research, and the third is public outreach as we have already been contacted by many who want to come and see the telescope," said Professor Garnavich.

The telescope was used for the first time on September 18, 2013, when the Department of Physics observed a planetary nebula, which is the cloudy remnants that stars produce when they shed their outer atmosphere. "It looked like the picture. It was so amazing to see it so clearly and bright with my own eyeball," said Professor Garnavich.

As the telescope reaches optimum status, it is important to remember the passion and imagination with which it was dedicated. The history of light collected with its mirror will serve as an illumination into the future, broadening the horizons of the students of Notre Dame.

Undergraduate Research at Notre Dame: The Push to Reach 100 percent

PATRICK DONEGAN

In just 20 years, undergraduate research has gone from an embellishment of one's resumé to a staple for people in any science field. According to the National Science Foundation (NSF), 72 percent of U.S. chemistry majors and 74 percent of environmental science majors have research experience. Increasing demand for qualified scientists to help solve some of the current challenges in such fields as health, energy, and the environment has driven competition among science students to higher and higher levels. But the question still remains: why is undergraduate research so important, and why is Notre Dame striving for 100 percent involvement? "Undergraduate research at Notre Dame gives students an opportunity to be creators of knowledge, not simply absorbers of it, very early in their careers," explained Dean Gregory Crawford, the man spearheading the push toward 100 percent involvement. For those who strive for a career in science, undergraduate research provides real world experience in the techniques and dynamics of a research lab. Undergraduate research will also help students to accurately determine what career path is right for them. Dean Crawford emphasized that for those who major in the sciences but wish to pursue other fields such as business, law or engineering, undergraduate research "provides a challenging experience on the role of research and discovery… it equips you with an approach that is both creative and logically systematic to think through a problem." While in lab, students can learn the values of patience, determination, and passion for their work along with invaluable communication skills acquired from working with fellow researchers and collaborators around the world.

Andrea Rosado, an undergradraduate researcher, in Stepan Chemistry Hall

Notre Dame has made significant progress toward reaching the goal of 100 percent undergraduate research participation in research in only a short period of time. "In the past five years," Dean Crawford said, "undergraduate participation in scientific research has increased from 20 percent of the students to more than 50 percent." One clear cause of this growth is the presidency of Rev. John I. Jenkins, C.S.C., who has spoken often about his goal to make the University of Notre Dame the premier Catholic research university. In less than a decade, he has been integral in the formation of Innovation Park, increasing the funding to major research projects, the construction of the Stinson-Remick Hall of Engineering, and the installation of a particle accelerator, the first to be funded by the National Science Foundation in nearly a quarter century. Changes have also occurred within the College of Science; one can simply look to the very journal you are reading, *Scientia*, as evidence of an increased focus on science and undergraduate research. Even when school is out for summer, students have the freedom to pursue many types of research at facilities around the world thanks to increased funding opportunities. Crawford also explained how the college has established formal and informal connections with other institutions, such as the Cold Spring Harbor Laboratory, Memorial Sloan Kettering Cancer Center, MD Anderson Cancer Center, and many others for summer placement of undergraduates. These are just some of the ways in which the University is carrying out its mission to be a "force for good".

Brian Shannon, an undergraduate researcher, in Harper Hall

Crawford summarized the purpose of undergraduate research perfectly in saying, "I believe that a research focus is important for a science degree. New research is central to what science is—not just information in a textbook or a prescribed laboratory recipe to repeat, but creativity, design, and virtues."

Dinners for Increased Scholarly Engagement

JEFF HANSEN

Becoming lost in a several hundred-person lecture class is easy; you sit in the back, take good notes and do well, but leave the class at the end of the semester unfulfilled. Achieving another "A" on the transcript is great, but how did you grow from the class itself? Several students in the College of Science began Dinners for Increased Scholarly Communication (DISC) in the fall of 2013 to attempt to increase students' intellectual engagement through informal dinners at professors' homes.

Various benefits are derived from these dinners. First and foremost, these dinners allow students to develop a meaningful relationship with a specific professor. This friendship allows for a more conducive environment for class, laboratory, or mentoring conversations. Having shared a meal with a professor in his or her home, asking a question in class, or attending office-hours can help to morph a nerve-wracking experience into a dynamic and enriching conversation, the ultimate seed for optimum learning. Additionally, speaking with professors who have completed schooling and experienced the post-student world allows undergraduates to see beyond traditional uses of a bachelor's degree in science.

Dinners for Increased Scholarly Communication owes much of its success to support from the College of Science. DISC has received generous funding from the College of Science, organizational support from Professor Dom Chaloner, and an appreciative willingness from each professor to open his or her home to students. The success of the program is a testament to the College of Science's readiness to support student ideas and the enthusiasm of professors to interact with undergraduate students.

Benefits from these dinners are already evident. One student who attended a dinner secured a research position shortly after learning the process of approaching a professor with related research interests. Additionally, feedback from both students and professors alike has been extremely positive. One student remarked, "As a freshman, it's sometimes easy to get lost in the shuffle of large lecture classes, so seeing that professors you might be taking classes with in future years are actually great people outside of the classroom as well makes you all the more eager to interact with them in the future." Professors who have hosted these dinners have also been supportive, stating that the dinner gave them the chance to talk to and meet students with whom they normally would not have had a chance to develop a relationship.

DISC was originally spearheaded by Junior biological sciences major Jeff Hansen, and has growth significantly since its inception. Originating in the Department of Biological Sciences, initial dinners were held at the homes of Professors Beth Archie and Jason McLachlan, Professors Patty and Matt Champion, and Professor Jennifer Tank. In 2014, the program's goal is to expand into the remaining departments of the College of Science. Progress towards this expansion has already begun with a dinner held in the Department of Physics hosted by Professor Renate Crawford and Dean Greg Crawford and a dinner in the Department of Chemistry and Biochemistry hosted by Professor Laurie Littlepage and attended by Professor Holly Goodson. DISC hopes that through these dinners, students will become more engaged in an active educational experience thus making the College of Science a dynamic and personable learning environment. Currently working towards this goal with Hansen are fellow students Mark Brahier, Zoe Volenec, Aaron Tarnasky, and Erin Lavin, and the group hopes to expand further. The program welcomes anyone who wishes to help organize future dinners or has new ideas and encourages those interested to contact Jeff Hansen (jhansen5@nd.edu).

The organizers of DISC: Aaron Tarnasky, Erin Lavin, Jeff Hansen, Zoe Volenec, and Mark Brahier

Paper Analytical Devices Identify Falsified Drugs

KATE GIRDHAR

At the University of Notre Dame, research often bridges gaps between communities separated by great distances and disparities. Professor Marya Lieberman's research is one such project interested in applying our resources to make scientific advancements more accessible for others.

In the United States, we often take for granted that the medications our physicians prescribe will be effective. Sometimes, we are even upset when they are less than perfect solutions for our ailments. In many developing nations, these expectations simply cannot be guaranteed. Without the reliability of regulatory agencies to conduct and monitor adverse side effect reporting, the prevalence of low-quality drugs continues to be a worldwide challenge. Hundreds of thousands of people are affected by substandard or falsified medications annually. Medications in prescriptions are replaced with other cheaper ingredients of lesser potency or even those that can cause harm to the patient. In the U.S., falsified drugs are identified primarily among nonessential medications such as internet prescriptions for weight-loss and herbal supplements. In many other countries, such common and vital drugs as acetaminophen, amoxicillin, and ampicillin fall victim to counterfeiting. Antimalarials and drugs fighting tuberculosis are also susceptible, creating dangerous risks for patients in countries where the targeted diseases are prevalent. The means to test drugs for active ingredients requires expensive technological equipment, laboratory space, and personnel, in addition to basic infrastructure to support electricity and temperature control.

In the Department of Chemistry and Biochemistry and in conjunction with Professor Toni Barstis at Saint Mary's College, Professor Lieberman is working to ensure patients have access to high-quality medicine. In order to make detection of low-quality drugs possible in regions without access to extensive laboratory supplies or even electricity, Lieberman and her team invented paper tests, known as Paper Analytical Devices (PADs) that use a version of liquid chromatography to colorfully display the contents of pills. The test cards are small, portable, and cost less than a dollar each. They require little training to use and reveal a series of colored streaks, which indicate the chemical composition of the pill being tested. Lieberman has been working closely with the Moi Teaching and Referral Hospital in Kenya, where the tests have been implemented into their pharmacy program. Pharmacists and even patients themselves have the potential to avoid the negative side effects associated with fake or substandard medication by using PADs. "When you are working in a developing country, it is really, really helpful to visit in person. In fact, I would say you cannot work effectively if you don't meet people face to face. It is so important to have those connections with people, said PRofessor Lieberman about working in Kenya." Her personal experiences in Kenya continue to impact her work and her desire to keep PADs inexpensive, portable, and accessible for regions without laboratory resources.

The test cards are currently in production and use, but more research is ongoing to expand the breadth of possibilities for detecting other drugs. "When we came to designing these tests, my goal was to give people a way to see chemicals. In science, we often learn things when we make an instrument that lets us see things in a different way…. We tried to make a tool that would let people tell one white powder from another white powder. Right now, I think it is at a crude but useable stage," explained Lieberman. Currently, the tests are qualitative, but Lieberman hopes that the team will soon be able to include a quantitative analysis to more effectively address substandard medications in which the active ingredient is present but in insufficient amounts. One such example of this quantification is the lab's current work aimed at determining the amount of iodine in salt. In partnership with St. Mary's College and Professor Barstis, the team is going forward to address a variety of new drug classes and to work in new locations. In addition to their work in Kenya, the program is expanding to address concerns in Nepal. Of the collaborations, Lieberman says, "I think that by combining our interests and our strengths, we can explore what we can do with this platform." The PADs project is already helping to alleviate the risks associated with falsified and substandard drugs and, with ongoing research, will continue to improve patients' and pharmacists' abilities to detect and avoid these medications.

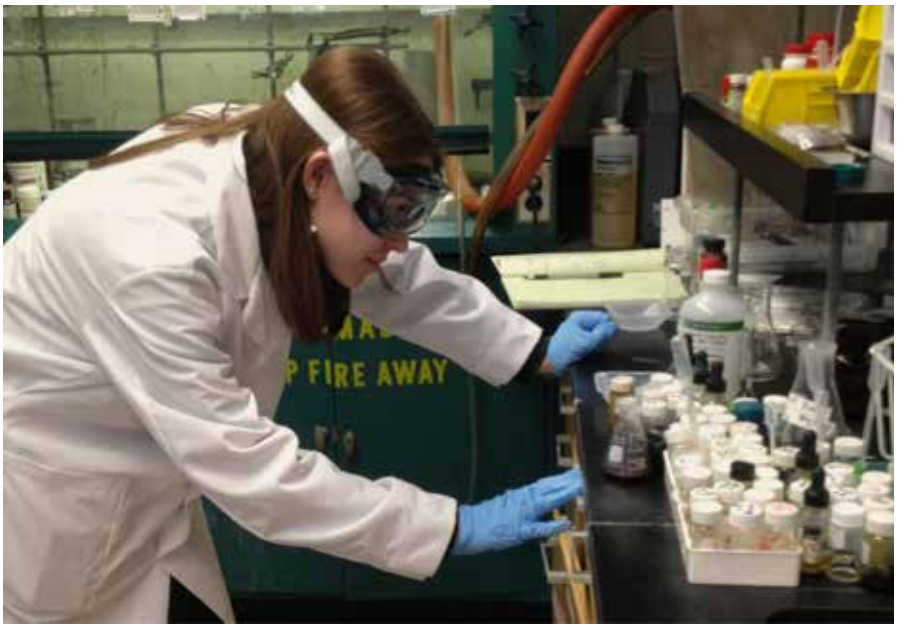

Catherine Ackley analyzes results while working on the PADs project in the Lieberman lab.

DNA Learning Center Expands Notre Dame's Community Presence

MICHAEL DINH

This summer, the College of Science will officially open the DNA Learning Center at Notre Dame. The center is a collaboration with the Cold Spring Harbor Laboratory and will provide services to the community including hands-on laboratory-based learning for students in middle school and high school.

The dedication took place on the morning of Saturday, September 28, 2013, at the center located in 139 Jordan Hall of Science. Remarks were made by Notre Dame and Cold Spring Harbor DNA Learning Center faculty including College of Science Dean Gregory Crawford, Biology Chair Gary Lamberti, and DNA Learning Center Director David Micklos. Highlighting the center's goal of expanding community outreach, artwork inspired by the DNA double helix was proudly created and presented by students from the Robinson Community Learning Center.

The DNA Learning Center began operations in Cold Spring Harbor, New York in 1988 and since then has had astounding success. This center offers faculty training workshops, student lab programs for middle school and high school students, and more. Dr. John Passarelli, a physician in New York and Notre Dame Alumnus, invited Dean Gregory Crawford, Professor Michelle Whaley, and Sean Kassen, Ph.D., to tour the center and meet with the staff of the Cold Spring Harbor Laboratory. Dr. Passarelli also generously donated the funds to start the center at Notre Dame, which includes a partnership with CSHL to access learning materials and staff expertise. Bringing this already established and successful program to Notre Dame is an ideal fit because of the strong Genetics, Genomics, and Molecular Biology research here.

The center plans to engage the South Bend community by partnering with local schools to offer excellent educational activities. Students will also be able to take field trips to the center and attend summer camps. Opportunities at the DNA Learning Center will not be limited to students, and there will also be weekend workshops open to the public. "The center is focused on hands-on and laboratory-based learning, which can be costly and difficult to accomplish during a school day," explained Professor Michelle Whaley, a teaching professor in Genetics and Cell Biology. "It will also provide instruction on the newer aspects of DNA technology such as genomics, bioinformatics, and pharmacogenetics."

The logo for the DNA Learning Center at Notre Dame

The DNA Learning Center will also educate College of Science students. "Undergraduates are going to play a key role," said Professor Whaley. "It is envisioned that they will be hired or volunteer as teachers in the center. It's especially good for people that want to go into education, but even for other students, it's valuable to learn communication skills for working with non-scientists. I can see this helping someone going into medicine because this is an integral skill when communicating with patients."

Yet another advantage of the program is its director, who is expected to be hired to start in the summer of 2014. "The Biology department will now have a faculty member whose primary responsibility is science education for middle school, high school, and college students," said Professor Whaley. "The director will also help develop curriculum for college lab courses or research projects." Camps for high school students will begin in summer 2014, with classroom visits and laboratory field trips beginning in fall 2014.

According to Professor Gary Lamberti, "We are excited to have the DNA Learning Center as part of our learning portfolio. The center complements our undergraduate and graduate curricula by bringing the wonders of the 'gene age' to local schools, and providing our own students with the opportunity to inspire the next generation of scientists."

The DNA Learning Center at Notre Dame is a collaboration between the College of Science, the Department of Biological Sciences, and the Cold Spring Harbor Laboratory that will provide access to genetics education to the entire Michiana community. This outward expansion will certainly benefit all parties involved for years to come.

College of Science Dean Greg Crawford with Dr. and Mrs. John Passarelli

Interactive Effects Between Ascorbic Acid and Glyceryl Trinitrate on Purine Metabolism in C2C12 Skeletal Muscle Cells Revealed by Untargeted Metabolomics

EUNICE LEE[1]
Advisor: Jan F. Stevens[2]
[1]*University of Notre Dame, Department of Biological Sciences*
[2]*University Oregon State University, College of Pharmacy*

Abstract

To unravel the biochemical pathways altered by the effects of ascorbic acid (AscH) and glyceryl trinitrate (GTN), metabolomics profiling of cell extracts from mouse skeletal muscle C2C12 cells were conducted using high resolution and high mass accuracy QToF-LC-MS/MS. Untargeted metabolomics analysis revealed significant differences in hypoxanthine, ADP and GMP levels between control and treated cells. The findings indicate that ascorbic acid supplementation suppresses the (hypo) xanthine/xanthine oxidase (X/XO) system, thereby decreasing cellular levels of oxidative stress. Without ascorbate supplementation, hypoxanthine levels were 40% lower in the GTN-treated cells, suggesting that GTN activates the X/XO system because hypoxanthine is an XO substrate. Ascorbic acid supplementation increased the intracellular levels of hypoxanthine 6-fold, even in the presence of GTN. Taken together, the findings suggest that ascorbic acid supplementation prevents GTN-mediated activation of the X/XO system, which could argue in favor of ascorbic acid supplementation to prevent XO-induced tolerance to GTN treatment in patients suffering from angina pectoris.

Introduction

Glyceryl trinitrate (GTN) has been used to treat angina pectoris, acute myocardial infarction, hypertension, and other cardiovascular diseases due to its vasodilatory effects caused by the release of nitric oxide (NO). However, studies suggest that patients on prolonged treatment of GTN may develop nitrate tolerance (1-4). Ascorbic acid (AscH) is an antioxidant that is predicted to prevent nitrate tolerance by scavenging free radicals and superoxides and/or preventing inactivation of aldehyde dehydrogenase, which is the enzyme that catalyzes bioactivation of GTN. Currently, the underlying mechanisms are not fully understood, but the present metabolomics study in mouse C2C12 skeletal muscle cells, which cannot synthesize AscH (5), may help understand the metabolic pathway, including the mechanisms of nitrate tolerance, and the protective effects of AscH. In a previous study, vitamin C deficiency was found to activate the purine nucleotide cycle (PNC) in zebrafish (6). The objective of this study was to determine how GTN affects cellular metabolism and whether ascorbic acid supplementation modifies the metabolic effects of GTN.

Materials and Methods

Cell Culture

Mouse skeletal muscle cells, designated C2C12 (American Type Culture Collection catalog number CRL-1772, Manassas, Virginia), were initially cultivated in 75 cm^2 flask using Dulbecco's Modified Eagle Medium (DMEM, Life Technologies catalog number 11995065, Grand Island, New York). After reaching 90% confluence, the cells were subcultured in 96-well plates for cell viability assay using MTT or in 6-well plates for treatment with GTN or AscH.

The C2C12 cells grown in the 75 cm^2 flask were washed twice with Hank's Balanced Salt Solution (HBSS) and trypsinized by adding 4 mL of 0.25% trypsin-0.53 mM EDTA. After a 5 minute incubation at 37ºC in a 5% CO_2, the cells were pipetted up and down to disperse the cells and then DMEM medium with 10% FBS was added to inactivate the trypsin. The cells were counted using a hemacytometer before plating in 96-well or 6-well plates.

Subculturing C2C12 cells to determine effects of GTN and AscH on viability using the MTT assay

A cell viability assay using MTT was chosen to examine the cytotoxicity of GTN and AscH in C2C12 cells. Viable cells were distinguished from non-viable cells by the ability of NAD(P)H-dependent cellular oxidoreductase enzymes to reduce MTT (3-(4,5-dimethylthiazol-2-yl)-2,5-diphenyltetrazolium bromide, a yellow tetrazolium dye, to a purple-color formazan. At 90% confluence, the C2C12 cells, seeded in 96-well plates, were treated with increasing concentrations of GTN (0, 1, 5, 10 and 25 µM) and AscH (0.1, 0.5, 1 and mM), either alone or in combination. After 24 hours incubation, the culture medium from each well were aspirated and 0.2 mL of complete DMEM with 0.5 mg of MTT per mL was added to each well. The cells were incubated for another 3 hours and then the MTT medium was aspirated. A volume of 0.15 mL of acidified isopropanol (isopropanol with 0.04 M HCl) was added to each well. Blank wells contained acidified isopropanol with no cells. The plates were shaken for 10 minutes at room temperature. The absorbance of the plates was read at 570 nm normalized to 650 nm.

Subculturing C2C12 cells to determine effects of GTN and AscH on the metabolome

A 2 x 2 factorial design was chosen to examine the role of GTN and AscH on the metabolome or small-molecule metabolite profiles of C2C12 cells. Thus, the cells seeded in 6-well plates were divided into 4 treatment groups: Group 1, control (vehicle); Group 2, AscH (0.5 mM); Group 3, GTN (10 µM); and Group 4 (10 µM GTN + 0.5 mM AscH). In treating Groups 2 and 4 with AscH, a stock solution of 5 mM sodium ascorbate (Sigma Chemical Company, St. Louis, Missouri) was first prepared in complete DMEM medium and filter sterilized before adding to the culture medium to reach a final concentration of 0.5 mM in a total volume of 3 mL/well. Group 4 was pre-incubated with 0.5 mM AscH for 30 minutes before the addition of 10 µM GTN. GTN was supplied as a stock solution of 1 mg/mL in acetonitrile from Cerilliant Corporation

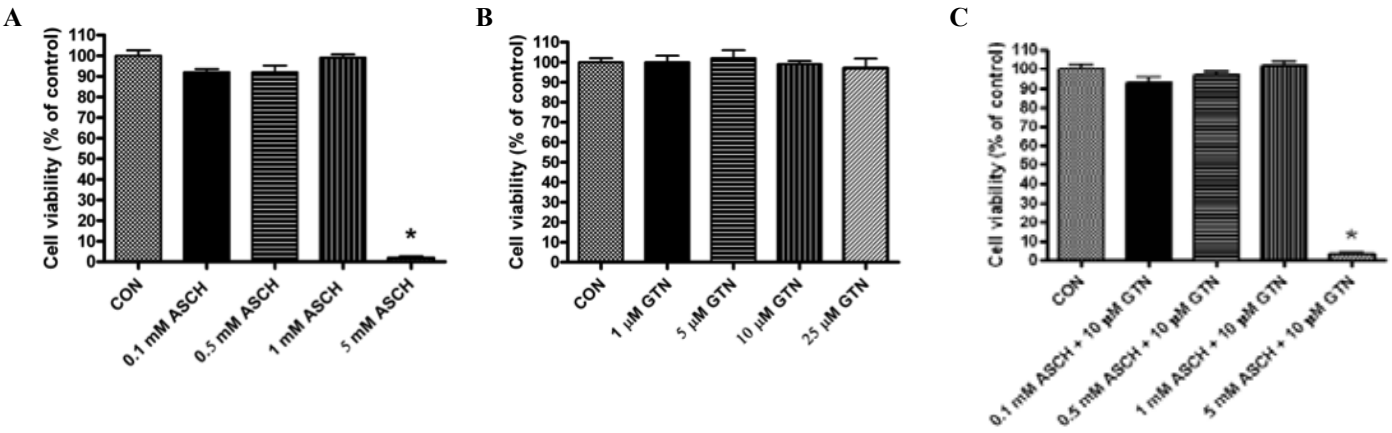

Figure 1. C2C12 cell viability determined by MTT Assay. Cells were treated with various concentrations of AscH and GTN for 24 hours before MTT assay determined cell viability. At 0.1, 0.5, and 1 mM, AscH was not toxic to cells, but was toxic at 5 mM (A). At 1, 5, 10, 25 μM, GTN was not toxic to cells (B). Combinations of AscH and 10 μM GTN were not toxic to cells except at 5mM AscH and 10 μM GTN (C).

(Round Rock, Texas). Group 1 (vehicle control) was treated with acetonitrile alone to a final concentration of 10 μM. After treatment, the cells were incubated for 24 hours at 37ºC and then the test media were aspirated, the wells washed with HBSS and 0.4 mL of 100% ethanol:methanol (1:1) was added to each well. The cells were scraped using a cell scraper and the cell suspension was transferred to 1.5-mL microcentrifuge tubes. The wells were rinsed with 0.2 mL of the ethanol:methanol mixture which was transferred to the corresponding 1.5-mL tubes. The tubes were vortexed for 30 seconds and then centrifuged at 13,000 rpm for 10 minutes in a microcentrifuge at 4ºC. The resulting supernatant was transferred to glass vials for analysis by mass spectrometry.

LC-MS/MS analysis

LC-MS/MS based metabolomics was performed on a Shimadzu Nexera system with a phenyl-3 stationary phase column (Inertsil Phenyl-3, 4.6 x 150 mm) coupled to a quadrupole time-of-flight (QToF) mass spectrometer (AB SCIEX, Triple ToF 5600) operated in information dependent MS/MS acquisition mode. A gradient solution at a flow rate of 400 μL/minute was applied with a mobile phase consisting of A: water and B: methanol containing 0.1% formic acid in each solvent. The elution gradient was as follows: 0 minutes, 5% B; 1 minute, 5% B; 11 minutes, 30% B; 23 minutes, 100% B; 35 minutes, 100% B; 37 minutes, 5% B; and 49 minutes, 5% B. The column temperature was held at 50ºC, and the injection volume was 10 μL.

Data Processing, Statistical Analyses, and Metabolites Identification

Statistical analysis was performed using GraphPad Prism software to determine significance by a one-way analysis of variance. Raw LC-MS/MS data files were initially imported using MarkerView (AB SCIEX) for data processing, including feature detection, peak alignment, peak integration, principal component analysis (PCA), and discriminant analysis (DA). The PCA-DA plot provided a visual distribution of the features and degree of discrimination among the sample groups. Using MarkerView, metabolites with the smallest p-values and largest fold changes were selected and plotted on a volcano plot to aid in identification of metabolites of interest. Following data processing and statistical analysis, metabolites of interests that were significantly different between the sample groups were initially identified by database searches using METLIN and Human Metabolome Database (HMDB) utilizing experimental mass measurements. Characterization of the metabolite was confirmed using MS and MS/MS spectra matching, retention time, experimental m/z values, and isotopic distribution.

Results

Effects of AscH and GTN on cell viability of C2C12 skeletal muscle cells

Cells were treated with various concentrations of AscH and GTN for a period of 24 hours. Cell viability was determined by the MTT assay conducted at different concentrations of only AscH, only GTN, and a combination of both. At 0.1, 0.5, and 1 mM, AscH was not toxic to cells, but was toxic at 5 mM (Fig. 1A). GTN was not toxic at 1, 5, 10 or 25 μM (Fig. 1B). Combinations of 10 μM GTN and various concentrations of AscH (0.1, 0.5, 1, and 5 mM AscH) did not cause toxicity to the cells except at a combination of 5 mM AscH and 10 μM GTN (Fig. 1C).

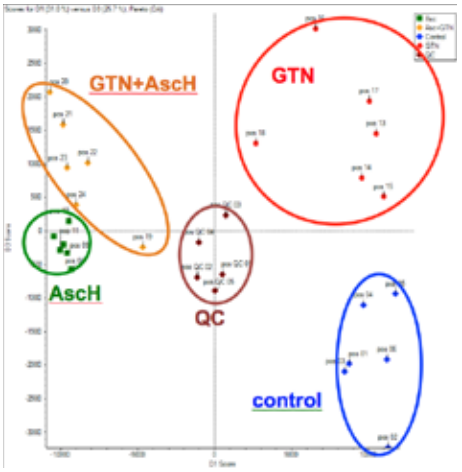

Figure 2. PCA-DA scores plot of control AscH treated with or without co-treatment with GTN (n=6). Analysis is on the basis of the polar features detected by LC-QToF mass spectrometry in the positive ion mode. QC: quality control sample analyzed five times; Control: cells neither treated with AscH nor GTN.

Discovery of Differentiating Metabolites and Identification

Principal Components Analysis coupled with Discriminant Analysis (PCA-DA) of the metabolomics dataset revealed significant differences in the polar metabolic profiles of the control and AscH with treated or untreated with GTN (Fig. 2). The control and AscH groups separated, demonstrating that AscH treatment had some effect on the metabolome of these groups. The PCA-DA plot also shows relatively tighter grouping from repeat injections of the pooled quality control sample, demonstrating instrument and system variance to be much lower than biological variance in these two groups.

Detection of untargeted metabolites with significant differences in sample groups

Metabolites of interest with small p-values from a Student's t test were plotted against large fold changes, as depicted in a volcano plot (Fig. 3) calculated by MarkerView, and were characterized using MS and MS/MS matching on METLIN, LIPID MAPS and HMDB online metabolite databases. Adenosine monophosphate (AMP) with m/z 346.1 and hypoxanthine with m/z 135.0 were detected as untargeted metabolites of interest with significant differences between the control (Fig. 3, group A) and the group treated with 500 µM of AscH (Fig. 3, group B). Differences between the two sample groups confirmed significance of the metabolites of interest. Following confirmation of significance, metabolite identification was conducted using high-resolution MS, MS/MS fragmentation, and isotopic distribution, and standard retention times. Extracted ion chromatograms (XICs) of AMP and hypoxanthine were obtained individually from the summed intensity across the entire range of masses detected in the total ion chromatogram (TICs). Identification of analytes of interests was confirmed through comparison of peaks at standard retention times (Fig. 4).

Effects of AscH and GTN on purine nucelotide metabolites in C2C12 cells

Exposure of AscH (0.5 mM) to mouse skeletal muscle cells with or without co-treatment with GTN (10 µM) caused a significant decrease in overall levels of metabolites from the purine nucleotide cycle (PNC), except for hypoxanthine. Treatment with AscH caused a marked decrease AMP and ADP (**p<0.005) and GMP (*p<0.05), but a significant increase in hypoxanthine (***p<0.00005; Fig.5, B). Individual analysis of hypoxanthine (Fig. 5, A) revealed that treatment with AscH increased levels of hypoxanthine with or without treatment with GTN.

Discussion and Conclusion

In our previous studies, AscH deficiency was discovered to activate the PNC in zebrafish (6). Without external AscH, C2C12 skeletal muscle cells operate under energy stress. Under oxidative stress, levels of purine metabolites, i.e., guanine, AMP, ADP, and GMP, were elevated presumably due to increased ATP and GTP turnover. Ascorbic acid supplementation caused a 6-fold increase in the cellular levels of hypoxanthine. We attribute this increase to suppression of the (hypo) xanthine/xanthine oxidase (X/XO) system by ascorbic acid, which would lead to reduced consumption of the XO

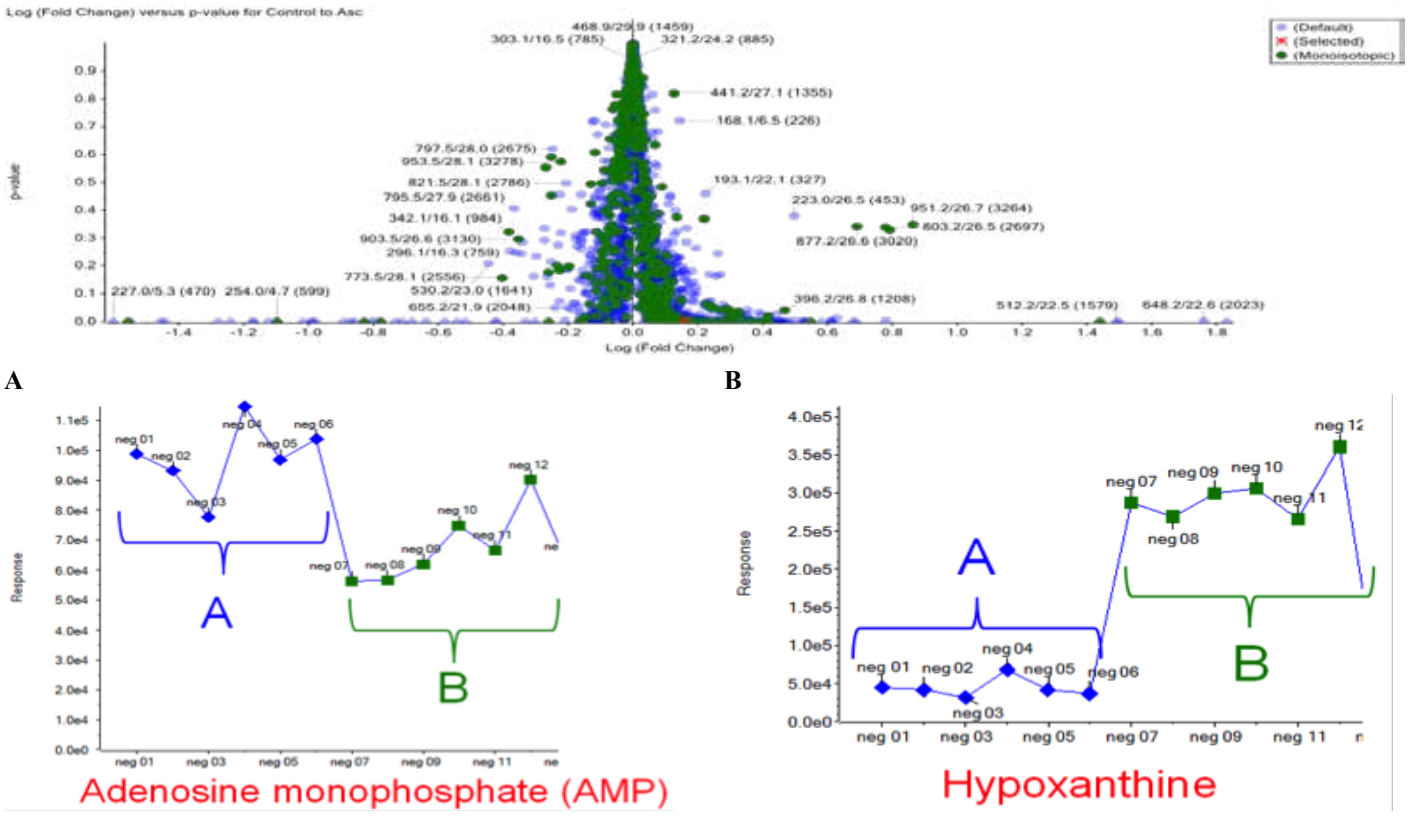

Figure 3. Detection of differentiating metabolites, AMP and hypoxanthine, by t-testing. The volcano plot (top figure) of p-value vs. log 10 (fold change) combines the fold change in the response of a variable between groups with the probability (p-value). The profile plot (bottom figure) shows relative levels of AMP and hypoxanthine in cells from group A (control) and group B (treated with 500 µM AscH).

substrate, hypoxanthine. A previous study showed that under anaerobic conditions, ascorbic acid activates XO, triggering significant nitric oxide generation from the organic nitrate, isosorbide dinitrate (7). Evidence from the previous study and this particular experiment suggests that ascorbic acid may play a role in the X/XO pathway.

In the ascorbate-deficient cells, GTN treatment caused a 40% decrease in the levels of hypoxanthine, which suggests that GTN activates the X/XO system. GTN treatment did not decrease but increase hypoxanthine levels in the ascorbate supplemented cells. This finding indicates that adequate intracellular levels of ascorbate prevent GTN-mediated activation of the X/XO system. The small increase of hypoxanthine in the cells co-treated with ascorbate and GTN can be explained by competition of hypoxanthine with GTN for XO, because GTN has also been identified as an XO substrate (7).

Taken together, our findings could bear relevance to the development of tolerance to GTN therapy. The X/XO system, activated by GTN, produces superoxide in addition to nitric oxide when GTN is the substrate. Both XO products, superoxide and nitric oxide, react with each other to form peroxynitrite (8), thereby further increasing oxidative stress and decreasing the formation of the vasodilatory GTN metabolite, nitric oxide. The untargeted metabolomics data point to an important role for the X/XO system in GTN therapy and revealed a possible mechanism by which ascorbate may increase nitric oxide production from GTN and prevent tolerance to nitrate therapy. These hypotheses will need to be substantiated by measuring the effects of GTN and ascorbate on XO expression and activity.

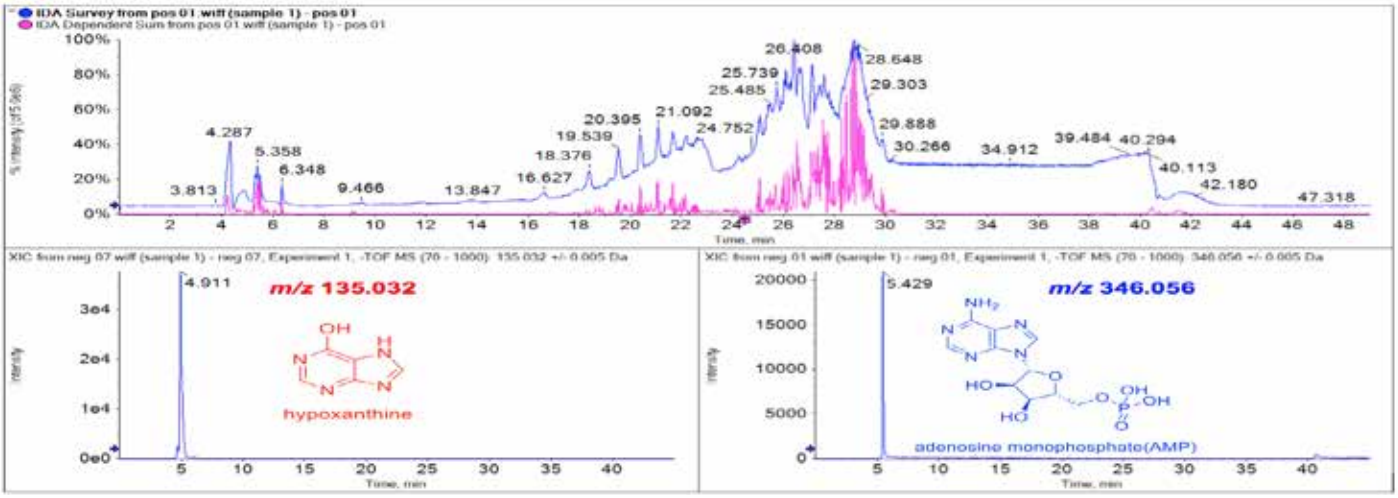

Figure 4. Total ion chromatogram (TICs) and Extracted ion chromatograms (XICs) of a selection m/z 135.032 and 346.056. Identification of the metabolites was confirmed by metabolite retention time and exact mass comparison with standards. The chromatogram intensity across the entire range of masses is seen in TIC (top). Specific m/z values representing hypoxanthine and AMP seen in the XICs (bottom) were extracted from the TIC.

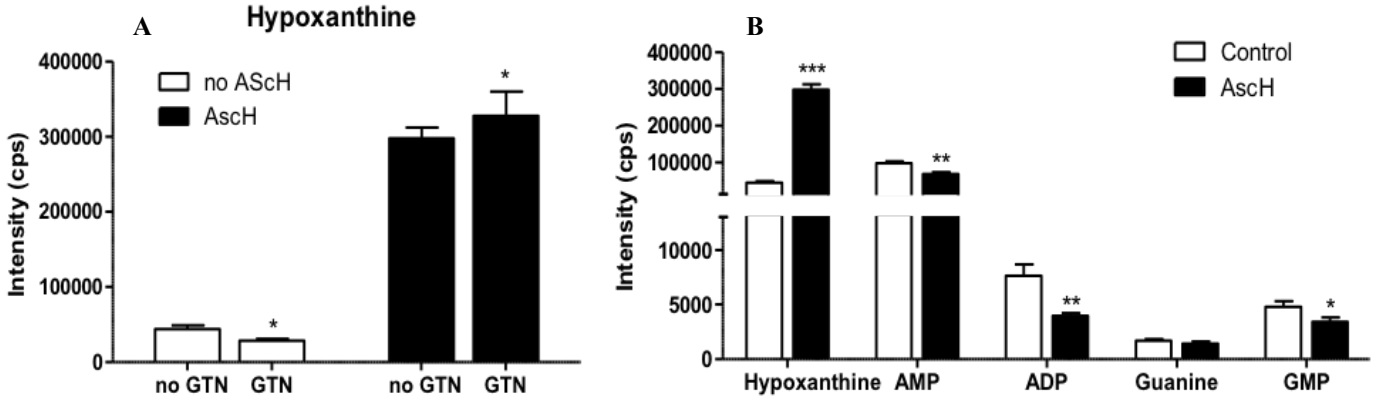

Figure 5. Measurement of purine nucleotide metabolites in C2C12 cells treated with or without AscH, GTN. After treatment of C2C12 cells with or without AscH, GTN, the means ± S.D. denoted by the error bars were calculated using the relative levels of hypoxanthine and purine nucleotide cycle metabolites from the profile plots. In the panel displaying the measurement of purine nucleotide cycle (Fig.5, B), most metabolites, including hypoxanthine, AMP, ADP, and GMP, differ significantly when treated with AscH. In the panel displaying specifically the measurements of hypoxanthine (Fig. 5, sA), treatment with AscH with or without GTN is significant. *p<0.05, **p<0.005, and ***p<0.00005

Acknowledgments

I would like to thank Jan F. Stevens, Jaewoo Choi, and Cristobal L. Miranda for their mentoring and support throughout the project and the First Year of Studies and the College of Science at the University of Notre Dame, Oregon State University College of Pharmacy (PHR007 PSFS), and NIH grant P30ES000210 for the funding of this project.

References

1. E. Bassenge, B. Fink. Naunyn Schmiedebergs *Arch. Pharmacol*. 353, 363-367 (1996).

2. E. Bassenge, N. Fink, M. Skatchkov, B. Fink. *J. Clin. Invest.* 102, 67-71 (1998).

3. H. Watanabe, M. Kakihana, S. Ohtsuka and Y. Sugishita. *Circulation.* 97, 886-891 (1998a).

4. H. Watanabe, M. Kakihana, S. Ohtsuka. and Y. Sugishita. *J. Am. Coll. Cardiol.* 31, 1323-1329 (1998b).

5. I. Savini, M.V. Catani, G. Duranti, et al. *Free Radic. Biol. Med.* 38, 898-907 (2005).

6. J.S. Kirkwood, K.M. Lebold, C.L. Miranda, C.L Wright, G.W. Miller, R.L. Tanguay, C.L. Barton, M.G. Traber, J.F. Stevens. *J Biol. Chem.* 287, 3833-3841 (2012).

7. H. Li, H. Cui, X. Liu, J.L. Zweier. *J. Biol. Chem.* 280, 16594-600 (2005).

8. R.E. Huie, S. Padmaja. *Free Radic. Res. Commun.* 18, 195–199 (1993).

About the Author

Eunice Lee is a sophomore at the University of Notre Dame, currently pursuing a major in biological sciences with a Korean minor. She spent the summer of her freshman year researching the effect of ascorbic acid and glyceryl trinitrate on C2C12 skeletal muscle cells at the Linus Pauling Institute at Oregon State University. She will return this upcoming summer to continue her work in researching the underlying mechanisms and the beneficial effects of ascorbic acid. She is passionate about researching to determine the role of essential micronutrients in extending healthy lifespan and preventing debilitating diseases. After her time at Notre Dame, she will pursue an M.D. degree.

TAG-320 Functions as a Brake on the Unfolded Protein Response in *Caenorhabditis elegans*

REBECCA NOBLE[1]
Advisors: Yair Argon[2], Marni Falk[2,3]
[1]*University of Notre Dame, Department of Biological Sciences*
[2]*University of Pennsylvania, Perelman School of Medicine*
[3]*Children's Hospital of Philadelphia*

Abstract

When the level of unfolded or misfolded proteins in a cell exceeds the folding capacity of the endoplasmic reticulum, a process called the unfolded protein response (UPR) is triggered. Part of this process involves the splicing of the xbp-1 mRNA transcript and its translation into a protein that serves as a transcription factor for UPR target genes, including those encoding many chaperones. Though UPR is necessary for proper cell function, prolonged UPR can cause cell death. PDIA6, a protein disulfide isomerase found in humans, regulates the response by attenuating UPR. This study investigates TAG-320, a protein found in Caenorhabditis elegans *(*C. elegans*) hypothesized to serve the same function as PDIA6. An assay was developed to quantify the level of xbp-1 mRNA splicing in order to measure the effect of TAG-320 down regulation. Results showed that xbp-1 mRNA splicing increases from the basal level when tag-320 expression is suppressed, suggesting that TAG-320 is an ortholog of PDIA6. If confirmed, these results will allow the use of* C. elegans *as a model organism for studying the modulation of UPR signaling. This could have great implications for diseases, such as diabetes and cancer, as well as numerous neurodegenerative diseases, for which excessive UPR has been identified in the pathology.*

Introduction

Proper protein function requires protein folding into a specific conformation, termed the native state. When proteins are not folded properly in the endoplasmic reticulum (ER), a stress pathway called the unfolded protein response (UPR) is triggered (Fig. 1). The primary cellular responses to an imbalance of misfolded/unfolded proteins and ER protein folding capacity involve decreasing the influx of proteins into the ER or increasing the ER's folding capacity. However, if neither of these responses is successful at reestablishing homeostasis, then the cell will undergo apoptosis (1) (Fig. 1).

Though UPR is traditionally considered a stress response, research has demonstrated that UPR is constitutively active in some cells as an integral part of eukaryotic development and metabolism. In particular, UPR appears to play an important role in specialized secretory cells such as plasma cells, pancreatic β cells, hepatocytes, and osteoblasts, which are under greater demand to translate, fold, and secrete large amounts of proteins (2).

Three main branches of UPR have been identified. Each is defined by a transmembrane protein signal transducer found in the ER membrane: inositol-requiring protein 1 (IRE1), activating transcription factor 6 (ATF6), and protein kinase RNA ER kinase (PERK) (3). A simple metazoan, *Caenorhabditis elegans* (*C. elegans*) has been found to contain counterparts to these three mammalian transducers (4). In this model organism, the most significant UPR regulation occurs through IRE1 pathway (2). Studies have shown that IRE1 is necessary for larval development in the model organism, and if both IRE1 and PERK are knocked out, the worm will arrest development before reaching the third larval stage (L3) (4).

The IRE1 signaling pathway in humans (Fig. 2) is initiated when the transmembrane IRE1 protein senses unfolded or misfolded proteins. In response, the protein oligomerizes in the membrane and trans-autophosphorylates. This phosphorylation activates the IRE1's endoribonuclease domain which specifically splices x box protein 1 (xbp-1) mRNA. An enzyme ligates the exons to produce a spliced mRNA transcript, and both the spliced (xbp-1s) and unspliced (xbp-1u) mRNAs are translated into proteins. The protein encoded by the unspliced mRNA is an inhibitor of UPR signaling, but the protein encoded by the spliced mRNA is stable and activates UPR target genes, including those encoding chaperones which will increase the protein folding capacity of the ER (3). Studies have revealed that the pathway in *C. elegans* is analogous with a few differences, one being that the proteins encoded by the spliced transcript and the unspliced transcript both act as effective transcription factors for UPR proteins in worms (5).

A recent study shows that Protein Disulfide Isomerase A6 (PDIA6) acts as a regulator of the IRE1 pathway in mammals. The data suggest that PDIA6 acts to suppress UPR, decreasing the amount of splicing activity (Fig. 2). When the gene encoding PDIA6 is knocked down prolonged UPR is observed, eventually leading to cell death. Conversely, when PDIA6 is overexpressed, mimicking the pattern seen in chemically-induced UPR, the duration of signaling is decreased (6). An ortholog to pdia-6, known as tag-320, has been predicted by bioinformatics analysis (6, 7) and was shown to be genetically important

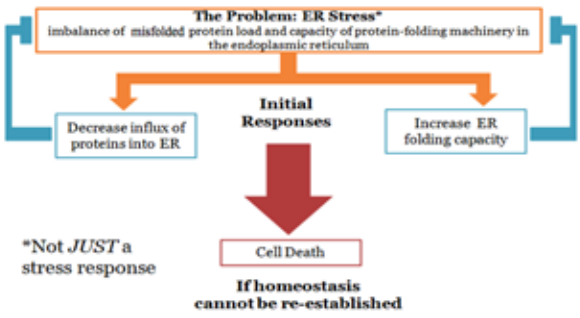

Figure 1. Unfolded Protein Response (UPR). When there is an excess of unfolded or misfolded proteins in a cell, UPR is initiated. If neither of the initial responses is sufficient to alleviate the stress, the cell signals for its death. While this process is generally considered in the context of cell stress, UPR is also an important part of normal development and metabolism. Adapted from Walter et al., 2011.

for UPR through the use of a UPR fluorescence reporter in *C. elegans* depleted of tag-320 (6).

The goal of this investigation was to develop a PCR assay to quantify xbp-1 mRNA splicing in *C. elegans*. If xbp-1 splicing is increased when tag-320 is knocked down, then it will support the notion that TAG-320 in *C. elegans* functions to suppress UPR.

Methods

All RNA extraction was carried out using L3 stage *C. elegans* from the 7.2 strain under various RNAi conditions: control RNAi, ire-1 RNAi, and tag-320. The 7.2 strain was made by Y. Argon and contains a GFP driven by the worm hsp4 reporter. In addition, the strain contains the mutation rrf-3, which makes the worm hypersensitive to RNAi silencing of gene expression. Other worm strains were obtained from the *C. elegans* genetics center (Minneapolis, MN).

RNAi Treatment

ire-1 and tag-320 RNAi bacteria were each streaked on separate LB plates treated with tetracycline (20µg/mL). These bacteria were picked and grown 6-12 hours in LB + 50 µg/mL ampicillin at 37°C. Once a dense culture was obtained, 100 µL were spread on small NGM plates with 25µg/mL ampicillin and 25mM IPTG. Plates were dried and induced overnight at room temperature. Worms were then grown on these plates at 20°C (8).

RNA Isolation

Worms were washed from OP50, ire-1 RNAi, and tag-320 RNAi plates, respectively. They were then homogenized and digested using Trizol (Ambion, Austin, TX) and a tissue grinder (Kontes Pellet Pestle Cordless Motor, Fischer Scientific, Hampton, NH) (9). Additionally, the worms were subjected to a freeze (-80°C)/thaw (37°C) cycle and vortexed until entirely dissolved in solution. The RNA was then isolated with chloroform and precipitated with isopropanol. Glycogen was used as carrier to maximize efficiency. Finally the RNA pellet was washed with 70% ethanol and quantified using spectrophotometry (NanoDrop) (10). Total isolated RNA was DNase-treated with the TURBO DNA-free kit (Ambion, Austin, TX) per standard protocol. Following treatment, the concentration and purity of the RNA sample were assessed by NanoDrop (9).

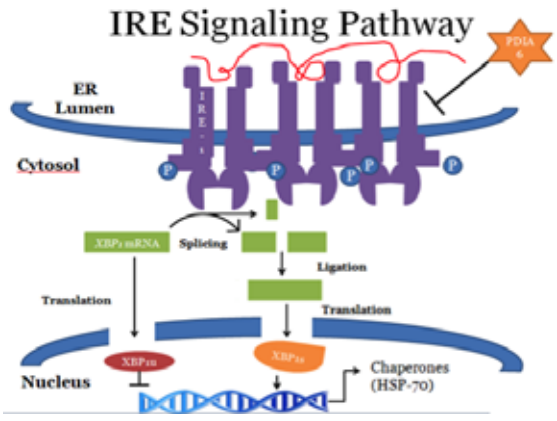

Figure 2. IRE Signaling Pathway The IRE signaling pathway is triggered by unfolded or misfolded proteins in the ER lumen. These proteins activate the transmembrane IRE proteins which contain an endoribonuclease responsible for xbp-1 mRNA splicing. The spliced transcript activates UPR target genes which encode proteins that increase ER folding capacity to alleviate cell stress. PDIA6 acts to attenuate this response. Adapted from Walter et al., 2007.

RT-PCR

cDNA was reverse transcribed from isolated DNase-treated RNA using the High Capacity cDNA Reverse Transcription Kit (Applied Biosystems, Foster City, CA) per standard protocol. The reaction was incubated at 25°C for 10 minutes, 37°C for 2 hours, and 85°C for 5 minutes (9).

PCR

To target the desired region of the cDNA for amplification, the ceXBP1_Fw ((Tm 56.8C) AGAAGTCGTCGGTGAGGTTG) and the ceXBP1_Rv ((Tm 53.6) CGATCCATGTGGTTGCATAG) primers were used, and the reaction was run through a thermocycler for 37 cycles. The first cycle was run for 3 minutes at 94°C to denature the genomic DNA. The next 35 cycles consisted of three steps: denaturation for 10 seconds at 94°C, annealing for 30 seconds at 52°C, and extension for 30 seconds at 20°C. The 37th cycle was a final extension cycle that ran for 7 minutes at 72°C. The PCR product was then run at 115V for 60 minutes on a 2% agarose gel with 0.5X TBE running buffer, using a 1kB DNA ladder (Promega, Madison WI) (9).

Results

To quantify the extent of IRE1-mediated UPR in *C. elegans* under various conditions, a PCR assay was developed to quantify xbp-1 mRNA splicing. Upon gel electrophoresis, xbp-1u mRNA was expected to produce a 231bp band and xbp-1s was expected to produce a 208bp band. RNA extracted from the control *C. elegans* population of worms grown on OP-50 plates produced two bands upon gel electrophoresis of PCR products: a strong band at 231bp and a weaker band at 208bp. When TAG-320 expression was knocked down, by exposure to tag-320 RNAi, the 208bp band intensity increased considerably (Fig. 3). When IRE1 expression was knocked down in worms, by exposure to ire-1 RNAi, only the 231bp band was produced (Fig. 3). In other experiments, knockdown of pdi-1, a gene from the same family as tag-320 did not increase xbp-1s above the basal level (data not shown).

Discussion

Previous studies had identified tag-320 as an ortholog of pdia-6, a human gene that encodes a known protein disulfide isomerase that functions as a brake on UPR (7). However, the function of tag-320 had yet to be investigated; it was unknown whether the worm protein played any role in redox signaling. The results of this paper suggest that tag-320 is indeed involved in UPR and support the hypothesis that TAG-320 functions in *C. elegans*, as the mammalian PDIA6 does, to suppress UPR. In addition to activating the UPR GFP reporter (Fig. 7 in ref. 6), knockdown of tag-320 promotes xbp-1 splicing, the signature activity of IRE1. This suggests that TAG-320 normally attenuates xbp-1mRNA splicing in *C. elegans*.

The persistent presence of xbp-1s at low levels suggests some constitutive xbp-1 splicing events. This is consistent with the presence of *C. elegans* UPR during development (4, 5, 11). Since worm preparations were not rigorously synchronized, the presence of larvae undergoing physiological UPR could account for this observation.

These results may be extended in several respects. First, the extent of RNAi knockdown needs to be quantified by a PCR assay that measures the level of tag-320 pre- and post- RNAi treatment. The level of splicing is then expected to correlate to the extent of tag-320 depletion. Second, quantification must be completed to compare the degree of increased splicing in the 7.2 strain to the maximal possible splicing. For this purpose, the effects of tunicamycin, a drug that causes ER stress, as well as other treatments that induce UPR will need to be compared to the tag-320 RNAi. Third, the xbp-1 mRNA splicing profile of RNAi of other genes should be compared with that of tag-320 RNAi. Multiple human protein disulfide isomerase orthologs have been identified in *C. elegans*, and comparing the splicing activity in knockout assays will establish the essentiality of TAG-320 in regulating UPR events (12). Fourth, if RNAi treatments demonstrate that the worm PERK homologue does not alter the xbp1 splicing, the evidence for TAG-320's role specifically on the IRE1 branch will be strengthened. Finally, a test of the worms in the L3 larval stage could be used to characterize the level of indigenous IRE1 signaling (4).

If further results confirm the role of TAG-320 as a repressor of UPR, then *C. elegans* can be used as a model organism to study pathways involving the human protein PDIA6. There are several disease pathologies in which UPR is implicated. Many genetic diseases are caused by mutations that disrupt proper protein folding and activate UPR, and excessive UPR ultimately leads to cell death (13). For example, in Type-II diabetes, prolonged UPR impairs insulin synthesis and causes apoptosis of pancreatic beta cells (14). Similarly, in neurodegenerative diseases such as Alzheimer's and Parkinson's, UPR activation in response to accumulation of abnormal protein aggregates ultimately leads to cell death (13). In cancer, on the other hand, UPR activated by hypoxia in solid tumors has antiapoptotic functions, leading to malignancy (13).

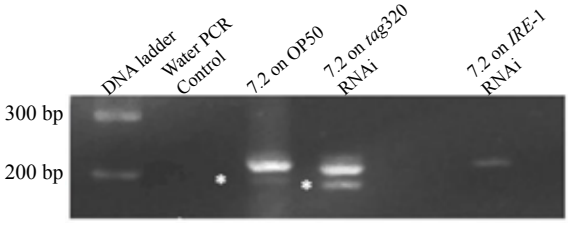

Figure 3. xbp-1 mRNA Splicing: An ethidium bromide stained agarose gel showing DNA fragments produced by PCR amplification of xbp-1u and xbp-1s mRNA from *C. elegans*. Lane one contains a 1KB plus DNA ladder (Promega); the 200bp and 300bp bands fragments are labeled. The UPR condition is indicated above each lane. For the negative control, sterile distilled water was used instead of template cDNA. The heavier band corresponds with 231bp xbp-1u mRNA and is present in all 3 UPR conditions. The lighter band (denoted by asterisk) corresponds with 208bp xbp-1s mRNA and is only present in control worms and tag-320 RNAi worms.

In each of these cases, therapies that attenuate UPR could be beneficial. Thus, gaining a better understanding of PDIA6 will be very important, and having identified tag-320 as an ortholog in *C. elegans* will facilitate further investigation.

Acknowledgments

I would like to acknowledge Yair Argon, Ph.D. and Dr. Marni Falk at the University of Pennsylvania and Children's Hospital of Philadelphia for their mentorship and guidance throughout the summer of 2013. I would also like to acknowledge the other members of the Argon Lab and Falk Lab for sharing their knowledge and expertise. Thank you to the Hesburgh Yusko Scholars Program for funding this summer research experience.

References

1. P. Walter, D. Ron. *Science*. 334, 1081-1086 (2011).

2. J. Wu, R.J. Kaufman. *Cell Death Differ*. 13, 374-384 (2006).

3. D. Ron, P. Walter. *Nature*. 8, 519-529 (2007).

4. X. Shen, R.E. Ellis, K. Lee, et al. *Cell*. 107, 893-903 (2001).

5. X Shen, R.E. Ellis, K. Skaki, et al. *PLoS Genetics*. 1.3, 355-368 (2005).

6. D. Eletto, D. Eletto, D. Dersh, et al. *Mol Cell*. 53, 562-576 (2014).

7. A.D. Johnston, P.R. Ebert. *J Toxicol*. 2012: 20 pages. (2012).

8. Worm base website. http://wormbase.org. Release WS240. (2014).

9. E. Polyak, Z. Zheng, and M. Falk. *Method Mol Cell Biol*. 837, 241-255 (2012).

10. V. Prahlad and M. Falk, personal communication

11. F. Urano, M. Calfon, T. Yoneda, et al. *J Cell Biol*. 158.4, 639-646 (2002)

12. A.D. Winter, G. McCormack, A.P. Page. *Dev Biol.* 15.308, 449-461 (2007).

13. R. Kaufman. *J Clin Invest.*110.10, 1389-1398 (2002).

14. M. Cnop, F. Foufelle, and L. Velloso. *Trends Mol Med*. 18.1, 59-68 (2012).

About the Author

Rebecca Noble is a junior Biological Sciences major with a minor in the Glynn Family Honors Program. She spent the summer after her sophomore year researching the unfolded protein response at the University of Pennsylvania and Children's Hospital of Philadelphia and will return this summer to continue her project. She has a passion for pediatric medicine and, following her graduation from Notre Dame, plans to pursue an M.D. degree. On campus, she is studying pediatrics from a different perspective, investigating how parenting styles impact children's moral development and physical well-being. She is committed to a holistic approach to medicine, recognizing that biological and social factors both play important roles in determining overall health.

The Effect of Dissolved Organic Carbon on the Diel Vertical and Horizontal Migration of Zooplankton

JULIA HART[1]
Advisor: Patrick Kelly[1]
[1]*University of Notre Dame, Department of Biological Sciences*

Abstract

Increased browning of global freshwater ecosystems, a result of increased dissolved organic carbon (DOC), can significantly alter both the biotic and abiotic characteristics of aquatic systems. Most prominent among abiotic changes is a darkening, or browning, of the water color. Research has shown that water color affects the diel migration patterns of freshwater zooplankton, an integral part of freshwater food webs and trophic interactions. While much is known about the diel vertical migration (DVM) patterns of zooplankton, little research has been done about diel horizontal migration (DHM) in freshwater systems. This study investigated how increased DOC affects both diel vertical and diel horizontal migration in north temperate lakes. Zooplankton were sampled for abundance across both vertical and horizontal transects in three lakes of various DOC levels. As water color increased across three lakes, diel migration, both vertical and horizontal, generally decreased. With darker water color, zooplankton are provided refuge from visual predators, allowing them to remain in the food- and oxygen-rich epilimnion or distribute across the entire surface of the lake at any time of day.

Introduction

There has been a steady increase in the amount of dissolved organic carbon (DOC) in freshwater lakes over the last few decades (1). Potential drivers of this phenomenon include increased carbon dioxide emissions, increased nitrate deposition, decreased sulfur deposition, changing land use, and climate change (1). An increase in DOC in a freshwater lake can significantly darken the water color while also altering other physical and chemical properties (2). For example, increased DOC attenuates UV radiation (3), impedes lake primary production, and decreases the depth of a stratified lake's thermocline which makes the epilimnion both shallower and warmer (4). Research has shown that the structure and functioning of lakes is tightly coupled to the terrestrial environment (3), and the exchange of materials between aquatic and terrestrial habitats is more ubiquitous than previously thought (5). Therefore, allochthonous carbon, originating from outside of the aquatic system, plays an important role in aquatic ecosystems.

Zooplankton are crucial to freshwater pelagic food webs and are thought to be good indicators of trophic state and ecological quality in lakes (6). As primary consumers, zooplankton reside in the center of many freshwater food webs. While feeding on phytoplankton, zooplankton are commonly consumed by many planktivorous fish and invertebrate species (7). It has been shown that DOC explains more variance in zooplankton community structure than other variables such as changes in pH, the presence or absence of predators, or chlorophyll levels (3). By attenuating light and darkening water color, DOC may provide zooplankton with a natural refuge from predators, especially visual predators like fish. Allochthonous resources, such as DOC, can also provide an additional food resource for zooplankton, albeit not a preferable one (8).

During the day, zooplankton exhibit diel vertical migration (DVM) to avoid visual predation in the lighted epilimnion of lakes (9). Sinking to the colder and oxygen-depleted hypolimnion during the day, zooplankton will return to the epilimnion at night to feed on phytoplankton under the cover of darkness (7). Recent research has shown that zooplankton are also capable of diel horizontal migration (DHM), migrating to the littoral zone of lakes during the day to avoid predators and returning to the pelagic epilimnion to feed at night. A study conducted by Burks et al. (2002) argues that DHM should be favored when macrophyte abundance is high and planktivore abundance is low. Diel horizontal migration might allow zooplankton to make use of alternate littoral zone resources (10).

This study examines both diel vertical and horizontal migration of freshwater zooplankton across a gradient of dissolved organic carbon in lakes. The purpose of this experiment is to determine how water clarity impacts zooplankton DVM and DHM. It was hypothesized that as DOC concentrations increase, zooplankton will be less inclined to migrate from the pelagic epilimnion. Both vertical and horizontal migration will decrease as a result of decreased predation in the pelagic zone.

Methods and Materials

Study Sites

Lakes were chosen for study based on previously recorded DOC concentrations spanning a gradient of water color. Bay Lake, Long Lake, and Hummingbird Lake were chosen as low (approximately 6 mg/L), medium (approximately 8 mg/L), and high (approximately 23 mg/L) DOC lakes, respectively. All lakes are located at the University of Notre Dame Environmental Research Center (UNDERC) in Land O' Lakes, WI.

Sampling and Processing

Two horizontal transects were randomly chosen on each lake. Sampling took place along four locations at each transect: shore 1, open water 2, open water 3 (both evenly spaced along the transect), and shore 2 at all lakes except Hummingbird Lake. The second horizontal transect on Hummingbird Lake had only one open water sampling site due to the short diameter of the lake. At each shore, one sample was collected in the littoral zone of the lake. Along the open water stops, three samples were taken: a shallow (~3m), a medium (~5m), and a deep (~7m) sample, representative of the stratified layers of the lake. All samples were collected using a zooplankton tow net.

To account for diel migration, samples were collected during the day and at night, approximately twelve hours apart. Day sampling began between 11 AM and 12 PM, and night sam-

pling between 11 PM and 12 AM. Each lake was sampled three times over a six-week period in June and July. Sampling start times extended later in the summer to account for the later sunset. All samples were preserved in 70% ethanol upon collection and brought back to the lab for identification. Zooplankton were counted and identified to order in the case of copepods, and genus for *Daphnia*, *Holopedium*, and *Bosmina* spp.

Statistical Analysis

Data were analyzed according to the type of migration pattern: vertical or horizontal. To analyze diel vertical migration, samples at each open water location were pooled according to depth, resulting in a shallow, a medium, and a deep zooplankton abundance per transect per time of day. A one-way ANOVA, followed by a Tukey's Multiple Comparison Test (MCT) if significant, was used to determine if zooplankton abundance was significantly different at each depth. A repeated measures ANOVA was used to determine if the sampling point in the summer was a significant factor between the three sampling episodes.

To analyze diel horizontal migration, all shore and shallow samples for each transect were analyzed together. This provided the most accurate comparison for horizontal movement along the entire transect. Again, a one way ANOVA with a subsequent Tukey's MCT was used to determine if zooplankton abundance differed across the surface of the lake. It is important to note that each sampling episode could be considered a true replicate, however, since they did not happen concurrently. A repeated measures ANOVA was used to determine if sampling time in the summer was a significant factor in zooplankton migration. All statistical analyses were performed with R statistical software (10).

Results

Diel Vertical Migration

Zooplankton in Bay Lake, the lightest lake, exhibited standard diel vertical migration patterns. In both transects, zooplankton were most abundant in the hypolimnion, or the deep sample, during the day, and in the epilimnion, or the shallow sample at night (Fig. 1). There was no significant difference in the abundance of zooplankton at each depth on either transect (p=0.221, p=0.504, p=0.246, and p=0.667). Repeated measures ANOVA was significant on both transects during the day (p=0.0026 and p=0.0113).

Zooplankton in Long Lake, the medium lake, showed little signs of any diel vertical migration. Regardless of the time of day, zooplankton across both transects were found mainly at the surface (Fig. 2). There was no significant difference in the abundance of zooplankton at each depth on either transect at either time of day (p=0.462, p=0.149, p=0.265, and p=0.499). Repeated measures ANOVA revealed that sampling point in the summer was a significant factor during the day in transect 1 (p=0.0195).

Zooplankton in Hummingbird Lake, the darkest lake, also showed little evidence of diel vertical migration. Similar to Long Lake, the highest abundance of zooplankton, regardless of the time of day, was found in the epilimnion (Fig. 3). A one-way ANOVA revealed that zooplankton abundance in the epilimnion was significantly higher than the hypolimnion on transect 1 at night (p=0.0499). There were no other significant differences in

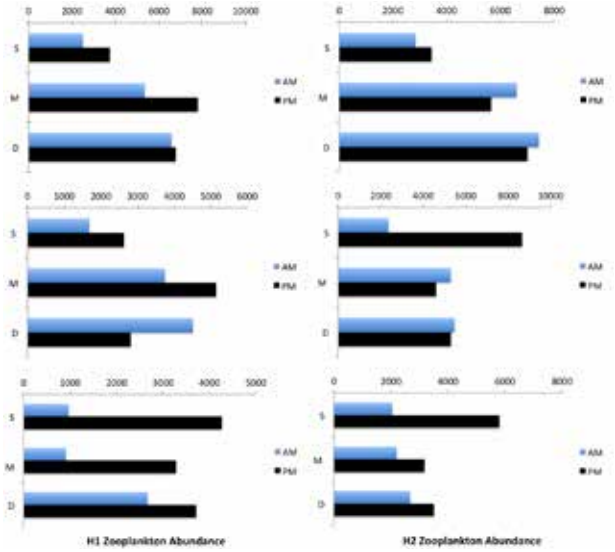

Figure 1. Diel Vertical Migration in Bay Lake (light).

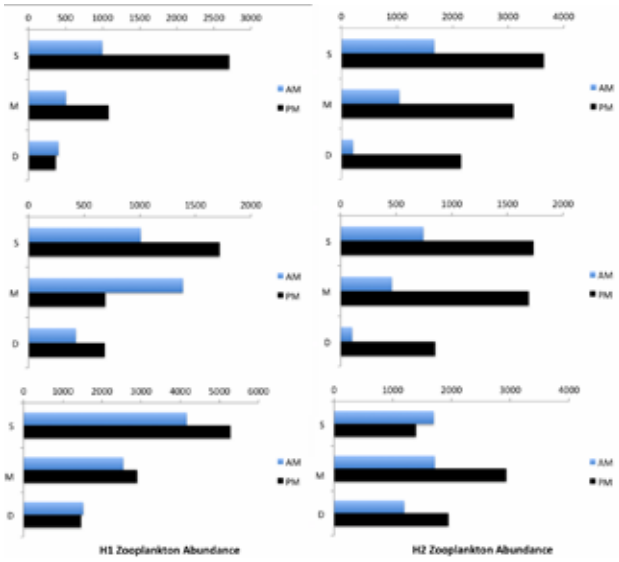

Figure 2. Diel Vertical Migration in Long Lake (medium).

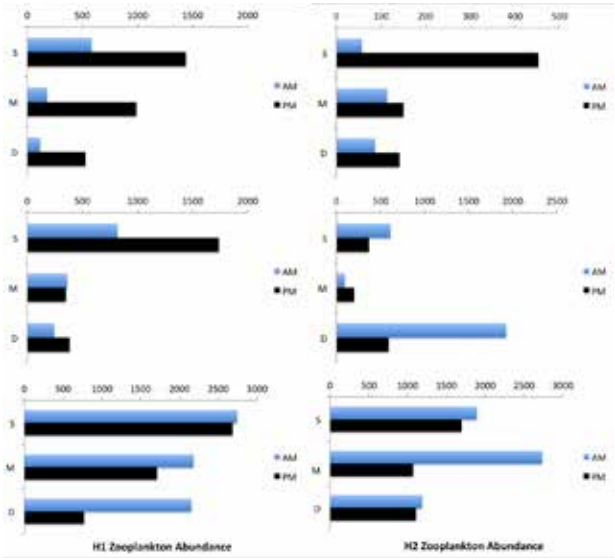

Figure 3. Diel Vertical Migration in Hummingbird Lake (dark).

the abundance of zooplankton at each depth (p=0.739, p=0.975, and p=0.759). Sampling point in the summer was a significant factor for transect 1 during the day (p=0.0054) and transect 2 both day and night (p=0.0318 and p=0.0090, respectively).

Diel Horizontal Migration

Zooplankton abundance on the shores was low in Bay Lake during the day, but increased at night, suggesting some diel horizontal migration to the littoral zone of the lake (Fig. 4). Zooplankton abundance was significantly greater in the shallow open water than shore 1 on transect 2 during the day (p=0.0337). All other abundances across the surface of the lake were not significantly different (p=0.0624, p=0.678, and p=0.481). Repeated measures ANOVA revealed that sampling point in the summer was only significant on transect 2 during the day (p=0.0395).

Zooplankton on Long Lake were fairly evenly distributed across the surface of the lake during the day on both transects (Fig. 5). At night, more zooplankton were found in the littoral zone, evidence of diel horizontal migration; however, there was no significant difference in zooplankton abundance across the surface of the lake on either transect at either time of day (p=0.548, p=0.0856, p=0.362, and p=0.842). Sampling point in the summer was not significant for either transect at either time of day (p=0.1976, p=0.1767, p=0.486, and p=0.0602).

Similarly, zooplankton abundance on Hummingbird Lake was evenly distributed across the surface during the day along both transects (i.e. no significant difference in horizontal distribution). Higher zooplankton abundance along the shores at night suggests diel horizontal migration (Fig. 6). There was no significant difference in zooplankton abundance across the surface of the lake on either transect at either time of day (p=0.754, p=0.385, p=0.934, and p=0.72). Sampling point in the summer was a significant factor for migration pattern on transect 1 during the day (p=0.0353) and on transect 2 for both day and night (p=0.0038 and p=0.0176, respectively).

Discussion

Diel vertical migration and diel horizontal migration patterns were reduced with increased DOC, supporting the hypothesis that as DOC concentrations increase, zooplankton will be less inclined to migrate from the pelagic epilimnion.

The DVM results in Bay Lake seem to reflect standard migration patterns. Zooplankton migrate to the hypolimnion during the day to escape fish predation and return to the epilimnion at night to feed. The light color of this lake combined with a substantial fish population and predation pressure in Bay Lake likely drives this process. The high DOC concentration of Hummingbird Lake, conversely, may provide a refuge for zooplankton in the epilimnion during the day. High zooplankton abundances are found at the surface during the day because it is not necessary for zooplankton to migrate during the day to avoid visual predators. Diel vertical migration in Long Lake appears most similar to that of Hummingbird Lake. It appears that water color provides zooplankton with enough cover that migration from the surface during the day is not necessary. Low fish populations in Long Lake could also be contributing to this phenomenon; risk of predation is lower in this lake to begin with. Overall, there was a trend of decrease in DVM

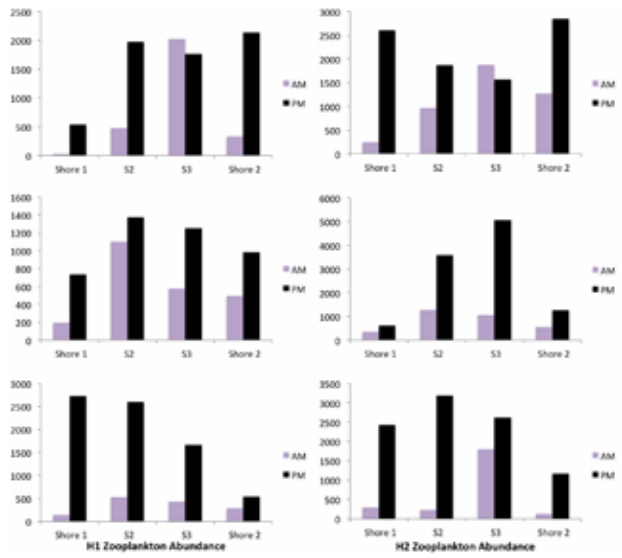

Figure 4. Diel Horizontal Migration in Bay Lake (light).

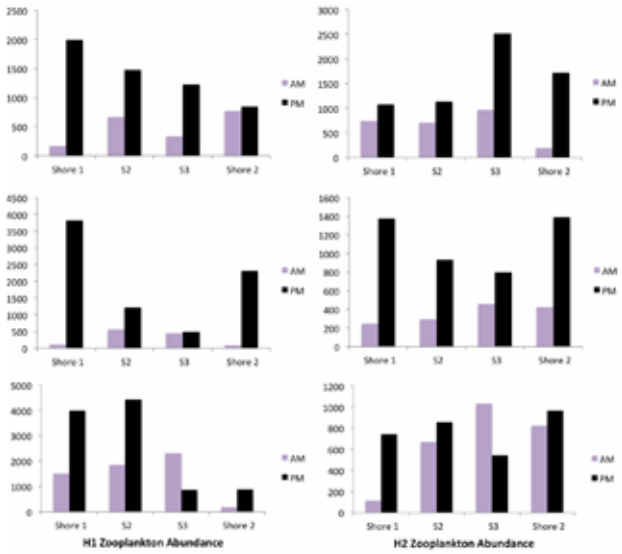

Figure 5. Diel Horizontal Migration in Long Lake (medium).

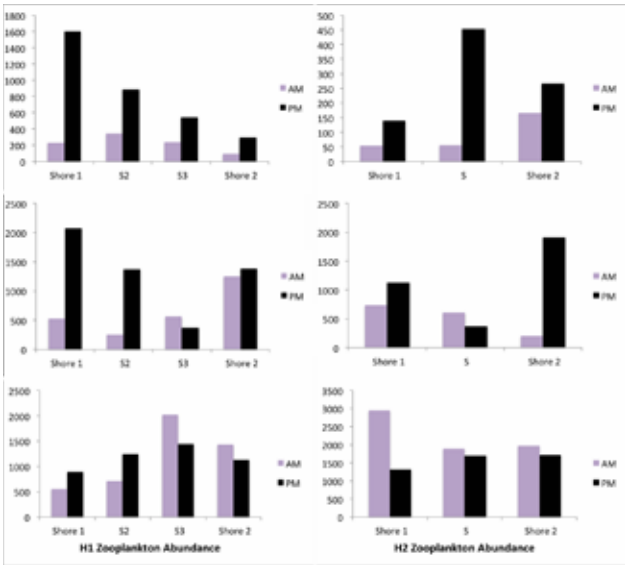

Figure 6. Diel Horizontal Migration in Hummingbird Lake (dark).

as DOC concentrations increased, implying that zooplankton are less likely to migrate from the food- and oxygen-rich epilimnion in darker lakes.

Zooplankton in the darker lakes, Long Lake and Hummingbird Lake, did not show significant diel horizontal migration compared to those in the lighter lake. During the day, the shores at Bay Lake showed low zooplankton abundance, but high abundances at night. This suggests that only under the cover of darkness will the zooplankton take advantage of the food resources found in the littoral zone of this lake. During the day, there is little refuge from visual predators in this area. In contrast, zooplankton in Hummingbird Lake are just as likely to be found in the littoral zone as the epilimnion during the day. The dark color of the water provides sufficient refuge across the entire surface of the lake. Across both transects, zooplankton abundance at the shores increased at night. Once again, migration in Long Lake most closely mirrored that of Hummingbird Lake. Though fairly evenly distributed across the surface during the day, there are much higher abundances found at the shores at night, even more so than Hummingbird Lake. This suggests that the water color of Long Lake does provide some refuge for zooplankton during the day, for the zooplankton are not afraid to remain at the surface or shores. But higher abundances at the shores at night suggests that the threat of fish predation is still a possibility. Overall, DHM decreased across the three lakes as DOC concentrations increased.

If the water color really does provide an ideal refuge, there should be no difference between the abundances in the littoral zone during the day and at night. These results, however, consistently show higher abundances at night, suggesting that zooplankton migrate to the shores only at night. It is difficult to conclude that purely horizontal migration is occurring at night, however. Zooplankton could be migrating from all points in the lake to the littoral zone. Tracking these migrations patterns would be very difficult with a small study organism.

These results are also the reverse of that suggested by previous research. Burks et al. (2002) predicted that if DHM was occurring, zooplankton abundance would be highest in the littoral zone during the day. They hypothesized that the zooplankton would use the macrophyte vegetation in the littoral zone as shelter from predators during the day and return to the pelagic epilimnion to feed at night. This pattern was not observed on any of the study lakes. Instead, zooplankton appeared to migrate to the littoral zone at night, indicative of some desirable quality of the littoral zone. This trend could be explained by the highly variable macrophyte densities on each transect as well. Burks et al. suggest that food resources might differ in quality in the pelagic epilimnion versus the littoral zone. The results might indicate a higher quality of food resources in the littoral zone since zooplankton make a point to migrate to the shores at night, regardless of DOC concentration.

The use of a repeated measures ANOVA indicates when and where the sampling point in the summer was a significant factor in determining the differences between sampling episodes. Where this factor was significant, conditions in the lake were changing over the course of the summer such that zooplankton migration also changed. As a result, one can see temporal changes in diel vertical and horizontal migration of zooplankton. These changes could be due to any number of factors, biotic or abiotic. For example, lakes could be increasing in DOC concentration over the course of the season. Climatic events and watershed changes could influence how much terrestrial carbon leaches into an aquatic system, leading to a constant flux of dissolved organic carbon (12).

Where the repeated measures ANOVA was not significant, the three sampling episodes could be used as replicates since conditions in the lake at those three times were not significantly different. Regardless, averaging abundances together provided a more complete look at the migration patterns along a specific transect. In most cases, however, transects were only significantly different at one point in the summer or at one time of day. To analyze diel migration patterns, both times of day would have to be significant to give an accurate representation of migration patterns.

In addition to water color, food web structures can also have an effect on the diel migration patterns of zooplankton. A study conducted by Loose and Dawidowicz (1994) found that above a threshold concentration, zooplankton migration increased as fish kairomone levels also increased. The presence or absence of predators such as planktivorous fish or aquatic invertebrates like *Chaoborus* spp. can determine to what degree zooplankton migration occurs. *Chaoborus* spp., more commonly known as the phantom midge larvae, live in the sediment of lakes and feed upon zooplankton. In this study, Bay Lake has high fish density, but low *Chaoborus* density. Long Lake has low planktivore density, but high *Chaoborus* density. Hummingbird Lake has high fish density and high *Chaoborus* density. Variation in predation pressure likely drives the direction and timing of migration (i.e. standard DVM, reverse DVM, or no DVM) rather than the magnitude of migration, which is predicted to be mediated more by water color (3).

In summary, diel vertical migration appeared to decrease as DOC concentrations increased across three lakes: Bay Lake, Long Lake, and Hummingbird Lake. While zooplankton in the light lake exhibited normal DVM, those in the dark lake rarely migrated from the surface. Diel horizontal migration also decreased as DOC increased. Bay Lake, the light lake, had low zooplankton abundance at the shores during the day, but higher abundances at night. Long Lake, the medium lake, and Hummingbird Lake, the dark lake, had relatively high zooplankton abundance in the littoral zone at both day and night.

Most studies of freshwater zooplankton migration focus on a strictly vertical profile of a lake by sampling at one part of the lake and identifying the zooplankton at various depths. Few studies have been specifically designed with the intent of sampling the horizontal distribution of zooplankton. Combining both vertical and horizontal distribution profiles might provide the most accurate profile of a lake's zooplankton population.

In the future, it would be interesting to replicate this experiment across a much larger gradient of dissolved organic carbon. Future studies could also isolate the drivers of these migration patterns. Perhaps food resources such as pelagic phytoplankton versus littoral phytoplankton are nutritionally different, providing more of an incentive for zooplankton to migrate to the shores. Variance in macrophyte abundance along the shores could also influence these migration patterns. Repeating this

experiment in situ, controlling for planktivore densities, could also improve the interpretation of these results.

As global browning of freshwater ecosystems continues to rise, zooplankton migration patterns stand to change. The more that is understood about diel migration of zooplankton now, the better we will understand the changes this phenomenon might inflict upon this process in the future.

Acknowledgments

First, I would like to thank my mentor, Patrick Kelly, for his help in experimental design, statistical analyses, and editing. Thank you also to the Jones Laboratory for allowing me to use their sampling equipment. Many thanks to my classmates Amarilis Silva Rodriguez, Michael Spear, Patrick Roden-Reynolds, Erin Hanratty, Cayla Bendel, and Michael Kipp for sampling assistance. Thank you to Gary Belovsky, Ph.D., Michael Cramer, Ph.D., Robert McKee, Claire Mattison, and Larissa Herrera. Finally, none of this would have been possible without the financial support of the Bernard J. Hank Family Endowment.

About the Author

Julia Hart is a junior at the University of Notre Dame currently pursuing a degree in environmental science. In the summer of 2013, she participated in the undergraduate program at the University of Notre Dame Environmental Research Center (UNDERC) in Land O' Lakes, Wisc. Her research interests include the effects of anthropological disturbance on aquatic ecosystems, with particular emphasis on aquatic conservation. On campus, she studies the effects of climate change in the Copper River Delta, Alaska with Gary Professor Lamberti. Upon graduation, she hopes to pursue a Ph.D. in aquatic ecology.

References

1. D.T. Monteith, J.L. Stoddard, C.D. Evans et al. *Nature* 450, 537-540 (2007).

2. J. Houser. *Can J Fish Aquat Sci.* 63, 2447-2455 (2006).

3. C.E. Williamson, O.G. Olson, S.E. Lott et al. *Limnol Oceanog*. 82, 1748-1760 (2001).

4. S. Sobek, L.J. Tranvik, Y.T. Prairie et al. *Limnol Oceanog*. 52, 1208-1219 (2007).

5. G.A. Polis, W.B. Anderson, R.D. Holt. *Annu Rev Ecol Syst* 28, 289-316 (1997).

6. E. Jeppesen, P. Noges, T.A. Davidson et al. *Hydrobiologia* 676, 279-297 (2011).

7. W. Lampert. *Funct Ecol.* 3, 21-27 (1989).

8. M.T. Brett, M.J. Kainz, S.J. Taipale, H. Seshan. *P Natl Acad Sci USA*. 106, 21197-21201 (2009).

9. S. Dodson. *Limnol Oceanog.* 33, 1431-1439 (1988).

10. R Core Team. *R Foundation for Statistical Computing*. ISBN 3-900051-07-0.

11. R.L. Burks, D.M. Lodge, E. Jeppesen, T.L. Lauridsen. *Freshwater Biol.* 47, 343-365 (2002).

12. M.L. Pace, J.J. Cole. *Limnol Oceanog.* 47, 333-342 (2002).

13. C.J. Loose, P. Dawidowicz. *Ecology* 75,- 2255-2263 (1994).

Microhabitat Choice as a Function of Ectoparasitism: Basking Behavior of *Chrysemys picta bellii* in the Presence of *Placobdella* Species

JULIA KRUEP[1]
Advisor: Michael J. Cramer[1]
[1]*University of Notre Dame, Department of Biological Sciences*

Abstract

The "desiccating leech" hypothesis proposes that differences in ectoparasite load between basking and bottom-dwelling freshwater turtle species occur because leeches abandon hosts that spend lengthy periods of time basking out of water and exposed to the sun. However, recent research has put this hypothesis under scrutiny, instead suggesting that leeches have simply evolved to avoid certain turtle species entirely based on the more favorable host environment provided by bottom-dwelling turtles. In order to examine the validity of the "desiccating leech" hypothesis from the standpoint of host behavior, the influence of Placobdella *spp. leeches on the basking habits of Western painted turtles (*Chrysemys picta bellii*) was investigated through a series of 3-day basking trials. If basking were to directly cause leeches to detach, one would expect turtles in the presence of leeches to spend more time out of water in an effort to remove or avoid parasitic individuals. Turtles were randomly assigned to three different treatment tanks: control,* Placobdella *spp., or* Macrobdella decora *(inert organism control). Results of an ANOVA indicated that no significant differences in basking behavior between treatments were observed over the course of the study. Baseline ectoparasite load for each turtle was also taken into consideration. Results of a linear regression analysis complemented the comparison across treatments; no significant relationship existed between baseline ectoparasite load and basking habits. These results support the idea that* Placobdella *spp. have instead evolved to selectively parasitize bottom-dwelling turtle species, regardless of individual basking behaviors.*

Introduction

Basking is a commonly observed behavior in a variety of freshwater turtle species. While basking serves the primary purpose of thermoregulation in ectothermic turtles (1-3), it may also have secondary benefits. Basking is not only important in the maintenance of body temperature within a functional range, it is also thought to facilitate increases in metabolic and digestive rates (4-7) and promote follicular egg development in females (3, 8-10). In addition, basking may be an integral component of skin and shell maintenance by aiding in the periodic shedding of carapacial scutes (1, 11-13).

Of interest to this study is the idea that frequent basking also promotes a reduction in parasite load, known as the "desiccating leech" hypothesis. A variety of North American freshwater turtle species harbor ectoparasites in the form of leeches, most notably the leech species *Placobdella parasitica* and *P. ornata* (14-16). The "desiccating leech" hypothesis proposes that turtles with a greater propensity to bask will have a lower leech prevalence due to lengthy periods of time out of water and exposure to the sun, forcing aquatic leeches to abandon their current host (1, 11, 13, 16-19). It has been shown that ectoparasite load is significantly greater in bottom-dwelling turtle species such as the snapping turtle (*Chelydra serpentina*) as compared to basking species such as the painted turtle (*Chrysemys picta*) (16, 18, 20, 21).

However, there is significant doubt to whether this hypothesis is the true explanation for differences in leech load observed between turtle species with contrasting microhabitat choices. MacCulloch (1981) reported no significant difference in leech load between turtles caught while basking and turtles caught in the water, although the "desiccating leech" hypothesis would predict that turtles caught in the water would harbor more leeches. Another study also noted a high leech prevalence in a *C. Serpentina* population that had an unusual tendency to bask (13).

Ryan and Lambert (2005) conducted a colonization experiment in which turtles of both a basking species (map turtles, *Graptemys geographica*) and a bottom-dwelling species (musk turtles, *Sternotherus odoratus*) were collected, cleaned of leeches, and placed in a common tank containing leeches but no basking sites. Initial data on leech prevalence was collected on the wild-caught turtles, showing that *S. odoratus* harbored greater than twenty times the amount of leeches than *G. geographica*. Despite the lack of basking sites under experimental conditions, musk turtles were still colonized by leeches at four times the rate of map turtles, indicating that basking is not the sole factor determining ectoparasite load (20).

Leech load may not be a function of basking habits, but rather of bottom-dwelling habits (20). Turtle species known to have larger leech loads, such as *C. serpentina*, often spend much of their time near bottom substrates where leeches reside when not attached to a host (23). This explanation may not be adequate either, however. Readel et al. (2008) found low relative leech prevalence in the spiny softshell turtle (*Apalone spinifera*) and *S. odoratus* in comparison to *C. serpentina* despite all three species sharing a common environment in close proximity to the substrate.

In 2005, Ryan and Lambert suggested an ultimate explanation for leeches' aversion to certain species: leeches have evolved to avoid particular turtle species based on their tendency to bask. Rather than abandoning hosts when threatened with desiccation, leeches simply bypass those specific hosts altogether.

As cited above, a multitude of studies have examined the "desiccating leech" hypothesis with an interspecific perspective, but few have examined the presence of leeches as potentially correlated with individual basking responses within a single species. This perspective may provide additional insight to

understanding patterns of leech parasitism in freshwater turtles. If the "desiccating leech" hypothesis were true, then one might expect individual basking behavior to vary in response to the presence of leeches in both an intraspecific and interspecific manner. It is accepted that basking serves first and foremost as a mode of thermoregulation, and therefore turtles found in the same temperature range would be expected to bask at similar rates, all other factors held constant (1-3). However, variations might arise if turtles displayed an increased basking response in the presence of parasitic leeches above and beyond their thermoregulatory requirements. If the ultimate explanation were true, then one would not expect to see differences in basking behavior depending on the presence or absence of leeches. *Placobdella* leeches would have evolved an aversion to entire species, disregarding individual basking habits within that species. In addition, turtles would not exhibit increased basking behaviors in order to rid themselves of leeches.

This study tested the "desiccating leech" hypothesis in an intraspecific manner by looking at leech loads in Western painted turtles. The Western painted turtle (*Chrysemys picta bellii*) is an ideal species with which to test this parasite-host relationship because it is both a basking species (1), as well as one that harbors *Placobdella* leeches, although in notably lower numbers than bottom-dwelling species (16, 17, 21, 22, 24). It was hypothesized that there would not be a significant relationship between leech presence and basking behavior in painted turtles, supporting the ultimate explanation for selective leech parasitism in freshwater turtles rather than the "desiccating leech" hypothesis. Learning more about these parasite-host dynamics allows for a greater understanding of the evolutionary process of ectoparasitism in freshwater turtles, as well as explores the validity of secondary benefits to basking behavior.

Materials and Methods

This study was conducted over a 3-week period during July 2013 at the University of Notre Dame Environmental Research Center (UNDERC) on the border of Northern Wisconsin and the Upper Peninsula of Michigan.

Western painted turtles were caught using basking traps, hoop nets, and by hand. Leeches were collected opportunistically from both painted turtles and snapping turtles. Captured turtles were measured (curved carapace length and width, plastron length, and depth) as well as sexed based on foreclaw length and distance between cloaca and carapace (3, 16, 25). Because the study occurred during nesting season, weight was not recorded as some females were likely gravid. Juvenile turtles were identified as those without male secondary sex characteristics and a carapace length less than 89 mm (3) and were not used in this study.

Turtles were cleaned of large leeches, after which a baseline ectoparasite load was determined for each turtle due to the presence of very small (approximately 1 cm or less) leeches that proved too difficult to remove. For the purpose of identification, each turtle was given an alphanumeric marking on the carapace using nail polish (26-28). Turtles were fed a diet of Tetra ReptoMin Floating Food Sticks.

Five basking trials were conducted. Three tanks 1.75 m in diameter were filled with fresh lake water (Tenderfoot Lake) to a depth of 30 cm before each trial. A basking platform with approximately 0.12 m^2 of space above the water surface was placed in each tank (Fig. 1). A heat lamp (65 watts) was angled approximately 25 cm over each basking platform, and was turned on for the 12-hour duration of each daily basking period. The experimental tank contained 10 large (over 3 cm) *Placobdella* leeches, while an inert control tank contained 10 *Macrobdella decora* leeches and a second control tank contained no additional leeches. Due to the limited supply of large leeches, assignment was non-random. North American Freshwater leeches (*Macrobdella decora*) do not primarily target turtles and provided an inert organism control. The entirety of the experimental tanks were enclosed in a tarped off area within the lab so that turtles would not be disturbed from their natural basking tendencies by the presence of people. The tarped enclosure was not entered for the duration of each daily basking period.

For each trial, three turtles were randomly assigned to a treatment. Both leeches and turtles were placed in treatment tanks at 8 AM on the first day of each trial. Trials ran for a period of 3 days, and basking behavior was recorded by video camera for a 12-hour period from approximately 8 AM to 8 PM each day. Basking footage was analyzed at 5-minute intervals, with individual turtles marked as present or absent on the basking platform at each interval. A turtle was considered basking if at least 75% of the carapace was visible out of water (3).

An ANOVA was used to determine whether a significant difference in basking behavior occurred between the three treatment tanks across five replicate trials. A replicate was considered one basking trial of 3 days in length. Basking behavior was quantified as the proportion of times a given turtle was present on the basking platform out of total time intervals checked. Linear regressions were also run to determine whether baseline ectoparasite load or size had an effect on basking frequency. Four different size measurements were used: carapace length (curved), plastron length, width (curved), and depth. Two-sample t-tests were used to compare mean basking proportion between turtles with and without leeches, as well as male and female turtles. All statistical analyses were conducted in SYSTAT 13.

Results

Across five basking trials, no significant differences were observed in basking proportion between turtles in the three different treatment tanks (F=0.266, treatment df=2, error df=12, p=0.771; Fig. 2). In addition, no significant relationship was found between baseline ectoparasite load and basking pro-

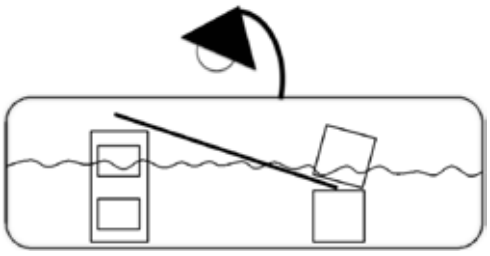

Figure 1. A schematic of the experimental basking platform setup in each treatment tank. Basking platforms were composed of a flat wooden surface secured by three cinder blocks. Plastic mesh was attached to the wooden surface for better grip.

portion (R^2=0.05, p=0.139; Fig. 3) or any size parameter and basking proportion (Table 1). No significant difference in mean basking proportion was found between turtles with and without a baseline ectoparasite load (df=43, p=0.722; Fig. 4), with and without large *Placobdella* leeches attached post-trial (df=13, p=0.151; Fig. 5), or male and female turtles (df=43, p=0.459).

An average of 1 out of 10 *Placobdella* leeches attached to turtles in the *Placobdella* tank at the end of each 3-day trial. No *M. decora* were found attached to turtles at the end of any of the trials. Post-trial, both leech species were often found concealed in crevices between the cinder blocks of basking platforms. Only in the first trial were all 10 leeches of each species recovered. An average of 1.8 *M. decora* leeches went missing per trial. *Placobdella* leeches were missing following only one of the five trials, an average of 0.8 per trial.

Discussion

Based on the results of this study, individual basking behavior does not predict or result from *Placobdella* baseline ectoparasite load. No significant differences in basking proportion were found between treatment tanks, indicating that the presence or absence of *Placobdella* leeches does not have an effect on the propensity to bask in Western painted turtles. In addition, no significant relationship was found between baseline ectoparasite load and basking proportion, nor a significant difference in mean basking proportion between turtles with and without leeches attached pre-trial. As expected, these results do not support the "desiccating leech" hypothesis.

It has been well documented that freshwater turtle species are targeted by *Placobdella* leeches at differing rates (16, 18, 21). Multiple explanations have been proposed for this phenomenon. According to the "desiccating leech" hypothesis, turtles with a greater propensity to bask will have a lower ectoparasite load. However, the results of a recent colonization experiment, in which a lack of basking sites did not deter unequal colonization rates between species, lead to another explanation: *Placobdella* leeches have evolved to selectively parasitize bottom-dwelling turtle species based on their more favorable microhabitat choice (20).

The lack of significant differences in basking proportion across treatments supports the ultimate explanation for selective leech parasitism, suggesting that although found in small numbers on *C. picta bellii*, *Placobdella* spp. have largely evolved to avoid these basking hosts in favor of bottom-dwelling species such as *C. serpentina*. This idea is further supported by the behavior of the leeches themselves. With an average of only one *Placobdella* leech attaching to a turtle host over each 3-day period, as well as most leeches exhibiting hiding behavior, it seems that both *Placobdella* spp. and *M. decora* actively avoided turtles. Missing leeches post-trial are also an indication that leeches might have been preyed upon by turtles, especially *M. decora*. Additionally, *Placobdella* leeches not attached to a host are often found in bottom substrates; the hiding behavior exhibited in the tank environment may have therefore resulted from the lack of a soft bottom surface within which to reside (23), as well as tank water with much less turbidity than found in the natural environment.

Even if *Placobdella* leeches were to parasitize *C. picta bellii* at rates similar to species such as *C. serpentina*, an increase in basking might not cause leeches to detach. Many of the leeches collected for this study were found on the shells of *C. picta bellii* and *C. serpentina* that had likely been out of water for several hours preparing to nest. *P. parasitica* has also been proven to resist desiccation. Hall (1922) showed that leeches could withstand up to 92% water loss, while Vogt (1979) noted that turtles remaining out of water for four days still retained tightly bound leeches. No reasoning was given for this observation, although it may be that leeches are able to obtain enough fluid from their host to avoid desiccation during periods out of water.

Table 1. Relevant statistical values for linear regressions testing the correlation between basking proportion and four different size parameters. No significant relationships were found.

	Carapace Length (Curved)	Plastron Length	Width (Curved)	Depth
p-value	0.817	0.645	0.333	0.313
R^2	0.001	0.005	0.022	0.024

Table 2. Comparison between leech species in attachment and disappearance rates. *Placobdella* leeches had higher attachment and recovery rates as compared to *M. decora*.

	Average Attachment	Average Recovery Post-Trial
Placobdella spp.	10%	92%
M. decora	0%	82%

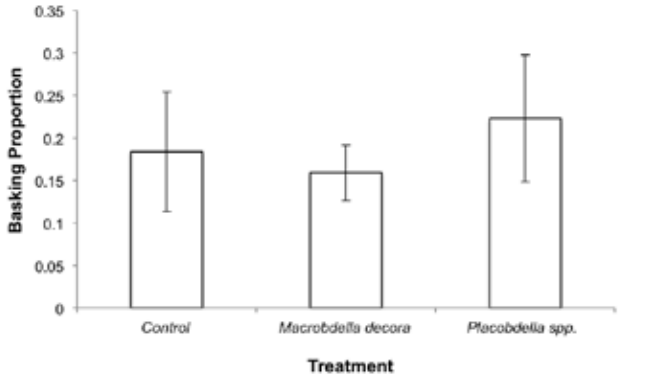

Figure 2. Overall mean basking proportion by treatment with standard error bars. No significant differences were observed between the three treatment tanks (p=0.771).

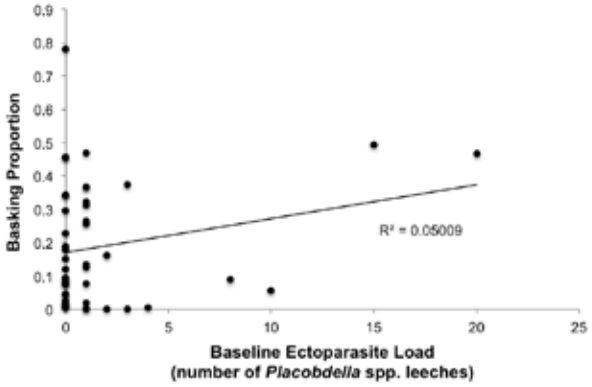

Figure 3. Linear regression between baseline ectoparasite load (*Placobdella* spp.) and basking behavior. Baseline ectoparasite load was found to be a poor predictor of basking proportion.

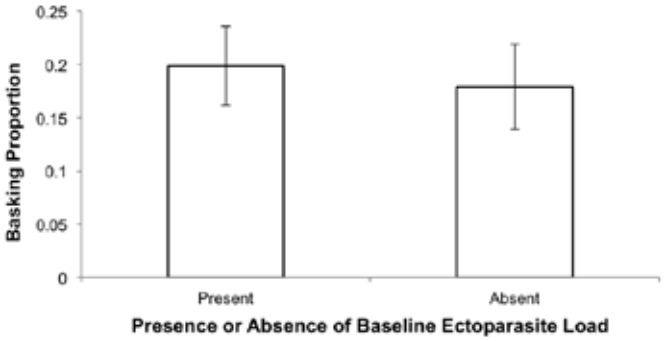

Figure 4. Average basking proportion by presence or absence of baseline ectoparasite load (*Placobdella* spp.) with standard error bars. No significant difference was found (p=0.722).

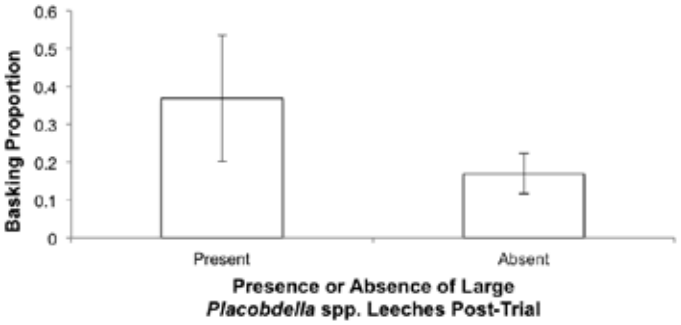

Figure 5. Average basking proportion by presence or absence of large *Placobdella* spp. post-trial with standard error bars. No significant difference was found (p=0.151).

Although *Placobdella* leeches have the ability to survive lengthy periods out of water, remaining in environments below the surface and in closer proximity to bottom substrates may increase survival and fitness rates. As for the discrepancies in leech colonization between *C. serpentina* and other bottom-dwelling turtle species such as *A. spinifera* and *S. odoratus* found by Readel et al. in 2008, perhaps *C. serpentina* provides a more adequate host environment for *Placobdella* spp. for reasons not yet understood. Future research might focus on the differences in parasitism between these bottom-dwelling species and how they might have originated over an evolutionary timescale. It would also be of interest to examine the interplay between host-parasite and predator-prey relationships that appear to coexist between freshwater turtles and *Placobdella* leeches. At least one case of *C. picta* predation on *Placobdella* spp. has been documented, a proposed feeding symbiosis between *C. picta* and highly parasitized *C. serpentina* (24).

More remains to be understood about selective leech parasitism in freshwater turtles and how the evolution of this parasite-host relationship may be a model for the development of other parasitic associations. However, as this study further supports, the "desiccating leech" hypothesis is likely not valid, and Western painted turtles do not exhibit a behavioral basking response to the presence of *Placobdella* leeches.

Acknowledgments

I would like to thank Matthew Michel, Ph.D., Professor Michael J. Cramer, and Professor Gary Belovsky for their support and guidance during the design of this study. I could not have completed this study without the help of Claire Mattison, who gave a lot of time and effort in getting this project up and running. I also thank Robert McKee for helping me with statistics as well as being generally encouraging. I am extremely grateful to everyone in the UNDERC class who went out of their way to find turtles and leeches for me, with too many to list. Riley Parrott was especially helpful in verifying turtle gender. I am also very grateful to graduate student Lindsey Sargent for bringing me turtles caught in her fyke nets. Lastly, I thank the University of Notre Dame Environmental Research Center and the Bernard J. Hank Family Endowment for providing the funding for both this project and the amazing experience that I had over the course of the summer.

References

1. D.R. Boyer. *Ecology.* 46, 99-118 (1965).

2. C.H. Ernst. *Copeia.* 1972, 217-222 (1972).

3. K. Lefevre, R.J. Brooks. *Herpetologica* 51, 217-224 (1995).

4. E.O. Moll, J.M. Legler. B. Los Angeles County Mus. *Nat. Hist.* 11, 1-102 (1971).

5. R.R. Parmenter. *Copeia.* 1980, 503-514 (1980).

6. K.A. Hammond, J.R. Spotila, E.A. Standora. *Physiol. Zool*. 61, 69-77 (1988).

7. H.W. Avery, J.R. Spotila, J.D. Congdon, R.U. Fisher, E.A. Standora, S.B. Avery. *Physiol. Zool.* 66, 902-925 (1993).

8. R.C. Vogt. *Tulane Stud. Zool. Bot.* 22, 17-48 (1980).

9. M.A. Krawchuk, R.J. Brooks. *Herpetologica* 54, 112-121 (1998).

10. M.A. Carrière, N. Rollinson, A.N. Suley, R.J. Brooks. *J. Herpetol.* 41, 206-209 (2008).

11. F.R. Cagle. *Ecol. Monogr.* 20, 31-54 (1950).

12. D.L. Auth. *B. Florida State Museum, Biol. Sci.* 20, 1-45 (1975).

13. R.M. Shealy. *B. Florida State Museum, Biol. Sci.* 21, 47-111 (1976).

14. R.J. Brooks, D.A. Galbraith, J.A. Layfield. *J. Parasitol.* 76, 190-195 (1990).

15. M.E. Siddall, E.S. Gaffney. *J. Parasitol.* 90, 1186-1188 (2004).

16. J.C. McCoy, E.L. Failey, S.J. Price, M.E. Dorcas. *Southeast. Nat.* 6, 191-202 (2007).

17. C.H. Ernst. *J. Parasitol.* 57, 32 (1971).

18. J.R. McAuliffe. *J. Parasitol.* 63, 580-581 (1977).

19. B.R. Koffler, R.A. Seigel, M.T. Mendonca. *J. Herpetol.* 12, 571-572 (1978).

20. T.J. Ryan, A. Lambert. *J. Herpetol.* 39, 284-287 (2005).

21. A.M. Readel, C.A. Phillips, M. J. Wetzel. *Copeia.* 2008, 227-233 (2008).

22. R.D. MacCulloch. *J. Parasitol.* 67, 128-129 (1981).

23. R.T. Sawyer, *Leech Biology and Behavior, Vol. 1 Anatomy, Physiology, and Behavior* (Clarendon Press, Oxford University Press, New York, NY, 1986).

24. M.A. Krawchuk, N. Koper, R. J. Brooks. *Can. Field Nat.* 111, 315-317 (1997).

25. L.E. Bayless. *Am. Midland Nat.* 93, 168-175 (1975).

26. J.E. Snow. *Copeia.* 1980, 534-536 (1980).

27. B.L. Choo, L.M. Chou. *Aquaculture* 40, 325-331 (1984).

28. G.S. Gaikhorst, B.R. Clarke, M. McPharlin, B. Larkin, J. McLaughlin, J. Mayes. *Zoo Biol.* 30, 79-94 (2011).

29. F.G. Hall. *Biol.* B. 42, 31-51 (1922).

30. R.C. Vogt. *Auk.* 96, 608-609 (1979).

About the Author

Julia Kruep is a junior biological sciences major from the San Francisco Bay area who plans on attending veterinary school after she graduates. This past summer, she participated in the UNDERC-East Practicum in Environmental Field Biology, where she carried out a research project with painted turtles. While on campus, she works in Professor Beth Archie's lab on parasitology in savanna baboons.

[$^{13}C_{10}$] AP_4A Substrate is a Novel Marker for Localizing the Binding Site of Adenosine Monophosphate in Adenylate Kinase

BRIAN TONG[1]
Advisors: Christoph Randak[2], Lokesh Gakhar[3], Marshall Pope[4]
[1]*University of Notre Dame, Department of Biological Sciences*
[2]*University of Iowa Carver College of Medicine, Stead Department of Pediatrics*
[3]*University of Iowa Carver College of Medicine, Department of Biochemistry and Protein Crystallography Facility*
[4]*University of Iowa Carver College of Medicine, Proteomic Facility*

Abstract

A sensitive and quick MALDI-MS method has been developed to identify the peptides close to the active center of adenylate kinase (ADK). Compounds capable of being photo activated (8-N_3-AP_4A and 8-N_3-[$^{13}C_{10}$]-AP_4A) have been employed to label peptides near the adenosine monophosphate (AMP) binding site. MALDI-MS analysis and mass selective sequencing of tryptic digestion products of ADK revealed two peptides containing the photoactive probe. Prior crystallographic work and computational modeling of a homologous ADK structure bound to an AP_5A shows the two peptides are in proximity to the AMP binding site. The coordination to peptides proximal to an AMP binding site belies the utility of the marker 8-N_3-[$^{13}C_{10}$]-AP_4A to help identify residues that may be involved in pertinent catalyzed phosphoryl transfer activity of ADK. The photo labeling technique described here leverages a distinct 10 Da mass difference between 8-N_3-AP_4A and 8-N_3-[$^{13}C_{10}$]-AP_4A photo-crosslinkers into a successful strategy to overcome vast amounts of background in MS, detecting pertinent ion peaks even in large and complex biomolecular structures.

Introduction

In the past decade, Matrix Assisted Laser Desorption/Ionization (MALDI) and Electrospray Ionization Mass Spectrometry (ESI-MS) have had significant applications in many studies, including the following: analysis of noncovalent interactions between substrates, sequencing of nucleic acids, in vitro analysis of drug targets, and structural analysis of proteins. The utility as a powerful analytical tool for proteomics results from high sensitivity and resolution (1-4). Mass spectrometry is currently the leading technique utilized in investigations of protein post-translational modifications (5). This investigation employs MALDI and ESI to evaluate the effectiveness of markers 8-N_3-AP_4A and 2-N_3-AMP to target and identify residues near AMP binding sites in adenylate kinase.

The model protein studied is the ubiquitous phosphotransferase enzyme adenylate kinase (ADK) derived from chicken muscle (myokinase). Two photo-activatable ligands 2-Azidoadenosine 5' monophosphate (2-N_3-AMP) and 8-Azido-diadenosine 5', 5"-tetraphosphate (8-N_3-AP_4A) along with a congener containing 10 ^{13}C isotopes ([$^{13}C_{10}$] 8-N_3-AP_4A) were utilized to target and identify the AMP binding site of ADK. The adenylate kinase used in this study is comprised of 193 amino acids (21.6 kDa, Uniprot Accession number P05081) (6). Adenylate kinases have a critical role in cellular energy metabolism where they catalyze a reversible transfer of either beta or gamma-phosphate groups, converting magnesium adenosine triphosphate (MgATP) and adenosine monophosphate (AMP) to two adenosine diphosphates (Mg^{2+}-ADP + ADP ↔ Mg^{2+}-ATP + AMP) (7). Adenylate kinase has been expansively studied; its genetics, expression, intracellular distribution, structure, and function have all been extensively elucidated (8). Adenylate kinase epitomizes the role of model proteins particularly for investigations of nucleotide binding domains and phosphoryl transfer mechanisms (8).

Adenylate kinases are composed of two binding domains with differing affinities for ATP and AMP substrates (9). Typically they have three domains: the core scaffold, the ATP binding LID, and NMP-binding core. Two independent conformational changes take place at each binding domain, namely: opening and closing (7, 10). In the absence of substrates, ADK transitions among these four states. In the presence of substrates (ATP, AMP, and Mg^{2+}), the LID and NMP-binding domains undergo allosteric alterations that cause the enzyme to close into a ternary complex, which prevents hydrolysis of either ATP or AMP (7). This closed conformation maintains coordination of the AMP α-phosphate and ATP β- and γ-phosphates to promote associative phosphoryl transfer (7).

The substrates 2-N_3-AMP, 8-N_3-AP_4A, and [$^{13}C_{10}$] 8-N_3-AP_4A bind to the adenylate kinase AMP binding site (Fig. 1). Upon irradiation with UV light, the aryl azide forms a nitrene group and loses two nitrogen atoms making the substrate very reactive toward nucleophiles (Fig. 2) (11). Photo cross-linking to the residues nearby on the AMP binding pocket is utilized to designate peptides that are targeted by AMP. A distinct mass shift caused by probe ligation is easily recognized by compari-

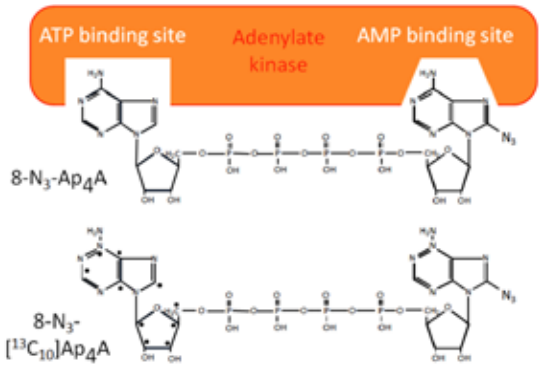

Figure 1. Model of 8-N_3-AP_4A and [$^{13}C_{10}$] 8-N_3-AP_4A binding simultaneously to the ATP and AMP binding sites of an adenolyte kinase. Substrates 8-N_3-AP_4A and [$^{13}C_{10}$] 8-N_3-AP_4A differ in mass by 10 Da.

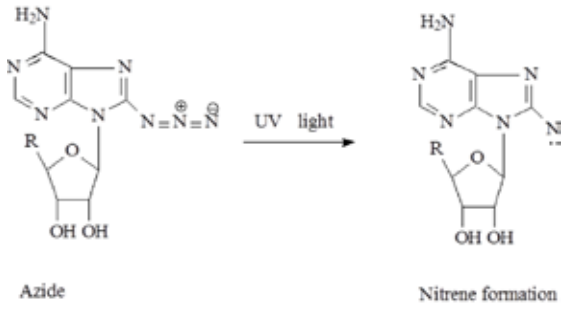

Figure 2. Aryl Azide Crosslinks upon exposure to UV light. Substrate aryl azide loses two nitrogen atoms and 28 Da mass which forms a nitrene intermediate that is reactive with nucleophiles found on amino acid side chains.

son to unlabeled samples. Other studies utilizing NMR analysis have been utilized to characterize AMP binding involvement of T39, L43, R45, G64, L66, V67, V72, Q101 (6).

This system, which utilizes ^{13}C isotopes of 8-Azido-diadenosine 5', 5"-tetraphosphate to label adenine binding residues, seeks to derive the location of functionally important residues in AMP binding through mass spectrometry. Peptides identified via analysis of distinct ionization patterns are suggested to carry the marker substrates using MALDI-MS and MS/MS analysis. Proximity of the labeled peptides to the AMP binding site is examined via structural models through open source software. Utilizing the distinct labeling pattern of the AP_4A isotopes, this investigation is interested in the feasibility of localizing potential AMP binding peptides using MALDI and ESI-MS analysis.

Materials and Method

Reagents and Equipment

Adenylate Kinase 1, P'-(adenosyl-5')-P_4-(8-azido-adenosyl-5'), [$^{13}C_{10}$] P'-(adenosyl-5')-P_4-(8-azido-adenosyl-5'), and 2-Azidoadenosine 5' monophosphate were purchased from Affinity Photoprobes, LLC (Lexington, KY). LC/MS grade organic solvent and water were obtained from Honeywell. Trifluoroacetic acid (TFA), Formic Acid (FA) and sequencing grade Trypsin were obtained from Pierce Thermo. α-Cyano-4-hydroxycinnamic acid (CHCA), Sinapinic Acid (SA), 2,6-Dihydroxyacetophenone (DHAP) and Ammonium Citrate Dibasic were obtained from Sigma-Aldrich (St. Louis, MO). Ultrafiltration cartridges used in FASP (Filter Aided Sample Preparation) device (10,000 MWCO) were obtained from PALL Lifescience (Port Washington, NY).

ADK Photo labeling

The photoactivatable P'-(adenosyl-5')-P_4-(8-azido-adenosyl-5') tetraphosphate (8-N_3-AP_4A), [$^{13}C_{10}$] P'-(adenosyl-5')-P_4-(8-azido-adenosyl-5') tetraphosphate ([$^{13}C_{10}$] 8-N_3-AP_4A), and 2-Azidoadenosine 5' monophosphate (2-N_3-AMP) probes (Affinity Photoprobes, LLC, Lexington, KY) were dissolved as triethylammonium salt in absolute methanol. Immediately before use the methanol was evaporated under a stream of argon and the azido-nucleotide was dissolved in a buffer of 20 mM Hepes (pH 7.5), 50 mM NaCl, 3 mM $MgCl_2$.

Labeling of 23 µg myokinase was done in 20 mM Hepes (pH 7.5), 50 mM NaCl, 3 mM $MgCl_2$ in a volume of 30 µl. Individual reactions were then irradiated with UV light (302 nm, eight watt lamp) for 1 minute on ice at a distance of 5 cm. 20 µl of stop buffer (25 mM dithiothreitol, 20 mM Hepes (pH 7.5), 50 mM NaCl) was added thereafter. Eight ADK samples were labeled. Sample A contained only ADK, sample B contained ADK with 150 µM 8-N_3-AP_4A, sample C contained ADK with 150 µM [$^{10}C_{13}$] 8-N_3-AP_4A, sample D contained a 1:1 mix of 150 µM 8-N_3-AP_4A and [$^{10}C_{13}$]8-N_3-AP_4A, sample E contained only ADK in presence of 5 mM MgATP, sample F contained ADK with 230 µM 2-N_3-AMP in presence of 5 mM MgATP, sample G contained ADK with 690 µM 2-N_3-AMP in presence of 5 mM MgATP, and sample H contained ADK with 230 µM 2-N_3-AMP in the presence of 5 mM AMP and 5mM MgATP.

Mass Spectroscopy of Undigested Adenylate Kinase

Measurements of the molecular weight of probe-bound ADK were done on a Bruker Ultraflextreme MALDI time-of-flight (TOF) mass spectrometer (Bruker Daltonics, Bilerica, MA) equipped with smartbeam II laser. MALDI samples were prepared by combining 1 µl sample with 1 µl saturatured SA matrix in a 1 to 1 ratio of acetonitrile and 0.1% TFA. 1 µl of a mixture of the sample and matrix was spotted on MTP-AnchorChip target. The mass spectra were initially obtained in linear positive ion mode with a source at a homogeneous 25 kV positive bias. Following each laser pulse, a delay of 350 ns transpired before the second lens was dropped to an extraction voltage of 23 kV and lens voltage of 6.3 kV.

Trypsin Digest

ADK samples were purified using a FASP filter unit (10,000 MWCO) to remove unbound nucleotides. 100 µl of 25 mM NH_4HCO_3 were added to the samples, which were centrifuged (Beckman, Microfuge R) at 10,000 rpm at 5°C for 5 minutes to wash the filter. 7.5 µL of samples A, B, C and D (463 ng/µL) were dissolved in 45 µl 2M urea in 25 mM NH_4HCO_3 buffer and loaded into the FASP unit and centrifuged at 10,000 rpm for 5 minutes 100 µl of 2M urea buffer was added to the FASP unit to rinse the sample and centrifuged. The samples of E, F, G, and H were treated with 25 mM NH_4HCO_3 buffer in all steps instead of urea buffer. 50 µl of 10 ng/µL Trypsin in 1M urea in 25mM NH_4HCO_3 was added to samples A, B, C and D. 50 µL of 10 ng/µL Trypsin in 25 mM NH_4HCO_3 was added to samples E, F, G and H. All samples were digested in a 37°C water bath for 16 hours.

Digested sample preparation for MALDI TOF

The samples were centrifuged at 10,000 rpm for 20 minutes and acidified to pH=2-3 with 10% TFA. C18 Ziptip (Millipore, tip size: P10) was conditioned with 50% acetonitrile in 0.1% TFA three times followed by 0.1% TFA three times. The sample was loaded by slowly aspiring the Ziptip in 20 µL sample more than 10 times. The Ziptip was washed with 0.1% TFA twice and eluted with 10 µL of 50% acetonitrile in 0.1% TFA. MALDI samples were prepared by combining 1 µL sample with 3 µL DHAP matrix. A 1 µL mixture of sample and matrix was pipetted on MTP-AnchorChip. MALDI-MS experiments were recorded utilizing Bruker Ultraflextreme Reflectron positive ion mode (1:30 of 2,6-Dihydroxyacetophenone, 10 mg/mL ethyl alcohol, and ammonium citrate dibasic 20 mg/mL water).

MS/MS Sequencing

Distinct patterns of either double peaks in sample D when compared to samples A, B, and C, or appearance of peaks unique to samples F and G when compared to E and H were considered for additional fragmentation. Significant ions were further fragmented using the reflection linear method and LIFT technique. Fragmented ion patterns were sequenced into amino acid sequences using Mascot database.

Q-TOF LC/MS

Agilent 1200 LC system with 6530 QTOF (Santa Clara, CA) was equipped with a HPLC chip cube (150 µm length, 75 µm diameter, particle size 5 µm) with particle material ZORBAX 300 SB-C18 (Pure size of 30 A). A Q-TOF experiment was run on a gradient of 0.1% FA in water and buffer containing 95% ACN and 0.1% formic acid for 53 minutes. A Q-TOF Agilent Mass hunter survey scan was utilized to target specific m/z target ions determined previously from MALDI experiments with a spectral parameters range for MS of m/z 290 with a maximum at m/z 2400, with an acquisition time of 5 spectra per second for 200 ms per spectrum and Transients/spectrum 1934. Parameters for MS/MS were a spectral parameter range of 4867 m/z with a maximum at 2400 m/z, with an acquisition time of 5 spectra per second for 25000 ms per spectrum and Transients/spectrum 4867 and 2 spectra per second for MS/MS.

3D modeling

Sequenced peptides were highlighted onto homologous models of ADK_1 through PYMOL crystallography modeling software.

Results and Discussion

MALDI mass spectrometry was used to determine whether the photoactivatable probe AP_4A and 2-N_3-AMP would cross link to the amino acid residues of ADK in undigested samples. Samples contain a base peak of about 21.6 kDa, which correlates to the mass of adenylate kinase. Furthermore, B, C and D contain a second peak 849 Da larger than adenylate kinase, which suggests the photoactivative probe AP_4A was able to cross-link to ADK by reduction of two nitrogen atoms (Fig. 3).

A tryptic digest of ADK was used to define peptides spatially contiguous to the AMP binding sites of ADK. Peptides bound by N-AP_4A and N-[$^{13}C_{10}$]-AP_4A show up as complementary peptide ions 10 Da apart. Sample A, the negative control, does not contain cross-linked probes. Sample B, containing 150 µM N_3-AP_4A, has a peak at 2344 m/z, an ion not found in sample A. Sample C contains 150 µM of the $^{13}C_{10}$ labeled congener of N_3-AP_4A, (N_3-[$^{13}C_{10}$]-AP_4A) and produces a m/z 2354 ion peak. Finally, sample D contains both N_3-AP_4A and N_3-[$^{13}C_{10}$]-AP_4A probes and has two peaks at m/z 2344 and 2354. Laser-Induced Fragmentation (LIFT) was used to dissociate mass-selected ions of m/z 2344 in sample B and D and m/z 2354 in C and D (Fig. 4). Error tolerant searches implemented in MASCOT database search were able to define the peptide sequence as YGYTHLSTGDLLR and match the ion of m/z 2344 relative to the peptide mass of 1495 plus 849 Da.

2-N_3-AMP was added to the ADK protein to investigate the AMP site directly. No expected shift of 361 Da could be detected in the ADK region which would implicate an AMP adduct. Possibly due to equilibrium conditions favoring ADP, the detected shift is instead 440 Da. A comparison of samples E, F, G, and H identified a pattern of peaks detected only in F and G suggested that the ion at m/z 1256 contained an AMP residue ligated to the probe. MALDI mass spectrums of the tryptic digest of ADK with 2-N_3-AMP probes were also acquired. The signal at m/z 1256 is particularly strong in sample F and G which were incubated with 230 µM and 690 µM 2-N_3-AMP respectively. Mass-selected LIFT experiments confirmed a partial sequence containing LETYYK from β and γ ion fragments.

General Protein/Mass Analysis for Windows (GPMAW) was used to confirm tryptic peptides with zero, one, or two missed cleavages identified by MS as ions with signals too weak to identify by MS/MS analysis. An ion pair at 2821 Da and 2831 Da in samples B, C, and D was suggested to be a single missed cleavage trypsin cleavage of YGYTHLSTGDLLR. Similarly, the ion pair corresponding to 2784 Da and 2794 Da is suggested to be a single missed cleavage of the LETYYK peptide, while 2940 Da and 2950 Da corresponds to two missed cleavages. These additional observed signals originating from missed cleavages support YGYTHLSTGDLLR and LETYYK as targets to the studied substrate markers.

Upon comparing the peptides containing the markers to the complete amino acid sequence of ADK, the relative location of the peptides were determined. The peptide YGYTHLSTGDLLR corresponds to amino acids 32-44 in the primary sequence (6). The peptide LETYYK corresponds to amino acids 150-155 (6). Amino acids modified in the putative AMP epitope as determined by MALDI were also sequenced by LC-ESI/Q-TOF. This work confirmed the structural identity of the peptide YGYTHLSTGDLLR and further pinpointed histidine-36 as the site of modification by the AP_4A substrate which is in close proximity to residues threonine-39 and leucine-43 which carry

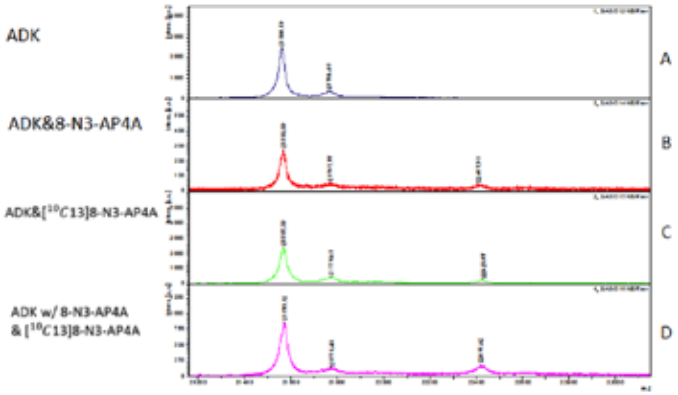

Figure 3. N_3-AP_4A probes are cross linked onto intact ADK samples. The samples A, B, C, D are graphed on Bruker Ultraflextreme MALDI time-of-flight mass spectrometer (Bruker Daltonics, Bilerica, MA) equipped with smartbeam II laser. The shift of about m/z 849 from the ion corresponding to ADK corresponds to the molecular mass of the N-AP_4A probe and likely the AP_4A probe cross linked onto the ADK. (A) was not labeled by the AP_4A probe and therefore does not have the peak shift. (B), (C), and (D) contain 8-N_3-AP_4A and/or [$^{13}C_{10}$] 8-N_3-AP_4A probes which corresponds to an approximate m/z 849 shift when cross-linked onto ADK and contains a defined ion peak.

AMP binding significance (6). A comparison to the 3D structure of homologous human ADK with the bound AP_5A substrate suggests the peptides LETYYK and YGYTHLSTGDLLR are both spatially close to the expected AMP binding site of the ADK (Fig. 5).

Conclusion

This work provided a proof-of-principle that photolabeling with 8-N_3-AP_4A and 2-N_3-AMP can be used to label amino acid sequences close to the AMP binding site of an adenylate kinase. MALDI-MS analysis with mass-selected LIFT confirmation of trypic peptides bearing substrate probes which, via UV induced ligation to residues near the AMP binding sites of ADK, revealed binding for precisely two peptides. The two peptides contain not only a target for nitrene functional cross-linking, but also are spatially contiguous to the AMP substrate. Computational docking methods applied to a close homology ADK structure with AP5A substrate bound substantiate this conclusion. Though only 23 µg of sample was used in these ligation studies, MALDI-MS was able to elucidate substrate-enzyme interaction and help map the functional domains of ADK. Using a novel label with a distinct mass difference such as the 8-N_3-AP_4A and 8-N_3-[$^{13}C_{10}$]-AP_4A it is possible to overcome the challenge of vast biological noise by using MS to detect epitope targets in large biomolecular structures.

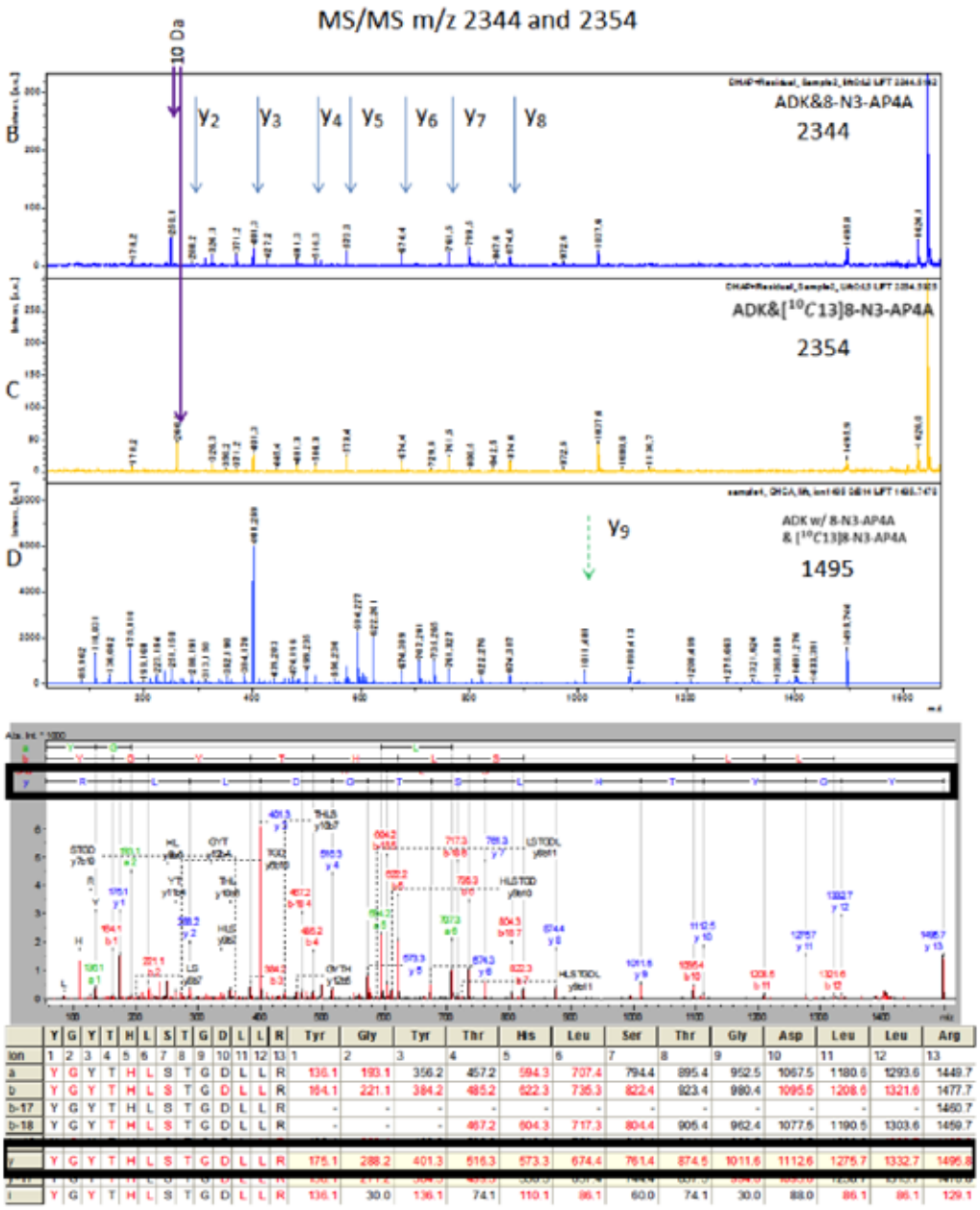

Figure 4. Peptides carrying the substrates 8-N_3-AP_4A and [$^{13}C_{10}$] 8-N_3-AP_4A are identified. A signal of 2344 Da and 2354 Da in sample B and C respectively were fragmented into Y ions using LIFT MS/MS. The 1495 Da peptide was identified using MASCOT database to be YGYTHLSTGDLLR. The ninth Y ion, histidine has a nucleophilic side chain.

Acknowledgments

I would like to thank Dr. Christoph Randak, Marshall Pope, Ph.D., and Lokesh Gakhar, Ph.D. at the University of Iowa Carver College of Medicine for their mentorship, support, and encouragement throughout the summer. This work was funded by National Institute of Health Grant K08HL097071. Finally, I would like to acknowledge Yalan Li and Chi-Li Yu for their patience while training me and for their invaluable contributions to the project.

References

1. G. Siuzdak. *P Natl. Acad. Sci. USA*. 91, 11290-11297 (1994).

2. M.J. Suh, S. Pourshahian, P.A. Limbach. *J. Am. Soc. Mass Spectr.* 18, 1304-1317 (2007).

3. W.H. Wang, A.M. Palumbo, Y.J. Tan, G.E. Reid, J.J. Tepe, M.L. Bruening. *J. Proteome Res* 9, 3005-3015 (2010).

4. R.L. Winston, M.C. Fitzgerald. *Mass Spectrom. Rev.* 16, 165-179 (1997).

5. M. Mann, S.E. Ong, M. Gronborg, H. Steen, O.N. Jensen, A. Pandey. *Trends Biotechnol*. 20, 261-268 (2002).

6. I.J.L. Byeon, H. Yan, A.S. Edison, E.S. Mooberry, F. Abildgaard, J.L. Markley, M.D. Tsai. *Biochemistry*. 32, 12508-12521 (1993).

7. H. Krishnamurthy, H. Lou, A. Kimple, C. Vieille, R.I. Cukier. *Proteins*. 58, 88-100 (2005).

8. P. Dzeja, A. Terzic. *Int. J. Mol. Sci*. 10, 1729-1772 (2009).

9. D.C. Fry, S.A. Kuby, A.S. Mildvan. *Biochemistry*. 24, 4680-4694 (1985).

10. P.C. Whitford, O. Miyashita, Y. Levy, J.N. Onuchic. *J. Mol. Bio*. 366, 1661-1671 (2007).

11. J.V. Staros. *Trends Biochem.* Sci. 5, 320-322 (1980).

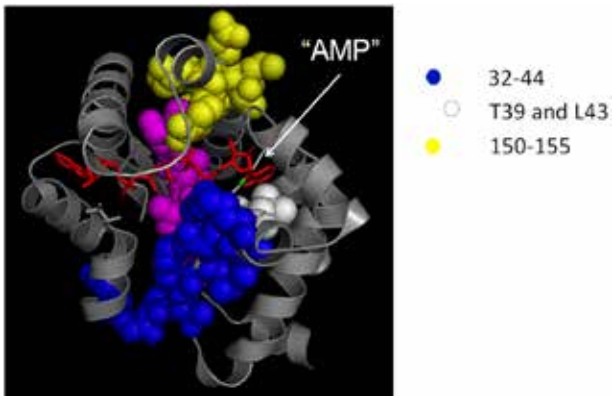

Figure 5. Localization of the labeled peptides. Utilizing PyMOL, a 3D modeling software, peptide sequences are highlighted in a homologous ADK crystal structure (PDB entry 1Z83) with an AP_5A substrate interacting with the ATP and AMP binding sites. Both labeled peptides containing amino acids 15-155 and 32-44 are spatially contiguous to the AMP binding site in the crystal structure.

About the Author

Brian Tong is a junior biological sciences major and a poverty studies minor. He spent the summer after his sophomore year testing techniques that aim to identify AMP binding activity in CFTR (Cystic Fibrosis Transmembrane Conductance Regulator) utilizing mass spectroscopy. His research interests lie in studying drug targets from a structural perspective, and he is passionate about understanding the impacts of living with currently incurable diseases. At Notre Dame he is studying protein-lipids interactions with Professor Robert Stahelin. This summer he plans to work with an organization that serves low-income individuals with HIV/AIDS. Brian hopes to attend medical school after graduation and continue to pursue his academic interests.

The Oxidation State of Non-innocent Ligands: What's the Verdict?

JUSTIN HOFFMAN[1]
Advisor: Seth Brown[1]
[1]*University of Notre Dame, Department of Chemistry and Biochemistry*

Abstract

"Non-innocent" ligands are readily oxidized, giving them many applications in coordination chemistry. When attached to a metal center, the resulting metal complex has been shown to have flexible oxidation states on both the metal and the ligand. However, this flexibility results in a confusing situation, as the oxidation state of the ligand may no longer be found using traditional methods. This paper reviews research on metal complexes involving non-innocent ligands and explains the methods used to determine the oxidation states of these ligands. By describing different analytical methods and presenting a few examples, this paper attempts to explain how one may find the oxidation state of a bonded ligand. Methods including high-resolution X-ray diffraction, absorbance spectroscopy, nuclear magnetic resonance (NMR) spectroscopy, and electron paramagnetic resonance (EPR) spectroscopy are explained.

Introduction

Coordination chemistry is used in a variety of fields, from alternative energy to biology (1, 2). Coordination chemistry is the study of metal complexes, which contain metal cations, such as Re^{7+} or Fe^{2+}, with various structures (ligands) attached to them. These structures can be uncharged molecules such as water and ammonia or charged molecules and atoms such as Br^- or OH^-. For example, in Fig. 1, *fac*-triaquatrichlorochromium(III) is shown. This complex has a chromium atom with an oxidation state of 3+. This is balanced by the three chlorine ligands, each with an oxidation state of 1-. Even though the three water molecules have an oxidation state of zero, they still interact with the central chromium.

These complexes are very useful in reduction and oxidation (redox) reactions, which involve the exchange of one or more electrons. Because metals can have different oxidation states (Iron can be Fe^{2+} or Fe^{3+}), these complexes are useful as they can accept or donate electrons, allowing for the addition or removal of functional groups. Because chromium can also have an oxidation state of 2+, the complex seen in Fig. 1 would be able to lose a chlorine atom and gain a neutral ligand. These reactions can be used in a myriad of ways, including the transfer of one or more electrons. However, not all electron transfers are possible. For example, a transfer of four electrons is not possible with many metals due to the limitations of possible oxidation states. This leads to a problem when this kind of electron transfer is needed.

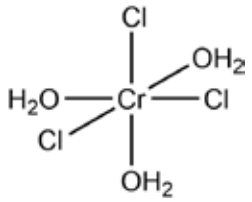

Figure 1. *fac*-triquatrchloro chromium (III), a simple metal complex with an octahedral structure

One proposed solution is through the use of "non-innocent" ligands, which are easily oxidized and reduced. When attached to the metal, these ligands may be oxidized and reduced along with the metal, creating additional oxidation states for the complex and allowing various new paths for reactions (3).

Several ligands are known to display these desired properties. They are known as catecholates when fully reduced, but removing one electron results in a semiquinone ligand. A second removal of an electron leads to a quinone. An example of one of these ligands in each of its oxidation states is seen in Fig. 2. This ligand is called ONO and will be discussed later (4).

When a complex involving a non-innocent ligand is created, the oxidation state of the metal is often identified to better understand the properties of the complex. The oxidation state suggests possible reaction pathways for a complex. If the only ligands in the complex are catecholates, the ligands will not be able to act as oxidants. The general method to determine the oxidation state of the metal considers what is attached to the metal and balances the total charge of the complex. However, for non-innocent ligands, this is no longer possible because the ligand oxidation state is not determined simply by the atoms that make it up. The ligand is too easily oxidized and reduced, so its oxidation state may vary depending on the structure of the compound in which it is found.

This paper focuses on different methods to determine the oxidation state of the constituents of these complexes. These methods include high-resolution X-ray crystallography, nuclear magnetic resonance (NMR) and absorbance spectroscopy, and electron paramagnetic resonance (EPR) spectroscopy. Three examples will then be given to clarify how these methods are used and when it is appropriate to use each.

Methods to Determine Oxidation State

The oxidation state of the non-innocent ligand has a measurable effect on the bonds in the ligand. The lengths of the bonds vary according to their π bond character. As π bond character increases, the length of a bond decreases. Adding or removing electrons changes the π bond character, meaning that the oxidation state of the ligand is associated with the lengths

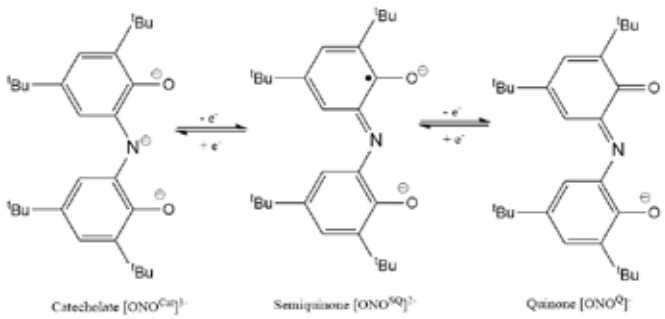

Figure 2. The three possible oxidation states of ONO (5).

of its bonds. In its quinone state, it has the fewest electrons. When electrons are added, they enter the lowest unoccupied molecule orbital (LUMO). The orbital in Figure 3 shows the LUMO of $[ONO^{Q}]^{-}$, a ligand previously mentioned. This orbital is anti-bonding with respect to some bonds while bonding to others. For example, to the far right of the diagram are the two C-O bonds with anti-bonding interactions in this orbital. Meanwhile, on the aromatic rings, the carbons bonded to oxygen and the carbons bonded to nitrogen form bonding interactions. When an electron is added to the LUMO orbital to make a semiquinone, some bonds (the ones which are anti-bonding) lose π character and are thus lengthened. Others (the bonding ones) gain π bond character and thus have shorter bonds. Adding a second electron creates the catecholate and continues this pattern.

These bond distances can best be analyzed using metrical oxidation state (MOS), which uses the lengths of all of the bonds to determine the oxidation state of the ligand. The use of MOS has been highly documented for many non-innocent ligands, and a formula has been created to relate all of the bond distances. This formula gives, to a rather high degree of accuracy, the oxidation state of the ligand (4). X-ray crystallography may be used to calculate the bond angles and distances that are used in this formula.

X-ray crystallography is also useful as it provides the geometry of the complex. The oxidation state of a metal is often the determining factor for its geometry. Because certain d orbitals are filled and others are open, the bonds can only be formed in certain places. Thus, if a ligand can take one of three states and two of the states require the metal center to have a different geometry from that which is observed, the oxidation state may be quite obvious (5).

NMR is also used to determine the oxidation state of the ligands. Because the π bond character changes based on the oxidation state of the ligand, the carbon atoms, particularly those nearest the bonding site, may be more or less shielded. In catecholates, the carbon bonded to an oxygen is an aryloxide, as the bond is single. However, in a quinone, the carbon forms a double bond with the oxygen, meaning that it is not an aryl carbon, causing it to be less shielded and further downfield (6).

Absorbance spectroscopy is also very useful for determining oxidation state. Because of intense $\pi \rightarrow \pi^*$ transitions in non-innocent ligands, clear bands may be seen. This intraligand transfer varies depending upon the oxidation state of the ligand. For catecholates, the band is often not observed in the visible or near-IR region because the next orbital to be filled is much higher in energy. Because the highest occupied molecular orbital (HOMO) of the semiquinone is half-full and the same orbital in the quinone is empty, the absorbance bands are different. However, patterns to define this difference are not often found, making this difference between the two hard to distinguish. There are also ligand-to-metal charge transfers (LMCT), where the ligand loses an electron and the metal gains one. Catecholates show bands in the UV-violet region while semiquinones and quinones have bands further in the visible region. These only occur when a metal can accept another electron, so this may give insight to the oxidation state of the metal. For example, an aluminum(III) complex will not easily become an aluminum(I) complex, making these LMCT bands unseen

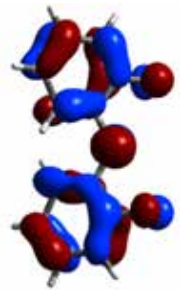

Figure 3. This orbital diagram shows the LUMO of $[ONO^{Q}]$ with its bonding and anti-bonding interactions.

in the spectrum (3). Finally, metal-to-ligand charge transfers (MLCT) occur when electrons go from the ligand to the metal (1). Like intraligand charge transfers, these bands cannot be seen in compounds with catecholate ligands, as the ligands cannot accept any more electrons. Although this logic is useful, problems arise when these three types of charge transfers all appear within the same range of the spectrum. Additional studies are usually necessary for further clarification.

For semiquinones, the electron spin state is important because not all electrons are paired. When two electrons share the same orbital, they are forced to hold opposite spin states, as in quinones and catecholates. However, in a semiquinone, one electron is unpaired, meaning that its spin state is not necessarily cancelled out by another electron. This gives the possibility of a magnetic moment caused by the unpaired electron. However, metals may also have unpaired electrons depending upon their oxidation states. To determine where the unpaired electron is located, electron paramagnetic resonance (EPR) spectroscopy may be used. This spectroscopy gives a value, known as the g value, based upon the location of the unpaired electron. The peaks in EPR spectroscopy are very different for those of ligands and for those of metals, making the unpaired electron easily identifiable. Thus, a semiquinone may be identified from both a magnetic moment and from the g value of its unpaired electron (7).

The next three sections of the paper review three different ligands and how their oxidation states were determined in metal complexes using the methods presented above.

ONO Ligand

N-(3,5-di-*tert*-butyl-2-oxyphenyl)-3,5-di-*tert*-butylquinoneimine (dbqdi or ONO) is a non-innocent ligand first synthesized in 1970 (8). ONO has three metal-binding sites, two at symmetrical oxygens and one at a nitrogen. ONO is very useful because its three oxidation states are all charged. Even the fully oxidized quinone ligand has a 1- charge, making all three states relatively stable when attached to a positively charged metal center (Fig. 2). Due to its useful properties, ONO has been widely studied, especially in its applications to coordination chemistry (9).

A recent example of determining the oxidation states in a metal-ONO complex involves $[ONO]ReO(PPh_3)$ (5). In this complex, the metal center is rhenium, which could have possible oxidation states ranging from 1- to 7+. The oxygen attached to the rhenium has an oxidation state of 2-, and the ONO ligand may carry a 1- to 3- charge, giving the central rhenium atom possible oxidation states of 3+, 4+ or 5+. The

oxidation states were determined based upon the geometry of the complex. A thermal ellipsoid plot of the complex may be seen in Fig. 4. X-ray crystallography indicates a square pyramidal geometry, which is strongly indicative of rhenium(V) complex, implying the presence of an ONO^{Cat} ligand. Because oxorhenium(III) complexes are rare and have not been shown to exhibit a square pyramidal symmetry, rhenium is not expected to exhibit a 3+ charge. The oxorhenium (IV) complex is also not expected to be stable. From this alone, the complex appears to have a catecholate ligand. However, more data may be used to confirm this.

Spectroscopic data was also used to confirm the oxidation state of the ligand. The carbon atoms that were bonded to oxygens were seen at 169.83 ppm in the $^{13}C\{^{1}H\}$ NMR, which is indicative of aryloxide and not a quinone, another indicator of a catecholate ONO ligand. Absorbance spectroscopy shows bands in the near-UV range, indicative of ligand-to-metal charge transfers. However, no bands have wavelengths long enough to represent the intraligand bands expected from quinones and semi-quinones. This lack of bands hints greatly at the presence of a catecholate ligand.

Tris-Iminosemiquinone

Determining the oxidation state of non-innocent ligands is made more complicated when multiple non-innocent ligands are within the same complex. This leads to even more ambiguities, as the question is no longer just whether the electrons are located in metal center or the ligand, but in which ligand the electrons are located. For example, if a complex has two ligands, and two free electrons are in the ligands, there are two possible situations. There may be two semiquinones with one electron each. However, there may be resonance with two ligands alternating between being catecholates and being quinones. One example is seen in Figure 5, the tris-semiquinone $Co^{III}(L^{ISQ})_3$, where L is 2-Anilino-4,6-di-*tert*-butylphenol. The different oxidation states of the ligand are seen in Fig. 6. The oxidation states of this complex have been determined through detailed analysis (7).

As in the other examples, X-ray crystallography was used to determine the oxidation state of the complex. The C-N bond distance in the complex was shorter than expected for the C=N bond seen in the quinone. The average C-O bond was shorter than that in a catecholate, falling in the range of a semiquinone. The short Co-N and Co-O distances also match the distances for Co(III) complexes more than that of Co(II) complexes. A Co(III) complex would be able to bind to three semiquinones while a Co(II) complex would only bind to up to two semiquinones.

Variable-temperature magnetic susceptibility measurements using a SQUID magnetometer were completed to determine the electron ground states in the compound. The result was an S=3/2 system, which is expected from three unpaired electrons, possibly from either three semiquinones or partially from the metal center. EPR spectroscopy showed that the three unpaired electrons were in fact from organic compounds, indicating three ferromagnetically coupled semiquinones.

3,5-$^{t}Bu_2$Catecholate Semiquinone

The catechol ligand has been known and studied for over a century (10). 3,5-$^{t}Bu_2$Catechol is a common non-innocent ligand used in coordination chemistry. It has two bonding sites, each an oxygen atom. It is less charged than ONO, so the quinone state binds more weakly than that of ONO^{Q} (Fig. 2). The oxidation states of this compound are seen in Fig. 7.

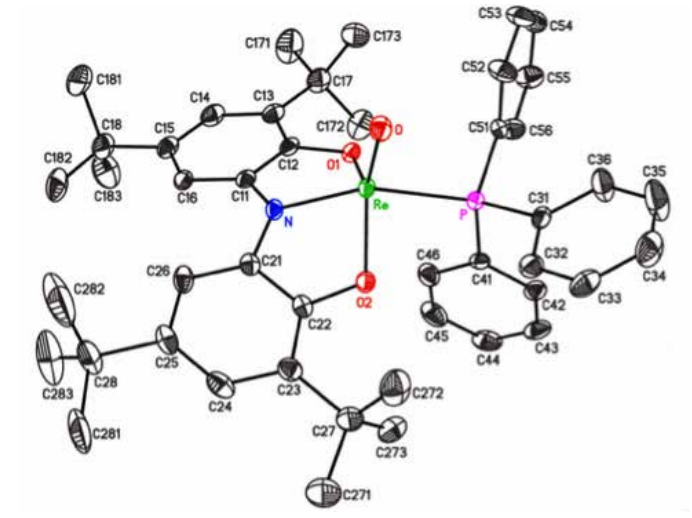

Figure 4 The thermal ellipsoid plot of [ONO]ReO(PPh_3) (edited for clarity). Selected bond distances (Å) and angles (deg): Re-O, 1.6873; Re-O1, 1.9515; Re-O2, 1.9733; Re-N, 1.9628; Re-P, 2.4359; O1-C12, 1.384; O2-C22, 1.381; N-C11, 1.412; N-C21, 1.402; O-Re-P, 99.85; O-Re-N, 113.26; O-Re-O1, 114.06; O-Re-O2, 116.31; O1-Re-O2, 129.55(5).

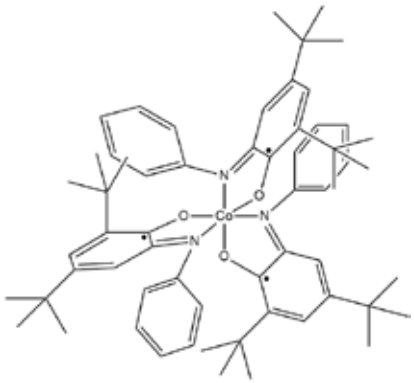

Figure 5 Schematic of $Co^{III}(L^{ISQ})_3$ (7).

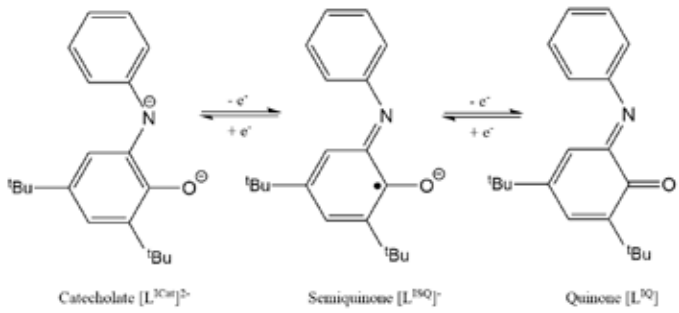

Figure 6 The three oxidation states for 2-Anilino-4,6-di-*tert*-butylphenol (7).

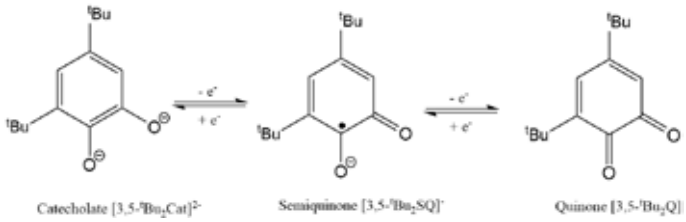

Figure 7 The three possible oxidation states of 3,5-^{t}BuCatechol (10).

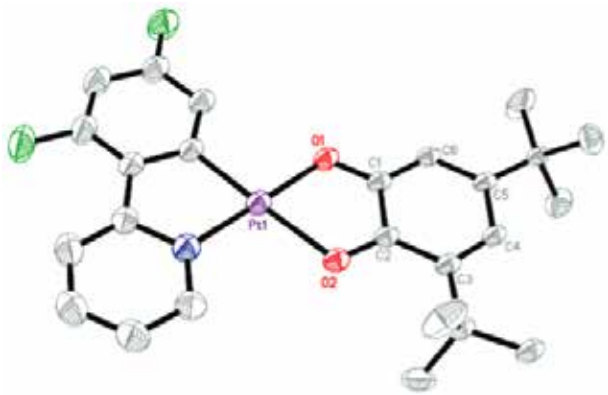

Figure 8 The thermal ellipsoid plot of Pt-sq. Selected bond distances (Å): Pt1-O1, 1.981; Pt1-O2, 2.123; C1-O1, 1.285; C2-O2, 1.296; C1-C2, 1.444; C2-C3, 1.440; C3-C4, 1.362; C4-C5, 1.428, C5-C6, 1.276; C1-C6, 1.406 (1).

A plantinum complex, (2,4-difluorophenylpyridine)Pt(3,5-di-*tert*-butylcatechol) (abbreviated Pt-sq), represents an interesting case using 3,5-^{t}BuCatechol. This compound was identified as a semiquinone through the analysis of bond distances, UV-Vis absorbance spectroscopy, and EPR spectroscopy (1).

X-ray crystallography was used to create the thermal ellipsoid plot seen in Fig. 8. The comparatively short C-O bond distance, like that in $Co^{III}(L^{ISQ})_3$, is clearly influenced by some π bond character, similar to that of other semiquinones. The bond distances are seen under Fig. 8. The C-O bond distances are similar to the semiquinones states of many complexes. The C-C bond distances are not like that of aromatic rings such as in catecholates, further suggesting the presence of a semiquinone.

Absorbance spectroscopy was used to further confirm the presence of a semiquinone. Intense bands in the UV region at 250 nm-500 nm match that expected of the $\pi \rightarrow \pi^*$ of the 2,4-difluorophenylpyridine ligand. Weak, broad bands in the visible-near IR region at 650 nm and up to 1200 nm are attributed to the MLCT bands of the 3,5-^{t}Bu$_2$Catechol ligand and platinum. These match the bands expected from 3, 5-^{t}Bu$_2$SQ, further affirming the presence of a semiquinone.

A magnetic moment was detected from this complex, so EPR spectroscopy was also used. At room temperature in toluene, the results show a radical signal at g=2.003. This value is similar to the values expected from other platinum dioxene complexes with semiquinone ligands. At 80 K in toluene, the spectroscopy shows g values at 2.042, 2.006, and 1.958. The values themselves along with the small range are indicative of a single electron in a ligand p orbital instead of an electron in a metal d orbital. This confirms the earlier suspicions that the ligand was a semiquinone.

Conclusion

In the confusing world of non-innocent ligands, there is hope for understanding what is happening. Though there is ambiguity when one tries to understand the oxidation states in the compounds using traditional methods, many techniques have been formulated to find the elusive oxidation state. Metrical oxidation state (MOS) uses the correlation between bond distance and charge due to the antibonding nature of the HOMO orbital. Using X-ray crystallography, the bonds distances may be measured and interpreted based upon what is already known about the ligand's oxidation states. X-ray crystallography also shows the geometry of the compound, which often limits the possible oxidation states for the metal, hinting at the nature of the ligand in question. NMR data also gives insight into the ligand, as the degree to which carbon atoms are shielded depends upon whether the ring is aromatic. Absorbance spectroscopy may also be used, as ligand-to-metal charge transfers and intraligand $\pi \rightarrow \pi^*$ transfers are clearly seen in the spectrum. The location of these bands depends on the oxidation state of the ligand, hinting at the oxidation state of the ligand. Finally, the magnetic moment may indicate electron paramagnetic resonance (EPR) spectroscopy may be very useful. Because semiquinones contain radicals, the free unpaired electrons show a radical signal in the spectroscopy.

Three examples were examined using these methods. [ONO]ReO(PPh$_3$) was shown to have a catecholate ligand based upon the lack of long-wavelength bands in the absorbance spectrum, the aromatic carbon peak in NMR, and the square pyramidal geometry. Next, $Co(III)(L)^3$ was shown to have a semiquinone ligand based upon measurements of intraligand bond distances and the S=3/2 electron spin state. EPR spectroscopy showed that the spin state was due to three semiquinone ligands and not from the metal. Finally, (2,4-difluorophenylpyridine)Pt(3,5-di-*tert*-butylcatechol) was shown to contain a semiquinone through the distance of intraligand bonds, absorbance spectroscopy, and EPR spectroscopy. Through the use of many methods, this complicated situation is made clearer, offering insight into the inner workings of these non-innocent complexes.

Acknowledgments

I would like to thank Prof. Seth Brown for all of his guidance in the past year I have worked with him and for all of the encouragement he has given me in my research, as well as in this paper.

References

1. B. Hirani, J. Li, P.I. Djurovich, M. Yousufuddin, J. Oxgaard, P. Persson, S.R. Wilson, R. Bau, W.A. Goddard, M.E. Thompson. *Inorg. Chem.* 46, 3865-3875 (2007).

2. S. Kundu, S. Maity, A.N. Maity, S. Ke, P. Ghosh. *Dalton Trans.* 42, 4586-4601 (2013).

3. R.F. Munhá, R.A. Zarkesh, A.F. Heyduk. *Dalton Trans.* 42, 3751-3766 (2013).

4. S.N. Brown. *Inorg. Chem.* 51, 1251-1260 (2012).

5. D.D. Wright, S.N. Brown. *Inorg. Chem.* 52, 7831–7833 (2013).

6. C. Camacho-Camacho, G. Merino, F.J. Martınez-Martınez, H. Nöth, R. Contreras. *Eur. J. Inorg. Chem.* 1999, 1021-1027 (1999).

7. Chaudhuri, C.N. Verani, E. Bill, E. Bothe, T. Weyhermuller, K. Wieghardt. *J. Am. Chem. Soc*. 123, 2213-2223 (2001).

8. (a) H.B. Stegmann, K. Scheffler. *Chem. Ber.* 103, 1279-1285 (1970). (b) H.B. Stegmann, K. Scheffler, F.A. Stöcker. *Chem. Int. Ed.* 9. 456 (1970). (c) H. B. Stegmann, K. Scheffler, F.A. Stöcker. *Chem. Int. Ed.* 10, 499-500 (1971).

9. T. Ren. *Inorg. Chim. Acta*. 229, 195-202 (1995).

10. C.G. Pierpont, R.M. Buchanan. *Coord. Chem*. Rev. 38, 45-87 (1981).

About the Author

Justin Hoffman is currently a sophomore chemistry and Chinese double major working in the Brown Lab. He researches the properties and reactivity of metal complexes involving non-innocent ligands. This is his first research project, which he began at the beginning of last summer, after his freshman year. He plans on continuing working in the Brown Lab on this project over the summer and in future semesters.

Predicting the Invisible Z Background in All-Hadronic Supersymmetry Searches Using SHERPA

CHRISTOPHER R. BARNES[1]
Advisors: Jay Dittmann[2] and Ken Hatakeyama[2]
[1]*University of Notre Dame, Department of Physics*
[2]*Baylor University, Department of Physics*

Abstract

The cross section for the production of Z + 3 jets in high-energy proton-proton collisions cannot be easily measured if the Z particle decays into two neutrinos, because neutrinos cannot currently be detected experimentally. However, the Z + 3 jets cross section can be estimated by the cross section of a γ + 3 jet interaction if the two maintain a constant ratio with one another as a function of several kinematic variables. This paper uses a Monte Carlo event generator called SHERPA (Simulation of High Energy Reactions of Particles) to explore whether the ratio is indeed constant over a range of kinematic quantities. Three quantities of interest within this paper are H_T, the scalar sum of jet transverse momentum, MHT, the missing transverse momentum within a particle interaction, and Δφ, the angle between the MHT vector and the least-energetic jet. The data within each histogram were subject to specific requirements, or cuts, that limited the events under study to those that exceeded certain threshold values of H_T and MHT, but these cuts did not have a significant effect on the behavior of the histograms. The results found that the ratio between the two cross sections remains fairly constant for all set cuts of the histograms of H_T, while the various cuts for MHT and Δφ show positive slopes for low values of these quantities. These data agree with prior theoretical work and offer insight into the invisible Z background in all-hadronic supersymmetry searches at the Large Hadron Collider.

Introduction

Throughout human history, philosophers have speculated about matter's constituents, the most fundamental pieces into which any object can be broken. Without having the necessary equipment to examine the universe on such a small scale, ancient thinkers had to use critical thinking to gain an understanding of the unobservable microworld. The Greek Democritus was the first to construct an atomic theory for the universe, stating that all matter consists of indivisible, indestructible particles known as 'atoms' (1). Plato was the first to characterize Earth, Wind, Fire, and Water as the 'elements,' understanding them to be the most basic building blocks of all other materials. Experiments throughout the twentieth century consistently showed that the atom is not solely fundamental, but rather that its constituent particles are composed of even smaller entities.

Today's understanding of particle physics rests upon the Standard Model, a theory that identifies the fundamental particles of the universe, how they obtain mass, and what forces act upon them. The three types of fundamental particles are quarks, leptons, and gauge bosons. All visible matter within the universe consists of quarks and leptons; the electron is a lepton, and protons and neutrons consist of three quarks each. In Table 1, the six different types of quarks are up, down, charm, strange, top, and bottom. Quarks combine together into structures called hadrons. Leptons are particles such as the electron, muon, and tau, as well as their corresponding neutrinos: the electron neutrino, muon neutrino, and tau neutrino. Shown in Table 2, bosons are the particles that mediate the fundamental forces: the photon, which mediates the electromagnetic force, the W and Z particles, which mediate the weak nuclear force, and the gluon, which mediates the strong nuclear force. The Higgs boson, discovered on July 4, 2012, is the mechanism by which a field of the same name generates the masses of the other fundamental particles. The Standard Model also predicts the existence of antimatter, which means that for every particle within the framework there is also a corresponding antiparticle. When a particle and an antiparticle meet, they annihilate and an enormous burst of energy is released (2).

The current instruments for micro-scale discovery are high-energy particle accelerators. These devices collide beams of particles traveling at close to the speed of light, which produce elementary particles that spray out from the collision point. The Large Hadron Collider (LHC) at CERN, the European Organization for Nuclear Research, in Geneva, Switzerland, is the most powerful particle accelerator ever built, accelerating protons to center-of-mass collision energies of 8 TeV. On February 13, 2013, the LHC began a shutdown period so that upgrades can be made to the accelerator. By the time the machine resumes operation in November 2014, energies as high as 13 or 14 TeV will be possible with the equipment, furthering the ability of physicists to explore particles at an even smaller scale (4).

This study is focused on the work of the Compact Muon Solenoid (CMS), a detector located along the LHC that takes data from particle collisions. CMS contains different subdetectors that are built to classify and track different types of particles, such as an electromagnetic calorimeter for electrons and

Table 1. The quarks and leptons of the Standard Model (3).

Particle name	Symbol	Charge (|e|)	Mass (MeV/c^2)	Spin
Quarks				
Up	u	+2/3	1.7–3.3	1/2
Down	d	−1/3	4.1–5.8	1/2
Charm	c	+2/3	1180–1340	1/2
Strange	s	−1/3	80–130	1/2
Top	t	+2/3	≈ 172000	1/2
Bottom	b	−1/3	4130–4370	1/2
Leptons				
Electron	e	−1	0.51100	1/2
Electron neutrino	ν_e	0	≈ 0	1/2
Muon	μ	−1	105.66	1/2
Muon neutrino	ν_μ	0	< 0.19	1/2
Tau	τ	−1	1776.8	1/2
Tau neutrino	ν_τ	0	< 18.2	1/2

Table 2. The gauge bosons of the Standard Model (1).

Boson	Symbol	Charge (|e|)	Mass (GeV/c^2)	Spin	Forces
photon	γ	0	0	1	EM
W	W^+, W^-	+1, −1	80.4	1	EM, weak
Z	Z	0	91.2	1	weak
gluon	g	0	0	1	strong

photons and a hadronic calorimeter for hadrons. In anticipation of higher energies at the LHC, physicists associated with CMS are preparing new searches for evidence of a theory that is coupled with the Standard Model: supersymmetry (SUSY). SUSY postulates that for every matter particle in the Standard Model there is a massive force-carrying particle, and that every force-carrying particle has a corresponding matter superpartner (2). Although supersymmetric particles have not yet been detected experimentally, searches have been performed at CERN and at Fermilab in Batavia, Illinois, the United States mecca for high-energy physics research, to detect these elusive particles.

Theorists are currently developing computer simulations to recognize the footprints of supersymmetric interactions, such as missing momentum in the plane perpendicular to the colliding protons. This inequality between the amount of momentum before and after the collision could be a result of equipment inefficiencies, but it also could be the result of the production of a SUSY superpartner particle. However, if the Z particle decays to two neutrinos, the neutrinos will account for missing momentum as well because the neutrinos cannot be currently detected. If the ratio between σ for the γ (photon) + 3 jets, streams of quarks and gluons that stream out from the collision point in the CMS detector, and σ for the Z + 3 jets remains fairly constant, then the cross section of the Z + 3 jets can be estimated using data from the γ + 3 jets interaction, which can be measured. The invisible Z background can be better modeled in this way.

This study utilizes SHERPA (Simulation of High Energy Reactions of Particles) to simulate processes with potential supersymmetric implications. SHERPA is a Monte Carlo event generator that simulates collisions of quarks, gluons, hadrons, and leptons from basic information about each of the particles, including momentum components and event ID (5). The information about the input particles was contained in histograms such as those in Figures 1 and 2, which bin the number of particles having certain kinematic quantities within the same range together. This paper discusses how the program may be ran to generate histograms of the ratio between σ for Z + 3 jets and σ for γ + 3 jets (6). These histograms are:

- σ (Z + 3 jets) / σ (γ + 3 jets) vs. H_T (the scalar sum of the momentum of the three jets)
- σ (Z + 3 jets) / σ (γ + 3 jets) vs. Δφ (MHT, jet3) (the azimuthal angle between the MHT vector and the third-most energetic jet, jet 3)
- σ (Z + 3 jets) / σ (γ + 3 jets) vs. MHT (the missing transverse momentum)

A jet cross section is approximated by using this infinite expansion:

$$\sigma=A_0 + A_1\alpha_s + A_2\alpha_s + A_3\alpha_s + ... \quad [1]$$

in which each coefficient AN is a set of matrix elements and αs is a constant predicted by the theory of the strong nuclear force, Quantum Chromodynamics (QCD). By truncating this expansion at the first term, the cross section is measured to leading-order (LO) accuracy by the following equation:

$$\sigma=A_0 \quad [2]$$

By truncating this expression at the first non-constant term, the cross section is measured to next-to-leading-order (NLO) accuracy by the following expression:

$$\sigma=A_0 + A_1\alpha_s \quad [3]$$

The most accurate approximation of the jet cross section is found by using an infinite number of terms, but theoretical calculations of more than the first couple of terms are extraordinarily difficult. Within this paper, the LO and NLO approximations are employed for all of the histograms to compare their resemblance to those found within (6) and (7), as well as to observe the behavior of the cross section ratio as a function of specific kinematic quantities.

Methods

Input Files

A set of input files containing information about the particles in the collision is needed to run a SHERPA analysis. They are contained in four separate subdirectories, each found within a directory for the photon and another for the Z particle:

- Born (B)
- Integrated Subtraction (I)
- Real Subtraction (RS)
- Virtual (V)

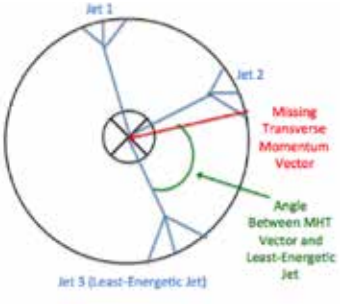

Figure 1. A diagram of the three jets accompanying a photon or Z particle with the MHT vector and Δφ angle drawn in. The two beams of protons travel perpendicularly to the direction of the jets, and the collision point is denoted by the X at the origin of the jets. H_T, not shown because it is a scalar and has no direction, is the mathematical sum of the magnitudes of the three jets' momentum.

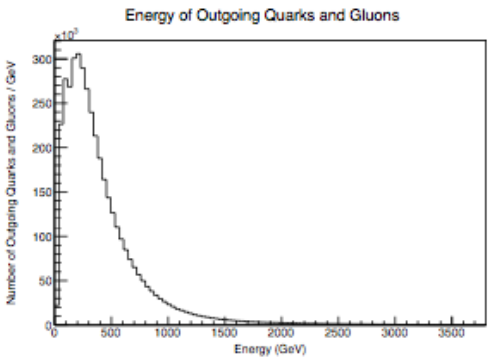

Figure 2. The amount of energy per outgoing quark and gluon (x-axis) vs. the number of quarks and gluons (y-axis) from a collision resulting in γ + 3 jets.

The name of the subdirectory specifies a particular type of theoretical contribution to the cross section calculation. Although a specific description of each contribution is beyond the scope of this paper, it is important to recognize that each of these subdirectories contain different information needed in the LO and NLO approximations.

The subdirectory for each type of theoretical contribution contains multiple data files to improve statistical precision:

Photon:
- Born: 10 files
- Integrated Subtraction: 30 files
- Real Subtraction: 160 files
- Virtual: 10 files

Z Boson:
- Born: 5 files
- Integrated Subtraction: 10 files
- Real Subtraction: 156 files
- Virtual: 20 files

The information about the particles in each of the collisions includes the following, among other quantities:

- The number of outgoing quarks and gluons from each interaction.
- The momentum components of the quarks, gluons, and the Z/γ.
- The energy of the outgoing quarks, gluons, and the Z/γ.

Examples of these are shown in Figures 2 and 3.

With this information, the SHERPA Analysis module generates files of text that contain differential cross sections for Z and γ production as a function of various kinematic variables.

Text Files

The text files generated by SHERPA are produced for each of the subdirectories (B, I, RS, V). Within each of the directories, there are seven distinct groups, or sets of text files that correspond to different requirements on the scalar sum of the jet transverse momenta (H_T), the azimuthal angle between the MHT vector and the least energetic jet, and the missing transverse momentum (MHT). The cuts for each of the sets are listed below (6):

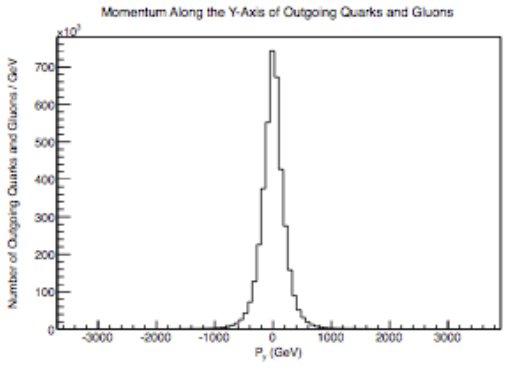

Figure 3. The amount of momentum in the y-direction per outgoing quark and gluon (x-axis) vs. the number of quarks and gluons (y-axis) from a collision resulting in γ + 3 jets.

- Set 1: H_T > 300 GeV, |MHT| > 250 GeV
- Set 2: H_T > 500 GeV, |MHT| > 150 GeV
- Set 3: H_T > 300 GeV, |MHT| > 150 GeV
- Set 4: H_T > 350 GeV, |MHT| > 200 GeV
- Set 5: H_T > 500 GeV, |MHT| > 350 GeV
- Set 6: H_T > 800 GeV, |MHT| > 200 GeV
- Set 7: H_T > 800 GeV, |MHT| > 500 GeV

Each of the text files contained rows describing the contents of each bin, a subsection of the histogram, with three values per row that specify the left edge of the bin, the value of the entry for the bin, and the uncertainty on the bin's entry.

The title of each text file specified the kinematic quantity that was plotted in the histogram.

The newest release of SHERPA was modified from its original version for the purposes of this study. The program as it is written includes an MHT vector that points in the direction opposite to that of the direction used by Zern et al. The orientation of the angles used in data collection matched that of Zern et al. to verify this study's results with his prior to generating the cross section ratio for the Set 2 cuts of missing transverse momentum. To correct this, a single sign was changed within the main tool through which SHERPA runs an analysis, thus establishing the correct azimuthal angle relationship between the direction of MHT and each jet. Additionally, the weights of the events were adjusted within the Virtual subdirectory to account for initial results that were many orders of magnitude too large.

A function exists within the SHERPA library that averages the bin entries in all of the text files of each of the input directories and then places the results in an output directory. The correct files in certain directories must be averaged together to create the text files that correspond to the histograms for the LO and NLO approximation of the cross section.

The Born directory within the framework contains the files needed to reproduce the histograms to LO approximation, because the Born calculation contains all of the matrix elements present in the A_0 term in the LO expression. An average of the bin contents for each of the ten Born files will produce these histograms. To produce the histograms to NLO approximation, an average of the files in each of the other calculations must be added to the average from the Born directory.

Histogram Production

To generate an image of this data, a C++ program was written to read the information from the file and plot the results within a histogram. Each histogram displays the ratio of the cross sections of the two physical processes, thus allowing for the modeling of one from the other, the goal of this study. The program runs within ROOT, a data analysis framework standardized by physicists at CERN. Although the program was revised throughout this project to accommodate distinct data files, its basic structure remained the same. The program opens the data file and reads the information per line in each of the three columns, storing the left edge of the bin, the entry in that bin, and the error on the bin entry in a vector. After all of the data was stored within the vectors, the histogram is declared in ROOT syntax with the number of bins, the minimum x-value, and the maximum x-value determined from the loop that read the file. The contents within the vectors are then used to fill the histogram's entries and its error before the histogram is saved

to a file. This program was updated to read two files, a γ + 3 jets file and its corresponding Z + 3 jets file, and then draw a histogram for a ratio of the Z + 3 jets cross section to the γ + 3 jets cross section.

Results

Scalar Sum of Jet Transverse Momentum

Set 1 Cuts: Fig. 4 and 5 display the histograms for the LO and NLO calculations of the ratio of the Z + 3 jets cross section to its γ + 3 jets counterpart vs. the H_T of all three jets combined. Each of these histograms starts at 300 GeV, which is the cut under consideration within Set 1. The MHT cut for these histograms, also per Set 1 standards, is 250 GeV.

Both the LO and NLO histograms are consistent with a constant ratio of 0.22. However, a slight increase in ratio at low H_T in the LO histogram is visible.

Set 5 Cuts: Fig. 6 and 7 display the histograms for the LO and NLO calculations, respectively, of the same quantities within the last section, but for the Set 5 cuts. Therefore, the first bin entry for both LO and NLO starts at 500 GeV and continues to 1000 GeV. Events with a smaller H_T are not considered under Set 5 cuts, which is why the histogram has a higher turn-on than the previous one. Additionally, the threshold for MHT of jets considered within this set is higher at a value of 350 GeV.

The distributions for these two histograms remain almost identical to their counterparts under the Set 1 cuts with the ratio remaining close to 0.22. The slight increase in the ratio at low H_T in the LO histogram is less pronounced for Set 5 cuts.

Δφ Between H/ T Vector and Jet 3

Set 1 Cuts: Fig. 8 and 9 display another relationship between the cross sections of the Z + 3 jets and γ + 3 jets interactions with another kinematic quantity, the angle between the missing transverse momentum and the least energetic of the three jets. The Set 1 cuts are the same as the ones for the Set 1 histograms of the scalar sum of jet transverse momentum.

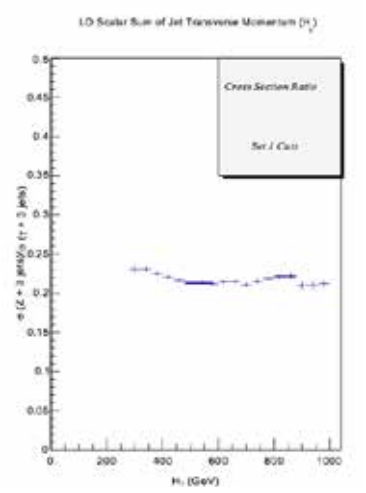

Figure 4. The LO approximation for the scalar sum of jet transverse momentum, Set 1 cuts.

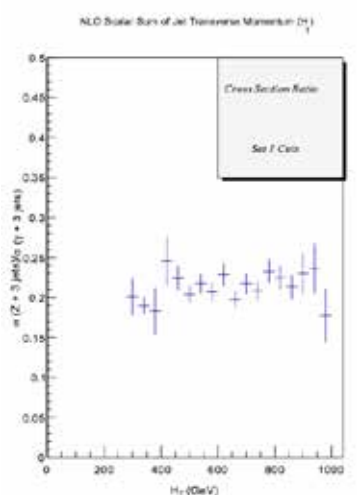

Figure 5. The NLO approximation for the scalar sum of jet transverse momentum, Set 1 cuts.

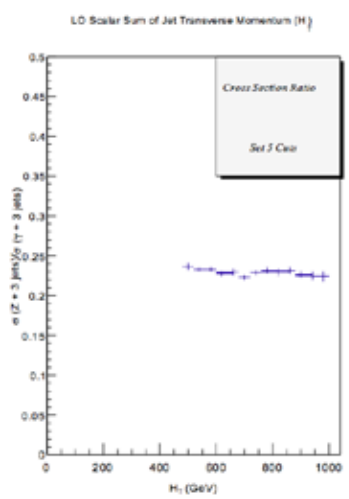

Figure 6. The LO approximation for the scalar sum of jet transverse momentum, Set 5 cuts.

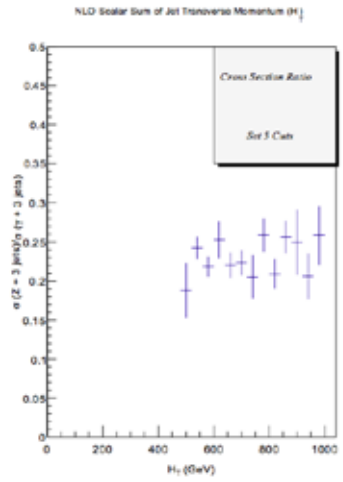

Figure 7. The NLO approximation for the scalar sum of jet transverse momentum, Set 5 cuts.

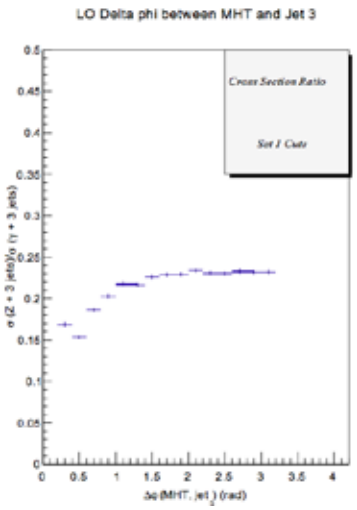

Figure 8. The LO approximation for Δφ between the MHT vector and jet 3, Set 1 cuts.

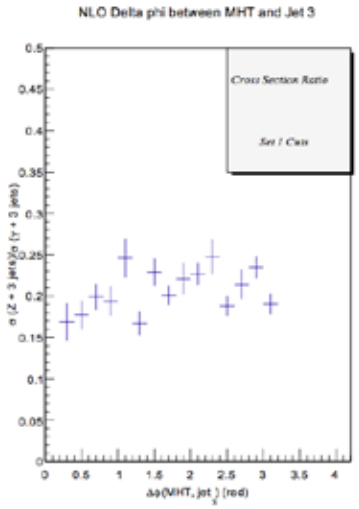

Figure 9. The NLO approximation for Δφ between the MHT vector and jet 3, Set 1 cuts.

Both histograms increase at values of low Δφ until a value in radians of 1.5, at which point they both settle at a value of 0.23. The rate of increase decreases until the histograms stop increasing altogether.

Set 5 Cuts: Fig. 10 and 11 display the same values as in the previous set of cuts, but with different requirements placed on the H_T and MHT thresholds. These minimum values are the same as those with the Set 5 cuts of the H_T histograms in the last section.

These two histograms display the same general trend that the histograms with the Set 1 cuts did, but these plots settle to a value of 0.24 after they are finished increasing.

Missing Transverse Momentum

Set 2 Cuts: The cross section ratio is plotted as a function of missing transverse momentum in Fig. 12 under Set 2 cuts, the same requirements used by another publication. This means that each jet must have a minimum H_T = 500 GeV and a value of MHT= 150 GeV. By implementing identical parameters of another program in the simulation, this plot can be compared to corresponding ones produced by a different event generator. The plot steadily increases until the value of MHT = 500 GeV is reached on the x-axis, at which point the histogram begins to level off. The errors on the individual bin entries also become much larger past this point. The histogram reaches the constant value of 0.22, which is similar to the plots in the previous subsections.

Discussion

The histograms within this paper greatly resemble similar plots from Bern et al., a publication written by the makers of SHERPA that contains the most accurate data that the program can generate. The shapes of the histograms agree from bin-to-bin, but the ratios within this paper are lower by a value of 0.01 or 0.02. Nevertheless, the strong correlation between the two demonstrates that the version of SHERPA used to produce the histograms within this paper is functioning properly and producing accurate results.

For the histograms displaying the scalar sum of the jet transverse momentum, the LO and NLO ratios are flat at 0.22 for both sets of cuts. The only slight fluctuation within this set of data is the small increase in the ratio in the LO histograms for both sets of cuts at low values of H_T. The ratios for Δφ between the MHT vector and jet 3 were slightly higher at values of 0.23 and 0.24, but the trend is an increase in the ratio for the first half of the x-axis range for these histograms. Similarly, the histogram of MHT shows an increase in the cross section ratio on the x-axis up until a value of 500 GeV, at which point the histogram remains at a maximum value of 0.25. The increase starting at low values of MHT agrees with previous findings (7). The histogram from the CMS Collaboration was produced using MADGRAPH, another Monte Carlo event generator, and produced only for the case of a Z/γ and two hadronic jets (9). The results between the two histograms are similar despite the large error on the bin entries at high MHT within the histogram of this paper.

Acknowledgments

Special thanks to Professor Jay Dittmann and Professor Ken Hatakeyama for overseeing the progression of this project and assisting whenever they could. Thank you to Professor Truell Hyde and Professor Lorin Matthews for leading this year's REU program and providing the undergraduates within the program with their knowledge and guidance. Lastly, thank you to Baylor University for hosting the REU program and to the National Science Foundation for funding the experience.

References

1. J.R. Dittmann, "Measurement of the W + ≥ 1 jet cross section in proton-antiproton collisions at √s = 1.8TeV," 1998.

2. The Particle Data Group, The Particle Adventure Website, The Particle Adventure, 2011.

3. M. Robinson, *Symmetry and the Standard Model: Mathematics and Particle Physics* (Springer, Bucher, 2011).

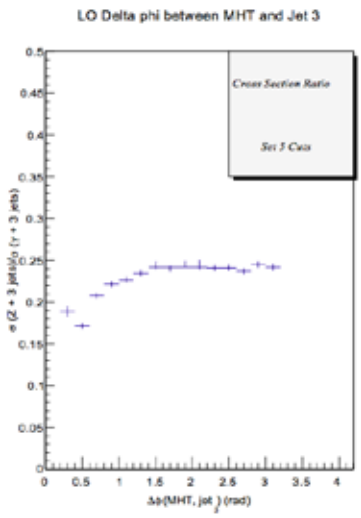

Figure 10. The LO approximation for Δφ between the MHT vector and jet 3, Set 5 cuts.

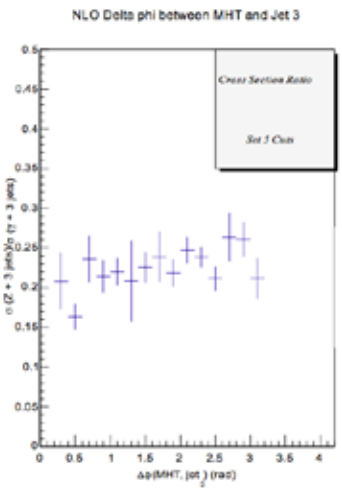

Figure 11. The NLO approximation for Δφ between the MHT vector and jet 3, Set 5 cuts.

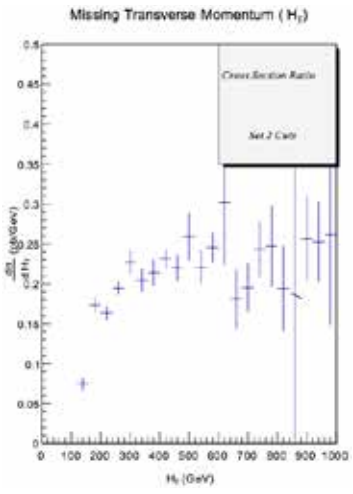

Figure 12. The NLO approximation for missing transverse momentum, Set 2 cuts.

4. R. Achintya, et al., "Long shutdown 1: An opportunity for consolidation," Compact Muon Solenoid Collaboration Website, 2013.

5. F. Siegert, "Sherpa 2.0.beta2," The Sherpa Homepage, 2013.

6. Z. Bern, et al. "Missing energy and jets for supersym- metry searches," *Phys. Rev*. 87, 034026 (2013).

7. CMS Collaboration,"Search for New Physics in the Multi- jets and Missing Momentum Final State in Proton-Proton Collisions at $\sqrt{s}$ = 8 TeV," CMS Physics Analysis Summary CMS-PAS-SUS-13-012, 2013.

8. Z. Bern, et al. "Driving missing data at next-to-leading order," *Phys. Rev*. 84, 114002 (2011).

9. J. Alwall et al., "MadGraph/MadEvent v4: The New Web Generation," *J. High Energy Phys.* 9, 028 (2007).

About the Author

Chris Barnes is a junior physics major from Royal Oak, Mich. He also has a minor in energy studies, a concentration in advanced physics, and is pursuing an Honors Physics distinction. He spent last summer working in high-energy physics on SHERPA, a Monte Carlo event generator, with Professor Jay Dittmann at Baylor University in Waco, Tex., and he will model the efficiency of new silicon chip electronics for Professor Matthew Jones at Purdue University in West Lafayette, Ind., this summer. After graduating from Notre Dame, Chris plans to pursue a Ph.D. in either high-energy physics or astrophysics and afterwards follow a career in research and teaching. In his free time, he enjoys reading, playing the clarinet, watching comedy, and spending time with his friends and family. Chris is also an avid fan of the Detroit Tigers and the Notre Dame Fighting Irish football team.

Nano Knowledge: American Scientific Illiteracy in the Age of Nanotechnology

SEAN MCGEE[1]
Advisor: Kathleen Eggleson[2]
[1]*University of Notre Dame, Department of Preprofessional Studies*
[2]*University of Notre Dame, NDnano*

Abstract

The nanotechnology industry has experienced a meteoric rise in development of new patents, uses, and fields and has even been called the dawn of the "New Industrial Revolution" by IndustryWeek (1). But what does the public, for whom developing technologies are regulated and implemented in the market, actually know about nanotechnology? Is it possible for the American people at this time to adequately address the gaping deficit of hazard and safety research in the nanotechnology industry? This case study addresses the shortcomings in scientific literacy with respect to the American public, explores the scale of the nanotechnology industry, lays out some of the potential hazards associated with it, and addresses the regulatory preparedness of the US government. We posit that, due to the relative uncertainty surrounding nanotechnology at all levels of the American public, not only does science education need to be more heavily emphasized but also that a discussion should be carried out to address the problems inherent in nanotechnology development and regulation for future generations.

Introduction

A democratic society shapes law and policy through the voting booth, and STEM policy is no exception. However, if the general public lacks basic literacy in STEM fields and is unaware of their developments, how can voters come to an informed and rational decision about the direction of societal advancement? As Carl Sagan suggested in his final interview with Charlie Rose on May 27, 1996, "We live in an age based on science and technology with formidable technological powers... and if we don't understand it—by "we" I mean the general public; if it becomes something that 'Oh, I'm not good at that I don't know anything about it'—then who is making the decisions about science and technology that are going to determine what kind of future our children live in?" It is true: scientific literacy in the United States is woefully low, and improving it is under-emphasized. Potential for adverse effects related to scientific illiteracy become clear when emerging technologies are considered. In the case of nanomaterials (NM), even the scientists who regulate and develop these materials do not believe that we are adequately prepared to properly regulate their responsible use, but many democratically active citizens lack the awareness and understanding needed to spur strong advocacy for regulatory reforms or increased environmental, health, and safety (EHS) research (2, 3). The confusion generated in the public over lack of understanding nanotech has made it so. This paper will consider the example of NM and their recent meteoric rise in public investment and in products that workers and consumers handle, all with minimal public consciousness. The number of patents related to NM has increased from 224 in 1991 to 12,776 in 2008. (4) Furthermore, during the 2009 fiscal year the US Government released $1.7 billion in grants for NM research, with only $90 million going to National Nanotechnology Initiative Environmental Health and Safety (NNI EHS) research (5, 6). Current estimates suggest over $1 trillion in NM-related products will be produced by 2015 (7). However, there is a significant deficit in research into the hazards of NM and as of now the jury is out on how to classify these materials and whether or not they can be thought of as "safe." How can it be possible for such a large industry to be built—in part on public funds—yet have such a significant lack in a body of knowledge on its own safety? We posit that emerging technologies and sophisticated materials such as NM are leaving a large portion of the American public even further behind with respect to the knowledge needed for informed civic and consumer choices. As the science and technology at the leading edge become increasingly complex, we argue, it is a moral imperative to devise and fund effective strategies for promotion of basic scientific literacy in the American public, particularly for those disadvantaged subpopulations who bear the brunt of poverty and related public health concerns. While crafting policy to address this problem requires interdisciplinary expertise and collaboration that goes beyond the scope of this paper; instead, we hope to make a compelling argument for increased urgency in the overall promotion of scientific literacy for the general public using the emergence of nanomaterials as an illustrative case.

The Pervasiveness of Nanotechnology

The first step in this procedure is determining what exactly the public knows about nanotechnology. News comes from more sources than ever before, and public opinion can often be very strongly divided on a particular topic. In general, it appears as though science is largely underemphasized in the United States: only 34% of American students possess scientific proficiency at a 4th grade level and, even more shockingly, that 40% operate below a 12th grade proficiency (8). In 2012 a Harris Poll was conducted on approximately 2,000 American adults from across the nation in varying demographics to determine the overall public knowledge of nanotechnology, from "none at all" to "a lot." In many cases the unawareness of nanotechnology is quite high (44% in the Midwest) (9). Additionally, approximately 32-36% of adults in the US believe that the potential risks of nanotechnology outweigh the benefits and that nanotechnology research should not be pursued further. However, many of those surveyed suggested that they would like to not only see nanotechnology research furthered, but also applied to healthcare and energy production (63% and 59%, respectively) (9). Interestingly, older individuals (those age 65 and above) were more likely to want to see nanotechnology applied across the board, despite being the smallest group to have heard about nanotechnology. This may be linked to their firsthand experience in seeing new technologies improve lives

throughout the last century (9).

In addition to the Harris Poll, the meta-study by Satterfield et al. from 2009 also explored the public's views on nanotechnology by combining the results of eighteen other studies from the past few years (10). One of the most striking pieces of data from this study is the strong correlation between those having learned extensively about nanotechnology and those who believe that the benefits outweigh the risks (10). As a result, this meta-study would suggest that careful education of the public, especially when it comes to shoring up the facts and "[exploiting] some of the more long-standing findings in the literature, including established theoretical propositions about the context of risk" (10). Another study suggests that the public's mindset is at this time particularly open to influence, which further highlights the need to properly frame the context and meaning of the findings of EHS research (11). Garnering public support would likely drive more interest in NM research and as a result, hazard and exposure research.

The meteoric rise in the prevalence of the ubiquitous usage of NMs extends far beyond what the public knows; some NMs are even used in foods and common cosmetics. The Project on Emerging Nanotechnologies, an organization backed by the Woodrow Wilson Center for International Scholars, tracks NMs research and their implementation in industry. This online resource has expanded its database of existing nanotechnology applications to over 1,600 items, up from only 209 when the database was founded in 2006 (12). Currently there are four types of NM: carbon based (CNTs and fullerenes), metallic (TiO2 and ZnO), dendrimers (polymer-based), and zero-valent metals (5). Each type has a myriad of uses:

1. CNTs and fullerenes: As of 2009, production of CNTs and fullerenes, soccer-ball like molecules made up of sixty carbon atoms, exceeded 1,500 metric tons per year. The usage of these NMs ranges from structural uses like in plastics to electronics. There is even research of stabilizing the agglomerating of CNTs for usage in aqueous (and, therefore, potentially biological) systems (14).

2. Metallic: Metallic NMs are most commonly derivatives of various metal oxides that are then ground into nanoscale or near-nanoscale particles. The two most common, titanium dioxide and zinc oxide, already have extensive use in dyes and sunscreen. A second class of metallic NMs, called quantum dots, are photoreactive compounds that are most commonly alloys of metals with semiconductors, such as cadmium selenide. Quantum dots are currently used in medical imaging and are expanding to be incorporated into solar cells, photovoltaics, security inks, and photonics and telecommunications (15).

3. Dendrimers: Dendrimer NMs are nanoscale polymers, chains of repeating molecular segments that form a larger structure. These are already being applied in a number of different fields ranging from biology to medical devices to surface chemistry (14).

4. Zero-valent metals: Zero-valent metal NMs include various metal compounds (like ferrous or ferric oxide) chemically treated to make them more reactive. These are often used in water remediation for nitrates and various pesticides (15).

In summary, NMs are currently most commonly used in eight industries: automotive, defense and aerospace, electronics and computers, energy and environment, food and agriculture, housing and construction, medical and pharmaceuticals, and personal care, cosmetics, and other consumer products, with the largest recent increase in NM use arising in healthcare and personal care products (5,16).

Current Research

While definitive concords in academia about the potential hazards of NMs are lacking, there have been some forays into hazard and exposure research. Initial results do show some potential hazards to environments and sensitive biota and to human models as well. Some studies have incorporated human cell lines over mammalian models.

Ecotoxicity

At this time, very little data exists on the fate of NMs in the environment. Lab tests would theorize that some NMs, like various metal oxides, would behave in similar fashions to their non-nanoscale counterparts in various ecosystems, as many of these already exist naturally. Especially difficult is the modeling of NMs in complex systems like large-scale marine environments: the variations in water chemistry throughout the ocean (depth, salinity, temperature, etc.) would likely exert very different effects on NMs suspended in them. Some preliminary research on fullerenes, nanotubes, and metal oxides has been shown to affect microbial populations, some algaes, and small freshwater invertebrates like *Daphnia magna* (17). In non-lethal concentrations there is a potential for biomagnification, especially in *D. magna* and other bottom-feeding organisms, as it is likely that many NMs will collect in sediments (15). Also interesting is the potential effects on an ecosystem would be if a large amount of silver-based NMs were suddenly released. Silver possesses very strong antibacterial properties, and such an incident would most likely have a substantial effect in the surrounding area. As of now it is difficult to pursue NM toxicity research on more complex organisms due to the requirements of raising such organisms in a laboratory setting. Despite this, there have been some studies on NM toxicity in some fish, amphibians, and freshwater and terrestrial invertebrates. Results vary, but preliminary signs for NM toxicity are seen in some cases (17).

Human health effects

Many of the potential dangers related to NMs and human health are linked to an increase in oxidative stress in cells in mammalian models and human cell lines (17). Some research has explored the toxicity of various NMs on the liver. In one particular study, it was shown that many metal oxides, especially silver nanoparticles, affected liver cell function (18). Cells exhibited irregular shape, leaked various molecules, and showed signs of oxidative damage. However, other metal particles, such as iron or tungsten, only became toxic at higher concentrations, sometimes ten to fifty times as high as silver. This data suggests that toxicity is incumbent on multiple factors, which will be discussed in further detail later in this discussion. Due to some CNTs' molecular similarity to asbestos (not all NMs in the same class are the same, see Fig. 1), much research on potential human health hazards has centered on pulmonary

damage that can be linked to NMs, especially mesothelioma. Adverse effects have been observed in laboratory studies that link lung damage and oxidative stress to high concentrations of inhaled or injected CNTs (19). Other studies, including one unpublished study by the NIOSH, have linked CNTs to increasing the likelihood of lung cancers in the presence of carcinogens. It is very important to note here that CNTs did not cause cancer on their own but only promoted or increased the cancer-causing efficacy of known carcinogens (20). As of now, there is very little research in the area of neurological damage that could be linked to NMs. Some, due to their chemical makeup, have the ability to easily cross the blood-brain barrier, which could cause problems, but as of now there has been no established link between them (21). In short, there have been several examples of potential health hazards observed in laboratory conditions for various NMs. However, it is important to remember that for these studies, dosages were controlled in the method of ingestion, dosage size, and duration. It is possible that, given proper protective equipment and procedures, these health risks can be avoided, but as of now significant study has not been done in this area.

Factors affecting toxicity

It is critical to remember that not all NMs have the potential to be toxic; many factors control the pathological mechanisms and overall toxicity of any given NM. The key to proper safety with NMs – or any material for that matter – is remembering the levels and pathways of exposure to any given one; as Paracelsus famously said, "The dose makes the poison."

There are many factors that can have an effect on the overall toxicity of a given NM:

1. Type: Toxicity of different NMs can vary merely by their chemical makeup; for example, a metal based NM like a gold nanoshell behaves differently than a carbon nanotube because of its chemical properties.

2. Purity: Many alternate constituents can make up a NM, especially in carbon-based substances (some actually make use of alternate materials to add more functionality). Current manufacturing techniques of NMs often make use of heavy metals, and improper purification and disposal of these ingredients can cause them to be incorporated into the NM structure (23).

3. Shape: Cells have to "ingest" various NMs when they are present in an organism so that they can be packaged and disposed of properly. This is most often handled by macrophages or similar cells. More irregularly shaped NMs like nanowires cause cytoskeletal strain on these cells and can cause problems with their functionality (24).

4. Size: Many studies differ on the role of size in the toxicity of a given NM, but most seem to correspond with the idea that an increase in diameter of the object consistently produces an increase in cytotoxicity (19, 22). As of now, current research has produced no consistent correlation between the length of an NM and cytotoxicity and carcinogenic activity (22).

5. Source/mechanism of exposure: NMs are used in a variety of industries and the same NM could be applied in different forms in each. For example, a CNT could be stored in a solution for one use and as a hard sheet or pellet for another. In addition to all this, release mechanisms of NMs into the local environment after disposal are poorly understood.

6. Functionalization: NMs, especially CNTs, have the ability to be chemically modified to affect their functionality. This provides them with an almost unprecedented ability to be used in multiple fields effectively. This also provides multiple facets to consider when determining the toxicity of a given NM. In some cases, like coating CNTs in polymers like polyethylene glycol, a common, biocompatible polymer, the toxicity is lowered when compared to unmodified CNTs (25). Other functional groups can lead to increased cell mortality, like the addition of an acetate group to a single-walled CNT (26, 27).

In short, the problem surrounding the nature and hazard research of NMs is very large and complex. It is essentially impossible to classify NMs as a whole but rather consider usage on a case-by-case basis. The variation in the potential factors that affect toxicity is simply too large. That being said, steps are being taken to be sure responsible use is regulated.

Regulatory Preparedness

One of the largest factors keeping the debate deadlocked is how to deal with NMs as a whole. The significant variance in size, scope, makeup, etc. of NMs makes them notoriously difficult to classify. As a result of all these variations in NMs, finding a "one size fits all" approach to properly regulating their usage will take some time and doing to fully accomplish. Some have suggested declaring NMs a new material and not subject to normal chemical regulatory procedure and that new laws must be written to account for these differences (29). Others, like the FDA, already believe that their standards will fit for NMs. Despite all this controversy, the FDA and some governmental institutions are taking steps to preemptively stop this potential issue. In 2011 the FDA published a draft guide to help provide some levels of guidance on how to best incorporate various NMs into new and existing technologies. In it, they cover best practices for the incorporation of NMs into food, medicine and medical devices, and cosmetics. They also state that they will not modify their existing regulatory policy for NMs, as "is consistent with relevant overarching U.S. government policy principles, and supports innovation under appropriate oversight" (30).

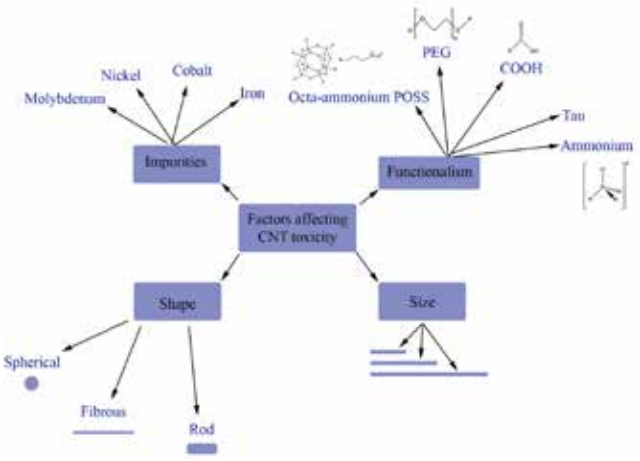

Figure 1. The various factors that affect CNT toxicity The sheer range of differences in chemistry for CNTs alone shows the issues surrounding the classifications and regulation of NMs as a whole. Adapted from Madani et al. (22).

Looking forward, the following question arises: "When would some sort of NM be classified as 'safe'? Can such a thing ever be accomplished?" Currently there are mechanisms by which this can be accomplished, the foremost being GRAS. "GRAS" is a government term that categorizes something as "Generally Recognized As Safe." There are some issues that could be associated with the GRAS label, however. NMs derive their utility from being the size that they are, and something that may be safe at nanoscale may not be at millimeter scale and vice-versa. This adds yet another level of complexity that must be considered when attempting to craft legislation for NMs.

Achieving the GRAS or label or something like it for many NMs will be difficult, as the appropriate channels to do so hold varying opinions on the nature of NMs and their usage. This is due to there being significant variances in opinion on how to address NMs between the scientists who develop the product compared to those who evaluate its safety (3). As of now there are few to no studies that try to classify opinion within a certain field (e.g. physics vs. biology, engineering, etc.), and this relative disorganization of information makes it difficult to perceive how to perceive opinions in context (3). The result of this disarray creates an air of doubt in the scientific community: in the study carried out by Beaudrie et al. scientists in all fields across nanotechnology felt the US government was inadequately prepared to deal with nanoregulation in 10 out of 14 presented scenarios. This is especially unsettling when regulatory scientists believe that the regulatory agencies are the most significantly lacking in preparedness.

Conclusion

The question of nanotechnology and all of its facets is not going to be answered today, tomorrow, or even this year. These issues surrounding how to characterize it and all its subcategories will continue to drive discussion. We need to sufficiently prepare for any potential hazards that all new materials, not just NMs, may produce. No one wants to have another incident on the scale of Exxon Valdes or asbestos or Chernobyl in the next twenty years. Multiple stakeholders invested in nanotechnology are concerned about general public backlash and financial fallout should a disaster associated with the term nanotechnology occur (not to mention the environmental and health effects following it). Doing things now could not only decrease the hazards, it could potentially keep some products that are actually hazardous out of the consumer marketplace and American homes, avoiding repetition of the folly of legacy chemicals like DDT or asbestos (Fig. 2) (31). However, this will not be possible without the intervention of the public. Adequate research cannot and will not happen in the absence of demands from the voting and consuming publics. In this multi-billion dollar industry, only $90 million of the $1.7 billion in tax dollars set aside for NM development per year by the US government are spent on hazard and exposure research (6). In addition to this, the US Government Accountability Office (GAO) reported that for fiscal years 2006-2010, approximately eighteen percent of the funds spent on hazard research did not go to projects with clearly environmental hazard and safety focuses. This may have been affected by many things, but the GAO recommends that "Director of the Office of Science and Technology Policy (OSTP), which administers the NSTC, (1) coordinate development of performance information for National Nanotechnology Initiative Environmental Health and Safety research needs and publicly report this information; and (2) estimate the costs and resources necessary to meet the research needs. OSTP and the seven included agencies neither agreed nor disagreed with the recommendations" (6). Could this gridlock have been avoided if the US had a higher level of scientific literacy and related consumer advocacy? Perhaps. As the sciences and technologies that define the "cutting edge" become more complex, however, people will need to be educated about them to participate in their proper development. In a world where trillions could be spent on a technology that few people know or understand, it becomes imperative that we make sure that the public be aware of asking the right questions for the best implementation of science. It is our job to provide the best future for our children to live in. Again, this paper does not serve to provide the overall solution to this problem, but instead foster the discussion that would lead to it. Recent events such as the "The Creationism vs. Evolution Debate" between Bill Nye and Ken Ham have cast such discussion in the public eye, and the 500,000 live viewers and the 830,000 subsequent views on YouTube show that people are interested and willing to explore this further (32). Let's get talking.

Figure 2. US Department of Agriculture and US Public Health Service urge domestic use of DDT.

References

1. SE. Rickert. "Taking the NanoPulse -- Nanotechnology: America's Next Industrial Revolution." IndustryWeek, April 10, 2010. http://www.industryweek.com/product-development/taking-nanopulse-nanotechnology-americas-next-industrial-revolution.

2. California Academy of Sciences. "American Adults Flunk Basic Science." ScienceDaily. www.sciencedaily.com/releases/2009/03/090312115133.htm

3. C.E.H. Beaudrie, T. Satterfield, M. Kandlikar, B.H. Harthorn. *PLOS One*. 8, 11 (2013).

4. Y. Dang, Y. Zhang, L. Fan, H. Chen, M. Roco. *J Nanopart Res*.12, 687–706 (2010).

5. Nanomaterials are widely used in commerce, but EPA faces challenges in regulating risk. GAO-10-549: Published: May 25, 2010. Publicly Released: Jun 24, 2010. http://www.gao.gov/products/GAO-10-549

6. Nanotechnology: Improved Performance Information Needed for Environmental, Health, and Safety Research. GAO-12-427: Published: May 21, 2012. Publicly Released: Jun 20, 2012. http://www.gao.gov/products/GAO-12-427

7. M.C. Roco. *Environ Sci Technol*. 39, 106A–12A (2005).

8. J.D. Miller, D. Jon. "The conceptualization and measurement of civic scientific literacy for the twenty-first century." Science and the educated American: A core component of liberal education. 136 (2010).

9. No Author. Regional and generational disparities in familiarity with and feelings toward nanotech are anything but small. Harris Poll. Sept. 6, 2012. http://www.harrisinteractive.com/NewsRoom/HarrisPolls/tabid/447/ctl/ReadCustom%20Default/mid/1508/ArticleId/1073/Default.aspx

10. T. Satterfield, M. Kandlikar, C.E.H. Beaudrie, J. Conti, B.H. Harthorn. *Nature Nanotechnology*. 10, 1038 (2009).

11. S. Lichtenstein, P. Slovic. *The Construction of Preference* (Cambridge Univ. Press, Cambridge, UK, 2006)

12. The Project for Emerging Nanotechnology online database: http://www.nanotechproject.org/cpi/

13. C. Buzea, I.I. Pacheco, K. Robbie. *Biointerphases*. 2, MR17–MR71 (2007).

14. R. Qiao, P.C. Ke. *J Am Chem Soc*. 128, 13656 (2006).

15. S.J. Klaine, P.J.J. Alvarez, G.E. Batley, T.F. Fernandes, R.D. Handy, D.Y. Lyon, S. Mahendra, M.J. McLaughlin, J.R. Lead. *Environ. Toxicol. Chem*. 27, 1825–1851 (2008).

16. C. Palmbery, H. Dernis, C. Miguet. Nanotechnology: an overview based on indicators and statistics; OECD: 2009.

17. J. Wang, J.D. Gerlach, N. Savage, G.P. Cobb. *Sci. Total Environ.* 442, 56-62 (2013).

18. S.M. Hussain, K.L. Hess, J.M. Gearhart, K.T. Geiss, J.J. Schlager. *Toxicol. in vitro*. 19.7, 975-83 (2005).

19. J.M. Gernand, E.A. Casman. *Risk Anal*. 34.3, 583-597 (2013).

20. V. Castranova, C.L. Geraci, P. Schulte. New Findings on Lung Tumor Formation in Laboratory Mice Exposed to Multi-Walled Carbon Nanotubes. NIOSH Science Blog – Centers for Disease Control. March 11, 2013. http://blogs.cdc.gov/niosh-science-blog/2013/03/11/mwcnt/

21. Y.L. Hu and J.Q. Gao. Potential neurotoxicity of nanoparticles. *Int. J. Pharm.* 394, 115-121 (2010).

22. S.Y. Madani, A. Mandel, A.M. Seifalian. *Nano Rev*. 4:10.3402 (2013).

23. K. Donaldson, R. Aitken, L. Tran, V. Stone, R. Duffin, G. Forrest, et al. *Toxicol Sci*. 92, 5–22 (2006).

24. S. Sharifi, S. Behzadi, S. Laurent, M.L. Forrest , P. Stroeve, M. Mahmoudi. *Chem Soc Rev*. 41, 2323–2343 (2012).

25. M. Bottini, N. Rosato, N. Bottini. *Biomacromolecules*. 12, 3381-93 (10 Oct 2011).

26. S.T. Yang, J. Luo, Q. Zhou, H. Wang. *Theranostics*. 2, 271-282 (2012).

27. S. Pichardo, D. Gutiérrez-Praena, M. Puerto, E. Sánchez, A. Grilo, A.M. Cameán, A. Jos. *Toxicol In Vitro*. 26, 672-677 (2012).

28. Y. Zhang, J. Deng, Y. Zhang, F. Guo, C. Li, Z. Zou, W. Xi, J. Tang, Y. Sun, P. Yang, Z. Han, D. Li, C. Jiang. *J Mol Med*. 91, 117-128 (2013).

29. D.M. Bowman, G.A. Hodge. *Regul. Gov*. 3, 145-164 (2009).

30. Draft Guidance for Industry; Considering Whether an FDA-Regulated Product Involves the Application of Nanotechnology. FDA; Public Availability. 76 FR 34715; June 14, 2011. http://www.regulations.gov/#!documentDetail;D=FDA-2010-D-0530-0001

31. F. Krupp, C. Holliday. "Let's Get Nanotech Right." Wall Street Journal, sec. Manager's Journal, June 14, 2005.

32. B. Chappell. "Who 'Won' The Creation Vs. Evolution Debate?" NPR. Feb. 6, 2014. http://www.npr.org/blogs/thetwo-way/2014/02/06/272535141/who-won-the-creation-vs-evolution-debate

About the Author

Sean McGee is a current senior science preprofessional and music double major at Notre Dame. For the past two years he has been an undergraduate research fellow for NDnano working with Kathleen Eggleson, Ph.D. and Marya Lieberman, Ph.D. In addition to the literature review that led to this publication, he has been carrying out research on a test for iodine deficiency for the PAD Project. Originally from Rossmoor, Calif., Sean hopes to return there following his graduate study in biochemistry and nanotechnology to research new treatments for disease.

Talk Science

September 12, 2013

Prof. Gregory Crawford
Dean of The College of Science

Using Scientific Tools to Aid in Child Abuse Cases

Elizabeth Owers
Science Preprofessional Studies '14

Visualization of Trabecular Bone Remodeling

October 10, 2013

Prof. Nicole Achee
Department of Biological Sciences

Mosquitoes, Politics, and Coconut Shells: Forging a Pardigm Shift for Vector Control

Elizabeth Nuter
Biochemistry '14

Biophysics of Immune Recognition: Flexibility of the Major Histocompatibility Complex

November 14, 2013

Prof. Nitesh Chawla
Department of Computer Science and Engineering

From Population Health Data to Personalized Health: Big Data for Common Good

Mitchell Faulk
Mathematics '14

Vertex Operator Algebras: Algebraic Realizations of the Geometry of String Theory

February 6, 2014

Prof. Matthew Ravosa
Departments of Biological Sciences, Aerospace and Mechanical Engineering, Anthropology

Integrative Approaches to the Evolution, Function, and Development of the Mammalian Skull

Michael Ahlers
Chemistry '15

Synthesis of GEX1A Analogues: A Potential Lead for Niemann-Pick Type C Disease

March 20, 2014

Prof. Patricia Clark
Department of Chemistry and Biochemistry

Protein Folding and Human Disease

Michael Kipp
Biological Sciences '14

Modeling Freshwater Methane Dynamics in a Changing Climate

April 10, 2014

Prof. Ani Aprahamian
Department of Physics

Nuclear Science and Society

Daniel Irvine
Mathematics '14

The Wild World of Knot Theory

Visit

Read past articles, browse new ones, and submit your own research online at scientia.nd.edu.

For more information about undergraduate research at the University of Notre Dame, visit science.nd.edu/undergradresearch.

Contact

Email questions or comments to the editors at scientia@nd.edu.

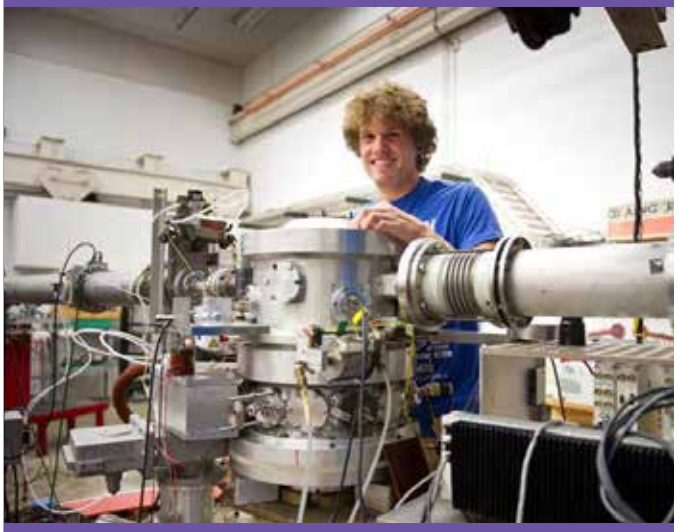

Join

Get involved with *Scientia* as an editor, news columnist, or graphic designer for the upcoming semester. Email for details.

UNIVERSITY OF
NOTRE DAME
College of Science